



OSLO METROPOLITAN UNIVERSITY
STORBYUNIVERSITETET

Department of Civil Engineering and Energy Technology
Institutt for Bygg- og energiteknikk
Energi og miljø i bygg
Postal address: Postboks 4 St. Olavs plass, 0130 Oslo
Visitor address: Pilestredet 35, Oslo

CANDIDATE No.

889

AVAILABILITY

Open

Telephon 67 23 50 00
www.oslomet.no

MASTER'S THESIS

TITLE Python-based modeling of the vapor compression cycle focusing on heat exchangers and user-friendliness with web page	DATE 2022-05-25
	NO. PAGES/APPENDICES 74/A-I
AUTHOR Eirik Jakobsen Svortevik	SUPERVISOR Rebecca Allen
IN COLLABORATION WITH OsloMet and Rebecca allen	CONTACT PERSON Rebecca Allen

SUMMARY <p>This research expands a Python-based heat pump cycle model to simulate three heat exchangers extensively. Utilizing Python and multiple codes to study the refrigerants R1270, R717, and R290. Heat load (Q_c) for results have been iteratively run through four convergence criteria. The study models the vapor compression cycle, monitors performance, and evaluates the coefficient of performance(COP), pump power, and efficiency trends across different heat exchangers. R717 consistently offers the highest COP, while the pump power varies with the heat exchanger types and condenser temperatures. Findings are presented by comparison of heat exchangers for three cases, and a web page in Python powered by Streamlit was built to introduce a new method to display results.</p>
--

KEYWORDS
Python
Heat Pump
Heat Exchanger

Preface

This master's thesis was written by Eirik Jakobsen Svortevik and will be the final work of a degree in Energy and Environment in Buildings, an engineering program at OsloMet.

I would like to extend my gratitude to my supervisor, Rebecca Allen, who always found time to help and gave excellent feedback. Would also say thank you to Arnab Chaudhuri who helped with some programming. Lastly, I would like to thank Jørn Stene from COWI and Ole Døsvik from Multiconsult for taking the time to answer questions and speak about the building industry.

Eirik Jakobsen Svortevik, 25/05/2023

Abstract

Research into simulating and calculating parameters for heat pumps has been on an upward trajectory, especially in recent years due to rising electricity prices. A pre-existing Python-based heat pump cycle has been extended and refined for more comprehensive calculations to heat pumps and, in particular, heat exchangers. This improved model includes three new heat exchangers: the shell and tube, double pipe, and plate exchanger, each offering an array of parameters to be calculated. An iterative Python code has been developed to generate a heat load (Q_c) and a user-input required heat load ($Q_{c,rec}$), with four convergence criteria, tolerance of: i) Q_c and $Q_{c,rec}$, ii) Q_{ev} and Q_{ev1} , and iii) condenser temperatures and iv) evaporator temperatures. The Python code has been validated against CoolTools.

Three cases involving different refrigerants (R2170, R717, and R290) have been computed to collect information and observe trends between the heat exchangers. The vapor compression cycle is then modeled in Python, using the converged results for calculated Q_c and $Q_{c,rec}$, and illustrated with T-s and P-h diagrams. This representation displays the findings by comparing the results of three cases. The computed results reveal that R717 consistently offers the highest coefficient of performance (COP) for all three heat exchangers across all cases. The study also measures the pump power required to circulate water through the condenser and evaporator. Of the three heat exchangers, the double pipe heat exchanger demands the most power due to its structure and length. Interestingly, as condenser temperatures rose across the cases, the pump power for water in the condenser decreased. This occurs in all three cases. In terms of efficiency, R717 emerged as the leader for the shell and tube exchanger, while R290 outperformed the other refrigerants in the double pipe exchanger. For the plate exchanger, the three refrigerants demonstrated equal efficiency, although this exchanger displayed the most significant decline in efficiency as Q_c increased.

To present these results in a more appealing and intuitive way, a web page was developed using Python and Streamlit. This digital tool provides an aesthetic and preferred method to illustrate and review the research outcomes.

Sammendrag

Forskning på simulering og beregning av parametere for varmepumper har vært i sterk vekst de siste årene, blant annet på grunn av stigende strømpriser. I denne masteroppgaven er en allerede eksisterende Python-basert varmepumpesyklus blitt utvidet og forbedret for mer omfattende beregninger til varmepumper og spesielt varmevekslere. Denne forbedrede modellen inkluderer tre nye varmevekslere: skallvarmeveksler, dobbel rør og plateveksler, som hver tilbyr en rekke parametere å beregne. En iterativ Python-kode har blitt utviklet for å generere en varmelast (Q_c) fra en opprinnelig varmelast ($Q_{c,rec}$) gitt av brukeren, med fire konvergenskriterier, toleranse for: i) Q_c og $Q_{c,rec}$, ii) Q_{ev} og Q_{ev1} , iii) kondensatortemperatur og iv) fordampertemperaturer. Python koden er validert mot CoolTools.

Tre caser som involverer forskjellige kjølemedier (R2170, R717 og R290) er beregnet for å samle inn informasjon og observere trender mellom varmevekslerne. Dampkompresjonssyklusen er deretter modellert i Python, ved å bruke de konvergente resultatene for beregnet Q_c og $Q_{c,rec}$. Dette er illustrert med T-s og P-h diagrammer. Denne representasjonen viser funnene ved å sammenligne resultatene fra de tre casene. De beregnede resultatene avslører at R717 konsekvent tilbyr den høyeste ytelseskoeffisienten (COP) i sammenligningen av de tre varmevekslerne i alle tilfeller. Studien måler også pumpeeffekten som kreves for å sirkulere vann gjennom kondensatoren og fordamperen. Av de tre varmevekslerne krever dobbeltrørsvarmeveksleren mest effekt på grunn av sin struktur og lengde. Interessant nok ble pumpe effekten for vann i kondensatoren redusert ettersom kondensatortemperaturene økt. Dette var tilfelle i alle tre casene. Når det gjelder effektivitet, er R717 best for skall- og rørveksler, mens R290 presterte best i dobbel rør eksleren. For plateveksleren viser de tre kjølemediene lik effektivitet, men plateveksleren viste stor reduksjon i effektivitet når Q_c øker.

For å presentere resultatene på en mer tiltalende og intuitiv måte, ble også en nettside utviklet med Python og Streamlit. Dette har gjort det mulig å presenter på en god estetisk måte hvilke av varmevekslerne som yter best i de ulike casene.

Nomenclature

ΔE_{sys}	Energy, [J]	$COP_{HP,2}$	Coefficient of performance, [-]
ΔP_t	Tube pressure loss, [Pa]	$COP_{HP,carnot}$	Coefficient of performance carnot, [-]
ΔP_x	Pressure loss, [Pa]	COP_{HP}	Coefficient of performance, [-]
ΔT	Temperature change, [K]	COP_{real}	'Real' Coefficient of performance, [-]
Δx	Length change, [m]	D	Diameter, [m]
\dot{E}	Power, [W]	d	Diameter, [m]
\dot{m}	Mass flow rate, [kg/s]	D_p	Real diameter, [m]
$\dot{Q}_{c,rec}$	Required heat load, [W]	D_e	Equivalent diameter, [m]
\dot{Q}_c	Heat load, [W]	D_h	Hydraulic diameter, [m]
\dot{Q}_{ev1}	Cooling load, [W]	$d_{i,ST}$	Innerdiameter ST, [m]
\dot{Q}_{ev}	Cooling load, [W]	D_i	Inner shell diameter, [m]
\dot{Q}_H	Heat load, [W]	d_i	Inner diameter, [m]
\dot{q}_H	Heat capacity, [kJ/kg]	$D_{o,b}$	Outer baffle diameter, [m]
\dot{Q}_L	Cooling rate, [W]	$d_{o,ST}$	Outer diameter ST, [m]
\dot{W}_{in}	Work input, [W]	D_o	Outer shell diameter, [m]
\dot{W}_{work}	Work, [W]	d_o	Outer diameter, [m]
ϵ_x	Efficiency(ST), [-]	E	Energy, [J]
γ	Inner channel factor, [-]	e	Energy, [kJ/kg]
λ	Volumetric efficiency, [-]	f	Darcy friction factor, [-]
μ	Dynamic viscosity, [kg/m * s]	F_{new}	Correction factor, [-]
ϕ	Enlargment factor, [-]	G_t	Mass velocity, [kg/s * m ²]
π	Pi, [-]	H	Enthalpy, [kJ/kg]
ρ	Density, [Kg/m ³]	h	Specific heat transfer coefficient, [W/m ² * K]
A_p	Heating area of plate, [m ²]	h_1	Enthalpy, point 1, [kJ/kg]
a_t	Tube flow area, [m ²]	h_o	Outside heat transfer coefficient, [W/m ² * K]
A_x	Specific area, [m ²]	H_p	Height, [m]
Ah_i	Inner area, [m ²]	h_t	Tube heat transfer coefficient, [W/m ² * K]
Ah_{oa}	Total heating surface area, [m ²]	$h_{2,a}$	Actual enthalpy, [kJ/kg]
Ah_o	Outer area, [m ²]	$h_{2,s}$	Icentropic enthalpy, [kJ/kg]
b	Corrugation pitch, [°]	k	Thermal conductivity, [W/m * K]
Be	Width, [m]	$K1$	Square factor, [-]
c	Rate for fluids, [-]	L	Length, [m]
c_c	Rate for water(cold), [kW/K]	$L_{p,tot}$	Total length of plate, [m]
c_h	Rate for hot fluid, [kW/K]	L_t	Length of tube, [m]
$C_{p,c}$	Specific heat capacity, cold, [J/kg * K]	$LMTD$	Log mean temperature difference, [K]
$C_{p,h}$	Specific heat capacity, hot, [J/kg * K]	m_{flow}	Mass flow rate refrigerant, [kg/s]
C_p	Specific heat capacity, [J/kg * K]	$n1$	Angle factor, [-]
		n_c	Icentropic efficiency, [-]

n_{el}	El. efficiency, [-]	s	SpesifiEntropy, [$kJ/kg * K$]
n_{kl}	Clamping efficiency, [-]	T	Temperature , [K]
$N_{p,pe}$	Number of plates, [-]	T	Temperature, [$^{\circ}C$]
n_{pump}	Efficiency, [-]	T_0	Ambient temperature, [$^{\circ}C$]
n_{tr}	Transfer efficiency, [-]	T_0	Temperature low reservoir, [K]
N_t	Number of passes, [-]	T_h	Plate thickness, [m]
N_t	Number of tubes, [-]	T_s	Temperature surroundings, [K]
NTU	Number of transfer units, [-]	U	Overall heat transfer coefficient, [$W/m^2 * K$]
Nu	Nusselt number, [-]	u	Internal energy, [J]
P	Pressure, [Pa]	V	Volume, [m^3]
P_o	Power output, [kW]	V_s	Compressed stroke volume, [m^3/h]
P_s	Plate spacing, [m]	V_x	Volumetric flow, [m/s]
P_t	Temperature factor, [-]	v_x	Flow per area, [m^2/s]
P_t	Tube pitch, [m]	V_{ins}	Real imbibed volume, [m^3/h]
Pr	Prandtl number, [-]	W_p	Width, [m]
Q_{conv}	Condenser, hot, [W]	$W_{p,tot}$	Total height of plate, [m]
R	Temperature factor, [-]	W_{pump}	Pump power, [W]
$R_{f,t}$	Fouling factor refrigerant, [$m^2 * K/W$]	$X_{\dot{Q}_L}$	Exergy, heat loss, [W]
$R_{f,x}$	Fouling factor water, [$m^2 * K/W$]	X_{dest}	Exergy destroyed, [W]
Re	Reynolds number, [-]	Y	Temperature factor, [-]
S	Entropy, [J/K]	Z	Temperature factor, [-]

Contents

1	Introduction	1
1.1	Literature review	2
1.2	Objective	5
1.3	Limitations	5
2	Theory	6
2.1	Thermodynamics	6
2.1.1	Enthalpy	6
2.1.2	Entropy	7
2.1.3	Exergy	7
2.2	Heat transfer	8
2.2.1	Convection	8
2.2.2	Conduction	8
2.3	Heat pump	9
2.3.1	Evaporator	10
2.3.2	Compressor	10
2.3.3	Condenser	11
2.3.4	Expansion valve	11
2.4	Coefficient of performance	11
2.5	Ground source heat pump	12
2.6	Vapor compression cycle	13
2.7	Heat Exchangers	14
2.7.1	Shell and tube HE	14
2.7.2	Double pipe HE	15
2.7.3	Gasketed plate exchanger	16
2.8	Refrigerants	16
2.9	Python	17
3	Method	18
3.1	Initial script	18
3.2	Set-up and learning programming	18
3.3	Assumptions	19
3.4	Starting foundation	19
3.4.1	Refrigerants	20
3.5	Heat exchangers	21
3.5.1	Shell and tube	21
3.5.2	Double pipe	24
3.5.3	Plate exchanger	26
3.6	General equations	29
3.7	Python	33
3.7.1	HPmain	33
3.7.2	HPIteration	36

3.7.3	App	38
3.8	Interviews with experts	39
4	Results	40
4.1	Validation of the code	40
4.2	Cycles that satisfy Q_{cond} values	44
4.2.1	Case 1	44
4.2.2	Case 2	50
4.2.3	Case 3	56
4.3	Web page with Streamlit	61
5	Discussion	63
5.1	Results and cases	63
5.2	User-friendliness	64
5.3	Web page	64
5.4	Phase change on refrigerant	64
5.5	Choice of refrigerant	64
5.6	LMTD	65
5.7	Components	65
5.8	Efficiency	65
5.9	Darcy friction factor	66
5.10	Overall heat transfer coefficient	66
5.11	Possibilities the script provide	66
6	Conclusion	67
7	Acknowledgements	68
	Appendix	75
A	Initial Code	75
A.1	Main script	75
A.2	P-h Plot	76
A.3	T-s Plot	77
B	Python values for validation	78
C	Python scripts	78
C.1	Start of function	78
C.2	Calling function	78
D	Mass flow rate and COP figures	79
D.1	Mass flow rate and COP, C1, DP	79
D.2	Mass flow rate and COP, C1, PE	79
D.3	Mass flow rate and COP, C2, DP	80
D.4	Mass flow rate and COP, C2, PE	80

D.5	Mass flow rate and COP, C3, DP	81
D.6	Mass flow rate and COP, C3, PE	81
E	Excel	81
F	T-s and P-h diagrams, Case 1	82
G	T-s and P-h diagrams, Case 2	83
H	T-h og T-s Python	84
I	T-s diagram modification	86

List of Figures

1	Imaginary exergy distribution shown.[55]	8
2	Main HP cycle from AutoCAD.	9
3	Condenser side from AutoCAD.	9
4	Evaporator side from AutoCAD.	9
5	Ground source HP illustration.[1]	12
6	VCC of sub-cooling.	13
7	VCC of super-heating.	13
8	Both sub-cooling and super-heating.	14
9	No sub-cooling or super-heating.	14
10	3D illustration of ST HE.	15
11	Simple schematic of an ST with two flow patterns.	15
12	Illustration of DP HE.[60]	15
13	Simple schematic of a DP with two flow patterns.	15
14	3D model of DP HE.[63]	16
15	Simple schematic of a PE with two flow patterns.	16
16	Caption	22
17	Schematic description of scripts	33
18	Illustration of PropsSI used in Python	34
19	Flow chart of HPmain script.	35
20	Flow chart of HPIteration script.	37
21	Flow chart of Streamlit app script.	38
22	CoolTools input screen with R134a as refrigerant.	40
23	Heat pump cycle from Python with R134a as refrigerant	41
24	All heat exchanger parameters possible to read from Python	42
25	Q_c and $Q_{c,rec}$ for all simulation points, C1,ST.	45
26	COP and COP_{real} for all refrigerants, C1,ST.	45
27	COP and COP_{real} for all refrigerants, C1,DP.	45
28	COP and COP_{real} for all refrigerants, C1,PE.	45
29	Water pump over Q_c for all refrigerants, C1, ST	46
30	Water pump over Q_c for all refrigerants, C1, DP	46
31	Water pump over Q_c for all refrigerants, C1, PE	46
32	Brine pump power for all three refrigerants, C1,ST	47
33	Brine pump power for all three refrigerants, C1,DP	47
34	Brine pump power for all three refrigerants, C1,PE	47
35	Efficiency for all refrigerants, C1,ST.	48

36	Efficiency for all refrigerants, C1,DP.	48
37	Efficiency for all refrigerants, C1,PE.	48
38	Mass flow rate for all refrigerants, C1,ST.	48
39	T-s diagram, R717, for Q_c equals 61 [kW], C1.	49
40	T-s diagram, R290, for Q_c equals 61 [kW], C1.	49
41	P-h, R717, for Q_c equals 61 [kW], C1.	49
42	P-h diagram, R717, for Q_c equals 61 [kW], C1.	49
43	Q_c and $Q_{c,rec}$, C2,ST.	51
44	COP and COP_{real} for all refrigerants, C2,ST.	51
45	COP and COP_{real} , C2,DP.	51
46	COP and COP_{real} all refrigerants, C2,PE.	51
47	Pump power required, water, C2,ST.	52
48	Pump power required, water, C2,DP.	52
49	Pump power required, C2,PE.	52
50	Brine pump power, C2,ST.	53
51	Brine pump power, C2,DP.	53
52	Brine pump power, C2,PE.	53
53	Efficiency for all three refrigerants, C2,ST.	54
54	Efficiency for all three refrigerants, C2,DP.	54
55	Efficiency for all three refrigerants, C2,PE.	54
56	Mass flow rate for all three refrigerants, C2,ST.	54
57	T-s diagram, R717, for Q_c equals 61 [kW], C2.	55
58	T-s diagram, R290, for Q_c equals 61 [kW], C2.	55
59	P-h diagram, R717, for Q_c equals 61 [kW], C2.	55
60	P-h diagram, R717, for Q_c equals 61 [kW], C2.	55
61	COP and COP_{real} for all refrigerants, C3,ST.	57
62	COP and COP_{real} for all refrigerants, C3,DP.	57
63	COP and COP_{real} for all refrigerants, C3,PE.	57
64	Water pump power for all refrigerants, C3,ST.	58
65	Water pump power for all refrigerants, C3,DP.	58
66	Water pump power for all refrigerants, C3,PE.	58
67	Brine pump power for all refrigerants, C3,ST.	59
68	Brine pump power for all refrigerants, C3,DP.	59

69	Brine pump power for all refrigerants, C3,PE.	59
70	Efficiency for all refrigerants, C3,ST.	60
71	Efficiency for all refrigerants, C3,DP.	60
72	Efficiency for all refrigerants, C3,PE.	60
73	First to see when opening web page.	61
74	Showing available refrigerants to choose from	61
75	Shows a table of the count, Q_c , etc.	61
76	More information of output and start of tables.	61
77	Q evaporator difference.	62
78	Q condenser and required, with evaporator difference.	62
79	The change in LMTD.	62
80	The change of temperature for condenser and evaporator.	62
81	Initial script handed over by bachelor groupe	76
82	P-h plot made by bachelor group	76
83	T-s plot made by bachelor group	77
84	Start of function	78
85	End of script "calling" the function	78
86	Mass flow rate for all refrigerants, C1,DP	79
87	COP for all refrigerants, C1,DP	79
88	Mass flow rate for all refrigerants, C1,PE	79
89	COP for all refrigerants, C1,PE	79
90	Mass flow rate for all refrigerants, C2,DP	80
91	COP for all refrigerants, C2,DP	80
92	Mass flow rate for all refrigerants, C2,PE	80
93	COP for all refrigerants, C2,PE	80
94	Mass flow rate for all refrigerants, C3,DP	81
95	COP for all refrigerants, C3,DP	81
96	Mass flow rate for all refrigerants, C3,PE	81
97	COP for all refrigerants, C3,PE	81
98	Values from Excel.	81
99	T-s diagram, R717, for Q_c equals to 61, 67, and 73 [kW], C1	82
100	T-s diagram, R290, for Q_c equals to 61, 67, and 73 [kW], C1	82
101	P-h diagram, R717, for Q_c equals to 61, 67, and 73 [kW], C1	82
102	P-h diagram, R290 for Q_c equals to 61, 67, and 73 [kW], C1	82
103	T-s diagram, R717, for Q_c equals to 61, 67, and 73 [kW], C2	83
104	T-s diagram, R290, for Q_c equals to 61, 67, and 73 [kW], C2	83
105	P-h diagram, R717, for Q_c equals to 61, 67, and 73 [kW], C2	83
106	P-h diagram, R290, for Q_c equals to 61, 67, and 73 [kW], C2	83
107	P-h plot.	84
108	T-s plot	85
109	T-s plot of 5 °C SH and 5 °C SC.	86

List of Tables

1	Refrigerants available.[64][66][65]	17
2	Assumptions made to the script	19
3	Parameters and values to each case	20
4	Refrigerants and measurements.[64][66][65]	20
5	Initial input values for shell and tube HE	21
6	K1 and n1 values to Shell and Tube HE	22
7	Initial input values for double pipe HE	25
8	Initial input values for plate HE	27
9	Convergence criteria for iterations.	36
10	Interviews with two individuals from the building industry.	39
11	Initial input values for double pipe HE	43
12	Input values Case 1	44
13	Rest of Case 1 input values	44
14	Input values Case 2	50
15	Rest of Case 2 input values	50
16	Input values Case 3	56
17	Rest of Case 3 input values	56
18	Initial input values for validation	78

1 Introduction

Today, the world faces a daunting challenge as rising temperatures lead to global warming.[2] This is largely due to countries worldwide contributing to increased carbon dioxide emissions by using materials and resources without considering the side effects or embracing a circular economy, with the building sector being a significant contributor. [3][4] A considerable amount of carbon dioxide from the building industry is released by BRICS countries, most of which are economically strong and recognized as developed. However, the European Union (EU) also has a severe impact on emission rates.[5] The building industry is responsible for approximately 39 [%] of global greenhouse gas emissions and 36 [%] of energy use, making it essential to take action worldwide to reduce these percentages. [6]

In recent years, the EU has brought more demands to the building industry and desired achievements on decreasing energy usage and greenhouse gas emissions, specially CO₂. [7] [8] With increasing electricity and gas prices, management of efficient energy usage in buildings is more emphasized than before.[9] Therefore, with electricity prices increasing by 500 [%] around Europe from 2020 to 2022 according to the international energy agency (IEA) the impact of making correct choices or innovative solutions that reduce energy use can be immense, both from an economical point of view, but also a step towards the widely known Paris Agreement that entered into force in 2016. [10][11] One of the solutions to the problems mentioned about emissions and energy is heat pumps(HP), where the potential for higher efficiency and lower energy use is enormous. The increase in sales of HPs across the EU over the period 2021 - 2022 was 35 [%] and it illustrates how residential and commercial buildings are dependent on this technology. [12]

Before the 2000 century, research on components such as compressors and technology for cold climates like Norway was limited, largely due to the country's low electricity prices compared to the rest of Europe. However, since the early 2000s, and particularly in the last decade, this field has experienced significant growth. As a result, HP technology has become a popular choice in Norway for addressing heating and cooling needs in buildings.[13] Since early 2000 and especially in the last decade this field of study has experienced enormous growth and as a result, HP technology is widely preferred in Norway to resolve especially heating- and cooling demands in buildings. By 2022 Norway was the leading country in Europe with the most HPs installed per capita and the Norwegian HP Association (NOVAP) states that 1,1 million HPs are in operation in Norway today. [14][15] That shows both private people and industry projects designing residential- and commercial buildings favor HPs for their high-efficiency potential and well-established technology. Air-to-air, air-to-water, and fluid-to-water cover most types of HPs in the wider picture, with fluid-to-water presenting many different possibilities where heat can be extracted from one/two meters down the soil, drill pipes down the bedrock, or use seawater.Renewable energy (solar panels) Utilization. [16]

Norway offers various subsidy programs through Enova, an organization established by the Norwegian National Assembly (Stortinget). Private homeowners can receive up to 15,000 NOK in support for fluid-to-water HP installations. Companies can apply for and receive funding of up to 2 million NOK for projects that include the installation of fluid-to-water HPs as part of a central heating system. A crucial factor to consider in current times, especially when applying for these subsidies, is the type of refrigerant used by HP. Refrigerants with high global warming potential (GWP) and ozone depletion potential (ODP) should be avoided when installing a new HP or replacing the refrigerant in an existing system. [17]

1.1 Literature review

HP technology has been around for a long time and the different types, liquid-to-liquid, air-to-liquid, or components, such as compressors, can be modeled, tested, and improved. With general searches on pages such as google scholar and ORIA one can reach 20 - 30 000 articles published after 2019 about the different variations of tests regarding HPs in general. Some testing upper limit performance of two-stage VCC for improving energy efficiency, where positive results for many experiments were obtained.[18] More creative studies with the subject as ejector-assisted two-stage evaporation VCC with single-stage VCC for condensation, with a cycle designed for specific refrigerants and the results yields a 22.0 [%] increase of Coefficient of Power (COP) in comparison to a 'basic' refrigeration cycle under rated conditions. [19] The determination to improve and build on simulation models or tools involving HPs is massive in today's science environment. Experiments associated with simulation tools and other modeling equipment are widely used and produced to illustrate progress within measurements, most commonly COP , Q_{cond} optimization, P_{com} , and type of refrigerant. [20] [21] Articles cover new technology and methods to improve future-built HPs, with examples such as permanent magnet engines in compressors and new technology to handle refrigerants with high pressure like carbon dioxide (R744). [22] Many articles also investigate improvements to already built HPs possible to implement without making major changes. [23] Experiments also consider the best possible refrigerant to use in HP cycles and the building industry development of environmentally friendly refrigerants in the last 5 - 10 years has been immense. [24] Refrigerants such as the widely known, R134a, were utilized, but now undergoing a phase-out process. Comprehensive studies are performed to analyze alternatives, such as R152a as a substitute. [25]

As the building industry shifts towards decarbonization, the VCC has become a focal point for enhancing performance prediction and system optimization. The VCC describes the relationship between pressure-enthalpy (P-h) or temperature-entropy (T-s), and enlightens the operation of the four principal HP components: the compressor, condenser, expansion valve, and evaporator.[26] The primary aim of most research in this area is to optimize the VCC. Through careful analysis and calculation of variables such as pressure, temperature, temperature lift, and the parameters of enthalpy and entropy, or through comparative studies of different refrigerants, optimization is typically aimed at achieving a low-pressure cycle and a reduced temperature lift.[27] [18] The most common computational tools for such optimization studies include IDA-ICE, MatLAB, Modelica, Energy Plus, TRNSYS, Excel, CoolPack, and CoolTools. More recently, the potential for Python to serve as a competitive, if not superior, tool for these calculations has emerged.[28]

IDA-ICE is a licensed simulation tool where heating demand on the building level, heating, cooling demand, and hot water often are simulated and calculated by using the "plant" which is the HP in IDA-ICE. With also in-depth temperatures of the building given as output. Persson Westermark wrote how an HP system could simultaneously produce domestic hot water and cooling spaces, with R744 as the working fluid. [29] Clauß et al. [30] analyzed predictive-based control for residential buildings and the use of HP to create energy flexibility. By utilizing compressor on and off control and schedule it yields the best results in case of energy saving. Solar-assisted HP to release less CO_2 and decrease the use of energy regarding domestic hot water and space heating is a combination where IDA-ICE is frequently used.[29]

Modelica is frequently employed for component-based dynamic simulations, which are particularly useful in the field of HPs. The software allows for the assembly of components drawn from various packages, constructing models through interconnections. It excels in analyzing transitions over time and initial conditions or start-up sequences. Ling et al. [31] developed a Modelica-based HP model that incorporated a compressor,

heat exchanger, controller, and expansion valve, and investigated the behavior of the cycle, particularly the compressor, during start-up and shut-down phases with various low GWP refrigerants. Factors such as COP, Q_{cond} , and pressure were examined. This foundation makes Modelica an excellent simulation tool for studies such as the one conducted by Verdnik et al.[32] which investigated the behavior of the compressor and heat exchanger under trans-critical operating conditions and a condenser temperature of 383 [K]. They found that increasing the suction gas superheat and modifying the heat exchanger led to an increased COP. Moreover, Modelica's refinement allows it to connect all four main components of an HP, the compressor, condenser, expansion valve, and evaporator, and even extend the model to more complex simulations by incorporating elements like a solar panel. Qian & O'Neill [33] designed a dynamic Modelica-based model of a solar-powered ground source HP. They calculated the COP at different time stamps and validated the model against test-rig data and manufacturer specifications, providing a foundation for future research once accurate results are obtained from validation and start tests.

Matlab is a licensed programming tool where components are built by providing parameters and supplying equations for each component, unlike Modelica where 'boxes' are chosen. Therefore, Matlab is a great tool for studying which parameters for example change output variables the most, by creating cases and changing one parameter at a time. Camdali et al. [34] present a study investigating ground source HP with HEs on 1.4 [kW] for different refrigerants and compare COP for against Solkane software program, and they yielded accurate results for calculated parameters. Luo Zou's [35] research exemplifies this approach by providing illustrations of the four components of an HP system, aligning the necessary equations, and presenting an analysis that concludes R245fa outperforms R600 in terms of COP, while also examining energy savings. Matlab also offers the capability to generate visually compelling plots of COP and corresponding VCC data. Matlab is commonly used in studies investigating COP and pressure lift, however, by incorporating equations related to exergy, a set of HP cycle equations can be adapted to calculate and analyze exergy destruction. Ozturk et al.[36] investigated the performance variation of an air source HP paired with a water heater under different ambient conditions. They utilized Matlab to assemble all thermodynamic properties and values, incorporating comprehensive exergy destruction calculations into the code. Rather than focusing solely on the final state, as it is often performed, they calculated exergy destruction for each state. Matlab also excels in traditional studies where energy savings and exergy are not considered, and the VCC and refrigerant are analyzed based on evaporator and condenser temperatures.[37] [38]

CoolPack is a comprehensive, freely accessible software designed to facilitate the analysis and evaluation of the performance and parameters of VCC. This tool provides users with the capability to generate P-h plots for various scenarios, thereby assisting in determining the most effective options. As demonstrated by Acharya et al.[39] it can be used to illustrate the effects of varying the speed of a condenser fan motor within a VCC system. Their study focuses on a P-h plot comparison of different scenarios, indicating the optimal case and providing the parameters for the subsequent COP calculations. This methodology could potentially be adapted to assess the effects of varying pump power on water flow through a HE. A similar application of CoolPack for the experimental investigation of a water-to-water HP is presented by Kolev et al.[40] Their work involves plotting the operation cycle on a log.P-h diagram, studying switch-off temperatures, and examining the impact of these temperatures on vaporization pressure variations. As such, CoolPack proves itself to be a highly effective tool for generating detailed and accurate P-h plots for various types of HPs. These plots yield valuable data for the various states of the HP, which can be instrumental in calculations such as determining the COP and different states.[41]

Components vice, compressor technology, condenser temperatures, and evaporation are the most widely discussed themes in research papers. This does indeed not insinuate that expansion valves are neglected in research performed, just that compressor and condenser/evaporator are the path of change chosen to analyze first because of their importance and impact. Šarevski & Šarevski [42] analyzed how high speed and high-pressure ratio affect a turbo compressor, also named centrifugal compressors by some, with water(R718) as a refrigerant. Their findings were a significant decrease in energy consumption by the application of a turbo compressor to the industrial plant and a more optimal temperature lift with increased COP. Mateu-Royo et al. [43] study the scroll compressor in depth by modification. Their conclusion was that a scroll compressor provided a significant improvement with regard to COP for a heat source temperature of 80 [°C] and heat sink temperature of 140 [°C], which is a high-temperature HP cycle. More research is also conducted on condensers by studying waste heat from gasses in HP cycles. The pressure of the condenser is likewise an extensively researched parameter that many research articles provide solutions to.

Python, a versatile programming language comparable to Matlab, is well-suited for equation-driven modeling and data plotting, as illustrated further down in this study. While Python lacks the component-based modeling capabilities of software like IDA-ICE and Modelica, it excels in calculating performance metrics such as *COP* and heating capacity. Ermel et al. [44], for instance, developed a Python-based framework for simulating an air-source HP under US conditions. Their model, which included thermodynamic states for all components and utilized an enthalpy marching solver procedure, demonstrated a deviation in *COP* values of just 1.43[%], with the maximum deviation for a single parameter being 10[%]. Moreover, Roskosch et al. [45] utilized Python to simulate variable capacity compressor cases, investigating the feasibility of refrigerant substitution without substantial redesigning of the system. Their findings highlighted the need for complex compressor modeling to generate useful results for potential replacement models. Python's utility extends to modeling both Variable Capacity Compressors and Organic Rankine Cycles, as demonstrated by Kamesh Koshti [46]. They showed that refrigerants R245fa and R404 were the most efficient choices for both systems, with Python being an effective tool for simulating and comparing their performances.[47] Further uses of Python in this field include simulation of novel ejector systems on air-source HPs for sustainability-focused studies [48], and educational applications. Aulicino Bakrania [49], for example, found Python to be an effective teaching aid for thermodynamics and cycle processes, even for students with no prior programming experience. In the broader research landscape, Python is frequently employed for performance analysis, especially in terms of *COP* and efficiency, refrigerant behavior simulations, and defrosting scenarios [50] [51]. These diverse applications strengthen Python's versatility and value in energy and building engineering.

The publication dates of research articles about various software platforms indicate a surge in studies focusing on Python as a simulation tool within the last 3-4 years. Meanwhile, more established programs have a wealth of information collected over the past 15-25 years. This pattern suggests that while Python is gaining traction, but still has considerable room for research expansion. The existing Python-centric literature predominantly covers thermodynamic properties and basic HP cycles, with only a handful delving into the component-level analysis. Among these, the compressor emerges as the most extensively studied component using Python. However, there's a notable lack of Python-based research on HEs within the HP cycle, indicating a knowledge gap ready to be explored.

1.2 Objective

The objective of this study is to develop a code using the programming language, Python, that simulates the processes involved in a HP cycle. Users should be able to input temperature values for the evaporator, which will perform calculations and provide new parameters to the compressor. Similarly, users should provide desired temperature values for the condenser, which will calculate the available heat for the water, that reaches the accumulator tank or circulation pipe. The Python code will perform calculations based on these input temperatures and parameters provided to the desired heat exchanger (HE), focusing exclusively on liquid-to-liquid HE in the thesis, but by simple modification, it is possible to calculate the values of an air-to-water HE.

User-friendliness and simplicity are crucial aspects of the code to make it accessible to more than just industry experts, such as student groups or engineers in other fields. With the necessary thermodynamics, fluid mechanics, and component inputs, the code should produce accurate outputs, including *COP*, *heat load* (\dot{Q}_c), *pump power*, *efficiency*, *mass flow rate*, and other relevant parameters. Validating the code is a priority to ensure its precision. A survey involving a focus group of individuals with expertise in the building industry, known to the author or supervisor, is conducted. The goal of this survey is to analyze their interpretation of the code and gather valuable feedback for further refinement and improvement. Desired objectives are:

- Extending a Python code previously made by OsloMet.
- Develop user-friendly code to function in both Spyder and Visual Studio Code.
- Conduct interviews with experts from the building industry (COWI and Multiconsult).
- Validation of the code against the suitable program.
- Analyze the *Vapor Compression Cycle* with regard to converged \dot{Q}_c .
- Calculate typical values for heat exchangers as stated: \dot{Q}_c , *COP*, *pump power*, and *efficiency* after convergence criteria are met, and then compare different types of heat exchangers.
- Make the code available online with a web page.

1.3 Limitations

The Python code will have some limitations because of a time limit. The main limitations to the code/thesis are as follows:

- 1 Liquid-to-air HE not available.
- 2 Water calculations outside the HE are not performed, only calculations for fluid inside the HE. Therefore, boreholes and pipes out of the condenser are not taken into account.
- 3 The cost of different heat exchangers is not included in the calculations because of the time limit. Life cycle costs are not researched.
- 5 Schematics only drawn inside the system boundaries.
- 6 System boundary with schematics from: Brine pump → **Heat Pump** → Water pump closest to HP.

2 Theory

Foundational theories that are essential for comprehending the computational modeling performed in Python. The section 2 should provide knowledge regarding sections described in the thesis that are difficult to understand.

2.1 Thermodynamics

Thermodynamics at broad specter can be defined as the *science of energy* and at its core, deals with the transfer of energy between systems and their surroundings. Energy itself is a very vast expression or term, but the core definition is described as the capability to cause change. [52] Thermodynamics is a fundamental field to study for engineers with applications in various fields such as power generation and refrigeration, but also as this thesis especially analyzes how a HP can be implemented with different HE to solve the heating load of buildings by transfer of heat between reservoirs using different mediums or fluids. For heat transfer, the two principles that have a foundation from laws of nature are the first- and second laws of thermodynamics. The first law of thermodynamics adheres to the principle of energy conservation, stating that in any interaction, energy cannot be created or annihilated, but merely transformed from one type to another while maintaining the total energy constant. The second law of thermodynamics describes the quality and quantity of energy, utilizing the concept of entropy. This results in energy always going from high quality to low quality in the respective system, and entropy is a measurement of the disorder of energy in the system.[52] These laws are critical in understanding the behavior of thermal systems and are essential when designing and optimizing thermodynamic processes and therefore HPs. Exploring the application of thermodynamics to building engineering, focusing on the first and second laws and their implications in designing efficient and sustainable building systems.

The energy balance is fundamental to thermodynamics, with the energy entering and exiting the system serving as its primary components. The energy flow in and out of a system can be calculated by equation 1, which is applicable to any process. Changes in internal energy, kinetic- and potential energy, are taken into account when performing the equation further.[52]

$$E_{in} - E_{out} = \Delta E_{system} \quad (1)$$

For time-dependent energy balance, it's written as *rate form*. This includes dividing the system changes on time. Equation 2 applies when the energy transferred by heat, work, and mass happens over a time period.[52]

$$\dot{E}_{in} - \dot{E}_{out} = \frac{dE_{system}}{dt} \quad (2)$$

Another commonly used approach to express the energy balance is per unit mass. Equation 3 is derived by dividing equation 1 by the mass of the system.[52]

$$e_{in} - e_{out} = \Delta e_{system} \quad (3)$$

2.1.1 Enthalpy

In thermodynamics, enthalpy can be viewed as a measurement of the energy present in place of a particular system. It gives an estimate of the amount of internal energy, most likely heat necessary to cause a system to

change, along with any energy acquired or lost during the process. The general equation for enthalpy is shown in equation 4, where u is the total internal energy, P is the system pressure, and V is the volume. [52] [53]

$$H = u + P * V \quad [kJ/kg] \quad (4)$$

If the process in a system is reversible and isobaric, the equation for heat alternated with surroundings is given with 5. But both conditions must be applied.

$$\Delta H = \bar{Q} \quad [kJ/kg] \quad (5)$$

2.1.2 Entropy

Entropy was mentioned above regarding the second law of thermodynamics and how it measures the internal molecule disorder, but now a deeper explanation. Entropy is something individuals can find hard to visualize or imagine because of its abstract magnitudes. Per definition, entropy can be defined as a system's internal energy divided by the countable temperature, that cannot be used or beneficial for productive work. The concept of entropy offers a method for encoding mathematically the intuitive understanding of which procedures are impractical, but not against the basic principle of energy conservation. With $S [kJ/K]$ representing entropy, $Q [kJ]$ describing the amount of heat, and $T [K]$ the temperature, equation 6 illustrates a simple way of showing the basic form of entropy. [54] [52]

$$\Delta S = \frac{Q}{T} \quad [J/K] \quad (6)$$

2.1.3 Exergy

Exergy correlates to the quality level and usefulness of energy. The definition is maximum shaft work that possibly can be performed by the compound of the given system and referenced to the environment. Exergy, therefore, provides information on available work when thermodynamic equilibrium with surrounding nature. Analyses of exergy present that all processes in the system and surrounding environment require to be reversible. At the exact moment where irreversible processes occur, exergy is destroyed. That is why performing an analysis of refrigeration facilities and power station takes into account the exergy destruction. Exergy destruction provides us with an amount of useful energy loss or wasted work/potential. Like energy, exergy also has the possibility to be transformed or transferred between the system boundary. Exergy transfer can occur with heat, work, and mass, but as this thesis focus on the HP cycle, the energy transfer associated with heat transfer and work is the most interesting. Equation 9 shows exergy transferred by heat in the case of a low-temperature medium. Figure 1 illustrates an example schematic of total efficient exergy available in a green box and how the wasted- and destroyed could be distributed. [52] [55]

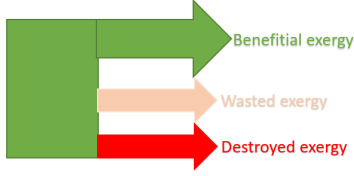


Figure 1: Imaginary exergy distribution shown.[55]

$$\dot{X}_{dest,4-1} = T_0 * \dot{S}_{gen,4-1} \quad [W] \quad (7)$$

$$\dot{X}_{dest,4-1} = T_0(\dot{m} * (s_1 - s_4) * \frac{\dot{Q}_L}{T_L}) \quad [W] \quad (8)$$

$$\dot{X}_{\dot{Q}_L} = \dot{Q}_L * \frac{T_0 - T_L}{T_L} \quad [W] \quad (9)$$

2.2 Heat transfer

Heat can be transferred between materials differently, but the three most common forms are convection, conduction, and radiation. These are the fundamentals for heat transfer aspects and are separated by what thermal applications are suitable for the desired demand. For both convection and conduction, thermal conductivity $[k]$ significantly influences the heat transfer process and can be characterized as a key factor.

2.2.1 Convection

Convection is the process where heat or mass is transferred by the bulk movement happening to the molecules of the fluid, most familiarly water and air. In most cases, convection appears when either advection or diffusion or in some cases both occurs. Convective heat transfer can be written as equation 10.[56]

$$Q_{conv} = h * A_s * (T_s - T_\infty) \quad [W] \quad (10)$$

The Reynolds number (Re) calculations can generally be conducted using two established methods, as demonstrated in equation ???. Given its specificity to various scenarios such as laminar, turbulent, or partially developed flows, a multitude of Re equations have been utilized. A selection of these is outlined in section 3.6.

$$Re = \frac{\rho * V * D}{\mu} = \frac{4 * \dot{m}}{\rho * \mu * d} \quad [-] \quad (11)$$

The Nusselt number (Nu) can be determined via various correlations involving Re and Pr . When these correlations are employed, the resultant equations depend on the type of flow, laminar or turbulent, which influences the applicability of different equations. A prevalent method for calculating the Nu is shown in equation 12.

$$Nu = \frac{h * L}{k} \quad [-] \quad (12)$$

The Prandtl number (Pr) can be calculated by using dynamic viscosity μ $[Ns/m^2]$, the thermal conductivity k $[W/mK]$, and the specific heat transfer coefficient (C_p) $[kJ/kgK]$.

$$Pr = \frac{\mu * C_p}{k} \quad [-] \quad (13)$$

2.2.2 Conduction

Conduction is the process of energy transferring from more energetic particles to their less energetic counterparts through inter-particle interactions. This phenomenon can transpire within gases, liquids, and solids.

In the HP cycle, conduction predominantly occurs when heat migrates from high-energy particles inside a pipe to lower-energy particles outside it. The conduction rate depends on the material's thermal conductivity, sectional area, temperature gradient, and the distance over which heat is conducted. These parameters are shown in the following equation 14. [56]

$$\dot{Q}_{cond} = k * A_s * \frac{T_1 - T_2}{\Delta x} = -k * A * \frac{\Delta T}{\Delta x} \quad [W] \quad (14)$$

2.3 Heat pump

HPs are assemblies of devices that typically employ electricity to leverage low-exergy energy sources, transforming them into high-exergy energy for applications such as heating buildings. While some countries may utilize gas or diesel to operate the compressor, regulations in Norway favor electricity. Various low-value energy sources can be used, including seawater, groundwater, outside air, and soil. The objective of an HP is to provide heat in a manner that maximizes energy extraction from these low-energy sources or reservoirs, supplementing it with the provided electricity. Figure 2 showcases a schematic of a heat pump, designed in AutoCAD for clarity and relevance to the calculations in this thesis. The dotted lines above and below the compressor and expansion valve denote the high- and low-pressure sides. Figure 3 and 4 illustrate the condenser and evaporator side respectively, of the HP. The four main components of a heat pump, along with their descriptions, are described in section 2.3.1 - 2.3.4. [57]

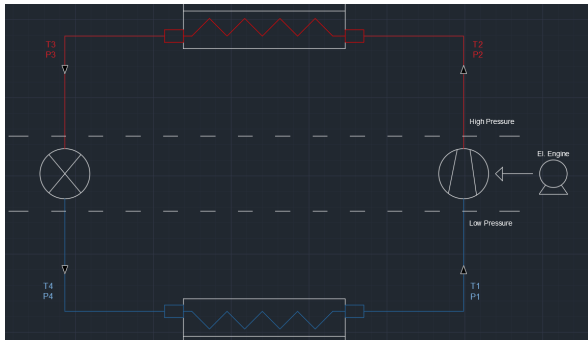


Figure 2: Main HP cycle from AutoCAD.

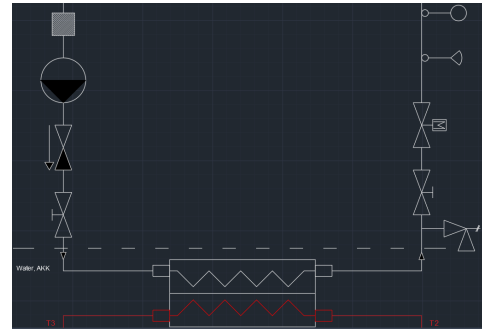


Figure 3: Condenser side from AutoCAD.

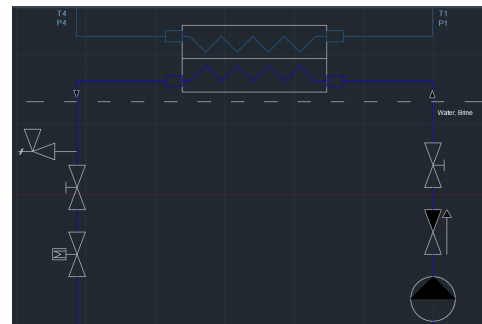


Figure 4: Evaporator side from AutoCAD.

2.3.1 Evaporator

The evaporator, equipped with a HE, plays a crucial role in the HP cycle. Upon its arrival from the expansion valve, the fluid should be in the form of a combination of saturated vapor and saturated liquid. The level of mixture, often described as X depends on the level of sub-cooling and the pressure reduction facilitated by the expansion valve. For the fluid to properly progress through the cycle, it needs to be in a saturated vapor state as it exits the evaporator because of the compressor. As illustrated in Figure 4, the evaporator capitalizes on the ambient heat from the designated reservoir to warm the fluid, typically between 2 to 6 degrees in Norway.[57] Equation 15 calculating relevant parameters from the evaporator.

$$\begin{aligned}\dot{E}_{in} - \dot{E}_{out} &= \frac{dE_{system}}{dt} \\ \dot{E}_{in} - \dot{E}_{out} &= 0 \\ \dot{m}_4 * h_4 + \dot{Q}_L - \dot{m}_1 * h_1 &= 0 \\ \dot{m}_1 * h_1 - \dot{m}_4 * h_4 &= \dot{Q}_L \\ \dot{Q}_L &= \dot{m}_R * (h_1 - h_4) \quad [W]\end{aligned}\tag{15}$$

2.3.2 Compressor

As the refrigerant transitions from the evaporator to the compressor, an engine usually powers the compressor to compress the saturated vapor. This compression process escalates the refrigerant's pressure, thereby raising its temperature. Various types of compressors, including scroll, piston, turbo, and screw compressors, are commonly employed in such systems. The temperature of the refrigerant post-compression is dictated by its thermodynamic properties and the prevalent conditions of pressure and temperature. Cooling assistance to the compressor is typically delivered through air or water mediums. The work done by the compressor to elevate the pressure from the system's low-pressure side to the high-pressure side, commonly referred to as states 1 and 2 in a standard VCC, can be calculated using the following equation. [52]

$$\dot{W}_{work} = \dot{m}_R * (h_2 - h_1) \quad [W]\tag{16}$$

Isentropic efficiency describes an ideal process that is adiabatic, meaning no heat is lost, and reversible. If a process is isentropic the entropy does not change, resulting in entropy before the compressor being equal to the entropy after the compressor. Isentropic efficiency is written with enthalpy differences in equation 17.

$$n_C = \frac{h_{2,s} - h_1}{h_{2,a} - h_1} \quad [-]\tag{17}$$

Volumetric efficiency (λ) is volumetric loss from the compressor. Real imbibed volume (V_{ins}) and compressed stroke volume (V_s) are deciding parameters for calculating λ . Equation 18 shows the relation between the parameters. [13]

$$\lambda = \left(\frac{V_{ins}}{V_s} \right) * 100 \quad [\%]\tag{18}$$

The clamping efficiency of the compressor can be defined as equation 19. This does indeed depend on what type of compressor the HP utilizes. A compressor without a belt to 'transfer' the rotation will not have a transmission loss, or it would be 1.0 [-]. [13]

$$n_{kl} = n_{el} * n_{tr} * n_c \quad [-]\tag{19}$$

2.3.3 Condenser

Upon achieving its peak pressure within the cycle, the refrigerant travels from the compressor to the condenser. In most cases, a HE facilitates the heat transfer, typically via a phase change, to another fluid, this applies particularly to liquid-to-liquid type HEs. Or a HE to supply heat for a new HP cycle. When employing an HP for building heating, the condenser plays a crucial role in carrying out this heat transfer directly. Once the refrigerant releases its heat, cools down, and undergoes complete condensation, it proceeds to the expansion valve. The energy balance for the condenser is encapsulated in equation 2, while equation 23 presents the final stage of the energy balance for \dot{Q}_H , assuming this is the parameter of interest.

$$\begin{aligned}
 \dot{E}_{in} - \dot{E}_{out} &= \frac{dE_{system}}{dt} \\
 \dot{E}_{in} - \dot{E}_{out} &= 0 \\
 \dot{m}_2 * h_2 - \dot{m}_3 * h_3 - \dot{Q}_H &= 0 \\
 \dot{m}_2 * h_2 - \dot{m}_3 * h_3 &= \dot{Q}_H \\
 \dot{Q}_H &= \dot{m}_R * (h_2 - h_3) \quad [W]
 \end{aligned} \tag{20}$$

The equation for unit-mass basis is 21.[52]

$$q_H = h_2 - h_3 \quad [kJ/kg] \tag{21}$$

For condenser, the equation can also be written as 22

$$\Delta h_{cond} = \Delta h_{comp} + \Delta h_{evap} \quad [kJ/kg] \tag{22}$$

The connection between heat output in $[W]$ from high and low can be analyzed with the following relation described with equation 23

$$\dot{Q}_H = \dot{Q}_L + \dot{W}_{in} \quad [W] \tag{23}$$

2.3.4 Expansion valve

The main task for expansion valves is lowering the pressure of the fluid from the condenser, which equals a reduction in temperature. With temperature reduction of the fluid, it arrives in saturated liquid or in a saturated liquid-vapor mixture.

2.4 Coefficient of performance

The coefficient of performance (COP) is a measurement of how much heat the system provides as output from the work the system requires. If a system has a compressor that requires 1 000 $[W]$ as work input and has a COP of 4.0 $[-]$, that results of heat output is equivalent to 4 000 $[W]$ from \dot{Q}_H . General equations that can be applied for different COP are shown below. Equation 24 illustrates COP for HP.[52]

$$COP_{HP} = \frac{\dot{Q}_H}{\dot{W}_{net,in}} \quad [-] \tag{24}$$

Equation 25 describes COP for HP following the Carnot cycle. [52]

$$COP_{HP,Carnot} = \frac{1}{1 - \frac{T_L}{T_H}} \quad [-] \tag{25}$$

Equation 26 illustrating the more thermodynamic method to analyze COP for HP.[52]

$$COP_{HP} = \frac{q_H}{w_{net,in}} = \frac{h_2 - h_3}{h_2 - h_1} \quad [-] \quad (26)$$

This thesis performs a COP_{real} value to describe COP regarding the pump work of water flowing through the HE in the condenser and the pump power of brine water flowing through the HE in the evaporator. Equation 27 illustrates the COP_{real} .

$$COP_{real} = \frac{\dot{Q}_H}{\dot{W}_{net,in} + \dot{W}_{pump,w} + \dot{W}_{pump,b}} \quad [-] \quad (27)$$

2.5 Ground source heat pump

As referred to in 2.3, there are numerous ways to harness ambient heat, but this thesis focuses on a code designed specifically for ground source HP. While other methods can be adapted with minor modifications, the thesis describes this particular approach. Ground source HP utilizes boreholes in the ground to store and extract heat from the environment, subsequently supplying this heat to the evaporator. The depth of these boreholes can range anywhere between 80 and 300 meters, but there are several considerations to bear in mind. Shorter pipes, 50 [m] or less, result in reduced pressure loss, but their heat extraction capacity is limited. Conversely, longer pipes, 200 [m] or more, may face challenges with the frost-secure fluid, glycol most widely used, losing heat on its return journey, not to mention the substantial cost associated with drilling deep boreholes. Figure 5 illustrates the boreholes. [58]

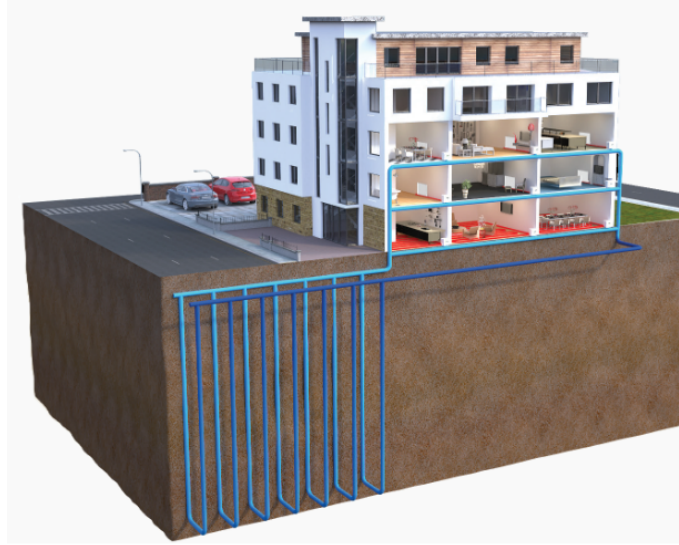


Figure 5: Ground source HP illustration.[1]

2.6 Vapor compression cycle

The VCC is a form of method to circulate a medium or a chosen working fluid to distribute heat from a cold reservoir to a hot reservoir, most widely used for buildings and automobiles. The compressor compresses the refrigerant with work input, which lifts the pressure as seen in Figure 6 The advantage is that heat output Q_{out} is higher than the input of energy or work W_{in} . One of the equations for power required for the VCC is the mass flow rate multiplied by the enthalpy changes.[13]

$$P_o = \dot{m}_R * \Delta h \quad [kW] \quad (28)$$

In the system, the equation is as follows.[52]

$$P_o = \dot{m}_R * C_p * \Delta T \quad [kW] \quad (29)$$

To illustrate the impact of choosing for example sub-cooling or super-heating for a VCC cycle, Figure 6 - 9 from CoolTools is displayed. Figure 6 has sub-cooling, but no super-heating. That means points four and five on the cycle are outside the outer black line resulting in a 100 [%] liquid state. The pair of external black lines delineate a region signifying a mixture of liquid and saturated vapor states, explained in section 2.3.1. In Figure 7, super-heating is exhibited, but no sub-cooling, implying that points one, seven, and eight represent 100 [%] saturated vapor, and thus are outside the external black boundary. Both super-heating and sub-cooling are evident in Figure 8, where points four and five, along with points seven, eight, and one, are situated beyond the black line. Conversely, Figure 9 withholds from incorporating any super-heating or sub-cooling, as all points are aligned along the black demarcations.

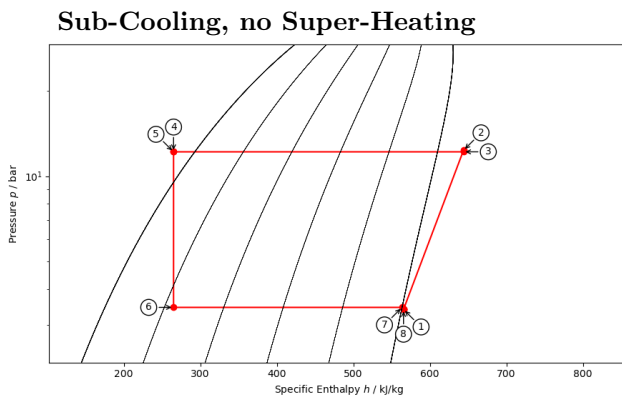


Figure 6: VCC of sub-cooling.

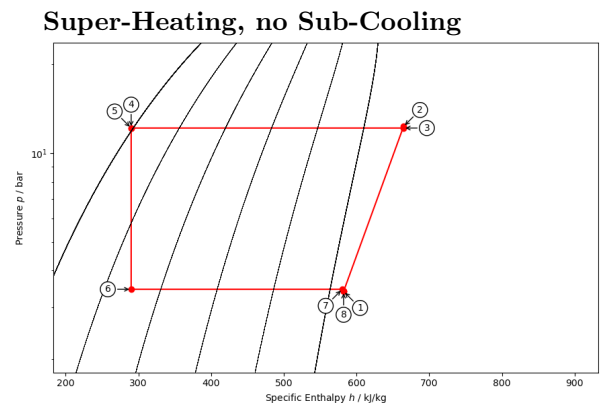


Figure 7: VCC of super-heating.

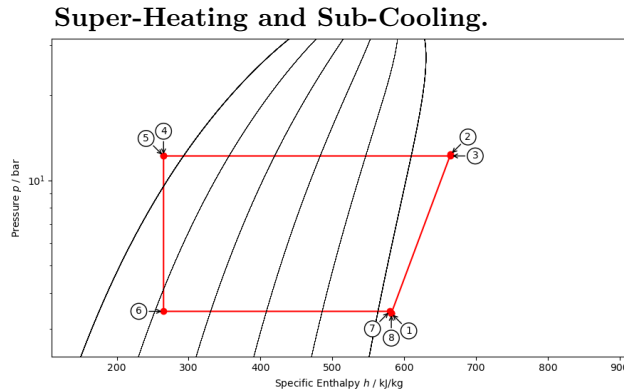


Figure 8: Both sub-cooling and super-heating.

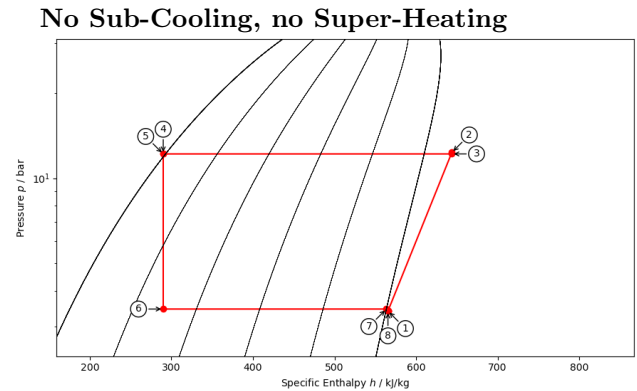


Figure 9: No sub-cooling or super-heating.

2.7 Heat Exchangers

HE is a device that facilitates heat transfer via conduction, typically occurring as a fluid moves through a pipe and heat is conducted through the pipe wall. HEs have a wide array of applications, spanning from power plants to building heating and air conditioning systems, among others. Within the building industry, there are primarily two methods for harnessing the heat generated. The first method involves a fan that directs air over the tubes, producing hot air for the surrounding environment, this is referred to as a liquid-to-air exchanger. The second method, known as a liquid-to-liquid exchanger, employs two sets of pipes where one heats the other. The Log Mean Temperature Difference (LMTD) plays a crucial role in heat exchanger operations as it quantifies the multiplication of temperatures relative to the flow pattern. Common flow patterns include counter-flow (or countercurrent) and parallel flow (or concurrent). Another important factor is the correction factor (F). The Effectiveness-NTU method is frequently used to gauge the performance of heat exchangers. Factors such as mass flow rate and C_p are significant in these calculations. Three prevalent types of heat exchangers include the Double Pipe (DP), Shell and Tube (ST), and Plate Exchanger (PE).

2.7.1 Shell and tube HE

An ST HE is essentially a large cylindrical tank filled with numerous small tubes, often serving the hot fluid. A different fluid or medium travels through the shell, absorbing heat from these small tubes. ST is a particularly preferred type of HE, owing to its inherent versatility and adaptable design methodologies, which accommodate a broad range of pressures and temperatures. This component is also notably simple to maintain and repair, making it cost-effective when dealing with potential malfunctions. Figure 10 shows the shell, the tube bundle, and the support structure. Figure 11, on the other hand, provides a basic schematic of the ST interior and illustrates the concepts of counter-flow and parallel flow, both made in AutoCAD.[59]

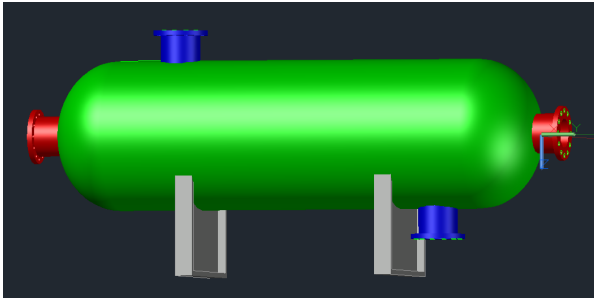


Figure 10: 3D illustration of ST HE.

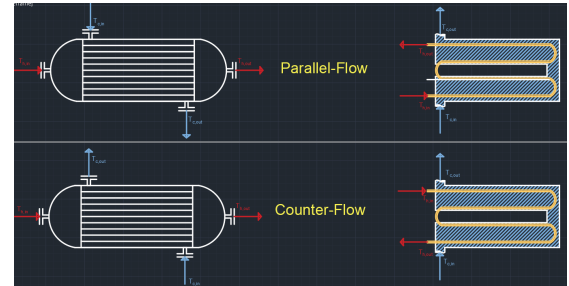


Figure 11: Simple schematic of an ST with two flow patterns.

2.7.2 Double pipe HE

Essentially, a DP HE shares the same principle as an ST HE, but instead of multiple small tubes, the DP employs one larger pipe encompassing a smaller one, thus forming a shell. Generally, the hot fluid circulates within the inner pipe, transferring heat to a colder fluid flowing within the shell, referred to as the annulus. These fluids are kept separate by the outside of the inner pipe. Factors such as the size and length of the pipe, as well as the number of bends, are deciding factors since they influence parameters such as pressure loss and temperatures. The DP HE, known for its simplicity and fundamental configuration, is illustrated in Figure 12.[60] A simplified schematic representation of the DP showing parallel flow and counter-flow, created in AutoCAD, can be seen in Figure 13.[61]



Figure 12: Illustration of DP HE.[60]

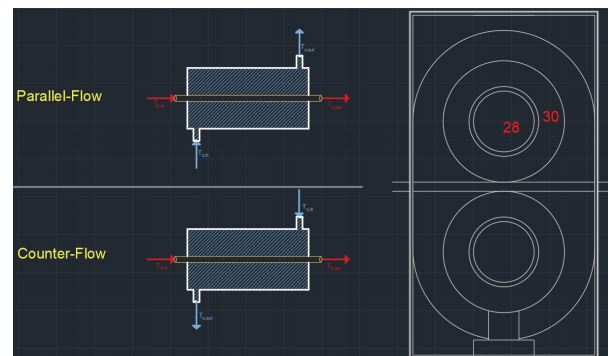


Figure 13: Simple schematic of a DP with two flow patterns.

2.7.3 Gasketed plate exchanger

PE is a device using thin plates and small openings between them to transfer heat from one fluid to another in different pipes by conduction. The space between each thin plate is small and therefore the PE is a very compact component and does not require a large space. There are different types of PE such as gasketed, brazed, and welded, but this thesis mostly refers to gasketed. PE has two bigger front and back plates where the pipes are mounted to help keep the heat in the component, illustrated in Figure 14. A simple schematic of the parallel flow and counter. The flow pattern is illustrated in Figure 15 [62] [63]

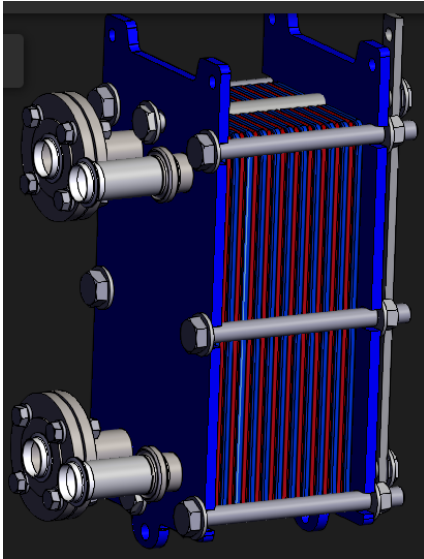


Figure 14: 3D model of DP HE.[63]

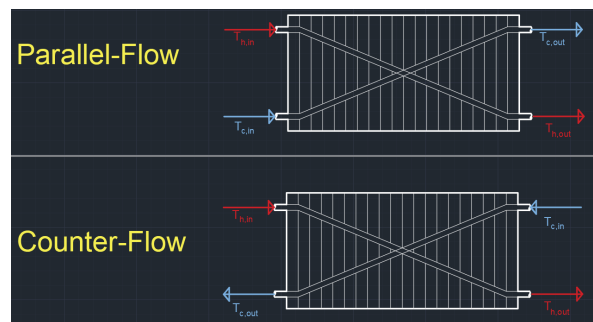


Figure 15: Simple schematic of a PE with two flow patterns.

2.8 Refrigerants

In thermodynamics, a refrigerant describes a working fluid for a given VCC where the fluid goes from evaporation to condensation in the refrigerant system. Working fluids used for the VCC are the main reason for the possibility to transfer heat from a low-temperature environment to a high-temperature environment. The fluid changes from gas to a liquid, or more correctly, saturated vapor to liquid to vapor again, which is the process where the fluid absorbs heat from the low-temperature and releases heat in the high-temperature environment. For the last 10-20 years manufacturers and producers have been working constantly to analyze and test more environmentally friendly fluids because the most polluting ones such as R134a, for example, are being phased out and will soon not be legal.

Refrigerants available naturally in the atmosphere or general surroundings are often referred to as *natural refrigerants*. Some examples are carbon dioxide, ammonia, propane, and sulfur dioxide. Not all natural refrigerants are called synthetic fluids and many synthetic fluids are produced with methane and ethane as a foundation. Some groups of refrigerants are Hydrogen Carbon (HK), Klor Fluoride Karbon (KFK), Hydrogen Klor Fluoride Karbon (HKFK), and Hydrogen Fluoride Karbon (HFK). Rxyz is the name method, where R is "Refrigerant", x is the number of carbon atoms subtracted with 1, y number of hydrogen atoms added

with 1, and z number of fluorine atoms. Two of the factors often used to categorize refrigerants are Ozone Depleting Potential (ODP) and Global Warming Potential (GWP). This gives a pretty good indication of how environmentally friendly a refrigerant is or how damaging it is.[13] [64] [65][66]

Table 1: Refrigerants available.[64][66][65]

Description	Refrigerant [–]	GWP [–]	ODP [–]	Molecular weight (<i>g/mol</i>)	T_{crit} °C
Propylene	R1270	2	0	42.08	301,9
Water	R718	0	0	18	373.9
Ammonia	R717	0	0	17	132.5
Carbon dioxide	R744	1	0	44	31
Pentane	R601	6	0	72.2	196.6
Butane	R600	20	0	58.1	152.0
Propane	R290	3	0	44.10	96.98
Tetrafluoroethane	R134a	1 430	0	102	101.1
Freon	R22	1 700	0	86	96.2

2.9 Python

Python is a programming language that presents almost endless possibilities with everything from making an app, website, scientific computing, artificial intelligence, and various data analyses, just to name a few applications Python is recognized for. Python’s strength lies in its readability and simplified coding, with clean syntax. As an open-source language, Python allows for unrestricted distribution and complimentary access to its source code. GitHub is also used to easily share codes between users. It can be swiftly installed on a computer within a matter of minutes, and the necessary packages for code writing are freely available and easily installed. This gives Python a significant edge in terms of cost-effectiveness. Unlike software such as Matlab, which requires a paid license, Python is available free of charge.[67]

3 Method

The methodology and path to creating the code in Python to produce the best possible results and a wide array of parameters. This section gives a detailed description of how equations regarding HEs and VCC are incorporated with Python to give output in the form of readable results, that engineers with or without expertise or high knowledge in the programming language Python can read/use.

3.1 Initial script

OsloMet had previously made a code, code also known as *script*, about the VCC and HP cycle in Python. [68] The calculations presented by the script dealt with the four components: compressor, condenser, expansion valve, and evaporator. The code editor chosen was Spyder, this open-source environment is written in Python. Therefore, Spyder was utilized in this master's thesis to develop the script further with added calculations especially surrounding HEs, with the high-pressure side of HP cycles in focus, but also take into account some calculations on the low-pressure side. Three scripts were initially handed over by the supervisor and this would represent the starting point of developing a final product of scripts calculating the desired equations to answer the objective. The main script had the equations and written packages, the second was a P-h script and the third was a T-s script. The initial three scripts are displayed in Appendix A.1, A.2, and A.3. Even though the code was written in Spyder as stated, the objective of this thesis is to make it as user-friendly as possible. Therefore, throughout the development of the code, there will be a goal to make it function in Visual Studio Code as well, for extra user-friendliness because this is a widely used programming language in Python. If one searches on youtube for help or how to execute a task or something with regard to Python, it's clear that Visual Studio Code will be seen as the programming environment preferred by the vast majority and taught.

3.2 Set-up and learning programming

The first step was analyzing the initial scripts provided by the supervisor and getting familiar with how equations in Python worked. Most of the time at the start went to changing something and examining differences in output to get a better understanding of the previous work in Python. The first time running all three scripts a couple of bugs were detected and some minor adjustments were necessary. The reason for bugs and error messages could have been updated versions in Python or changes in the packages used for the given script. After this was corrected and everything worked as it should, the work of expanding the code could begin.

Prior to implementing substantial modifications, a thorough examination of the various packages employed in the script and available on the internet was researched to identify those best suited to enhance its capabilities. Both PropsSI and Pyromath demonstrated their specialization in VCC and HP, owing to the more extensive information available on PropsSI, it was deemed the preferable choice for advancing the script's development. A comparison of the respective web pages for each package underscores the disparity in terms of accessible information. Since a talking point at the start of the thesis was the prospect of making a web page or an app, HyperText Markup Language (HTML) was utilized to learn and gather experience. HTML is a programming code, or set-up to make a browser/web page, and is commonly used by programmers around the world when creating web pages for all kinds of customers. Templates were downloaded to examine if this could be used in the thesis.

3.3 Assumptions

Thermodynamics is a complex field of study, and as a result, certain aspects may be simplified. Table 2 lists the assumptions made, along with a description of each, for the Python script created. These assumptions are introduced to simplify certain stages, allowing for the incorporation of additional calculations. Water is considered incompressible for the calculations, resulting in a consistent pressure of 101,325 [Pa] whenever it is used in equations. When evaluating the Re, Prandtl number, and Nu, it is important to note that the refrigerant undergoes a phase change from saturated vapor to liquid. The assumption that ST, DP, and PE are the most commonly used heat exchangers is based on literature reviews and discussions with professionals in the building industry. The compressor heat loss factor could have been analyzed more thoroughly, same goes for Q_{loss} . Outer walls for HEs are deemed to have minimal heat loss.

Table 2: Assumptions made to the script

Number	Assumption	Description
1	System operates at steady state	Kinetic and potential energy neglectable
2	Density water	Always at P = 101 325 [Pa]
3	Phase change	Percentage of liquid and vapor mixture not calculated
5	Closing valve and safety valve	Not taken into account for pressure loss
6	PE, DP and ST most used	On general basis
7	Heat load loss	Q_{loss} from compressor to condenser not calculated
8	Components to be well insulated.	Outer walls minimal heat loss

3.4 Starting foundation

The scripts mentioned in 3.1 serve as the foundation for the further development of the main script. Additional equations tailored to each HE will be incorporated, and the calculations will be executed. The script is responsible for generating P-h and T-s diagrams and will be updated to accommodate the new main script and ensure proper functionality, at least until new updates. An additional script will be developed to manage iterative calculations, where convergence between various set parameters should yield results for the chosen case. The objective is to execute three different cases with varying water temperatures entering and leaving the HE, enabling comparisons between them. As highlighted in the 1.1, key parameters for comparison include COP , Q_c , pump power, and efficiency. Other parameters yielding interesting results and additional insights will also be compared. As Table 3 shows the three HEs from 2.7 are utilized. The challenging aspect is in calculating and executing the three primary cases: *Case 1*, *Case 2*, and *Case 3*. Inspiration is gathered from parameters such as evaporator temperature used in [34], written about in the literature review.

Table 3: Parameters and values to each case

Number	$T_{w,in}[^{\circ}C]$	$T_{w,out}[^{\circ}C]$	Type HE	Refrigerants
Case 1	20	30	ST, DP, and PE	R1270, R717, and R290
Case 2	30	45	ST, DP, and PE	R1270, R717, and R290
Case 3	40	60	ST, DP, and PE	R1270, R717, and R290

3.4.1 Refrigerants

The refrigerants selected for validation in this study are derived from table 1, all listed in Table 4, encompassing those with the greatest current and future relevance in the HP industry. Tetrafluoroethane, R134a, is presently undergoing a phase-out in Norway because of high GWP values, however, due to its extensive use over the past decades, an abundant amount of testing data is available. [25] This wealth of information, particularly from academic syllabi, justifies the inclusion of R134a as a refrigerant in the validation process of this master's thesis. Ammonia (R717) and water (R718) was chosen to include because of their increased service over the past years. R290 is also a natural refrigerant and therefore included in the results. With low GWP and ODP, the refrigerants R601 and R600 will be tested and made sure that work if the user gives input values in accordance with critical temperatures and pressure. The field of the application describes what purpose the refrigerants have for the thesis.[66]

Table 4: Refrigerants and measurements.[64][66][65]

Field of application	Refrigerant	GWP	ODP	Fire class
VAL, SCR	R134a	1300	0	A1
VAL, RES, SCR	R717	0	0	B2L
RES, SCR	R1270	2	0	A3
RES, SCR	R290	3	0	A3
SCR	R744	1	0	A1
SCR	R718	0	0	A1
SCR	R600	20	0	A3
SCR	R601	6	0	A3
* VAL	=	Validation		
* RES	=	Results		
* SCR	=	Script		

3.5 Heat exchangers

First and foremost the types of HE were examined to get an understanding of the availability and different types of HE suitable for the task. Therefore, the building industry, primarily in Norway, showed elements written and some information gathered suggesting that PE was preferred on projects by engineers. [Jørn Stene, Ole Døsvik, Section 3.8] Since the PE seemed to be the type with the most acquaintance by engineers, it was essential to include the type as a choice when running the script. The information gathered from articles regarding DP gave information that high heating demands and temperatures were cases suitable for DP. ST seemed a preferable choice in the USA, but also widely known in Europe.[59]

3.5.1 Shell and tube

The ST HEs require certain input values to be set prior to performing calculations. When the area is not provided, parameters such as the inner and outer diameter are necessary to obtain a more accurate area and values for flow calculations. Table 5 illustrates the parameters that are essential for the script to perform calculations. The parameters listed in Table 5 were selected based on research from scientific articles and product descriptions from manufacturers. These values were considered standard and realistic for the manufacturer. Values in Table 5 also function as inputs if the user does not have any other preferences and wants to run the script by just changing U_{ST} for example.[69] [70]

Table 5: Initial input values for shell and tube HE

Explanation	Parameter	Value	Unit
Clearance	D_{cl}	0.080	[m]
Tube outer diameter	d_o	0.020	[m]
Tube Inner diameter	d_i	0.016	[m]
Length tube	L_t	4	[m]
Type of tube arrangement	<i>Triangular</i> (30)	$1.25 * d_o$	[m]
Number of tube passes	N_p	2	[-]
Number of tubes	N_t	185	[-]
Baffle spacing	B_s	0.133	[m]
Number of baffles	N_{ba}	6	[-]
Thermal conductivity wall	k_w	45	[m]
Overall heat transfer coefficient	U_{ST}	800	[W/m ² * K]
Initial correction factor	F_{ST}	1	[-]

To compute the tube pitch for a specified ST, equation 30 is employed 30. This has been included in table 5 to demonstrate its dependence on the chosen outer diameter for the HE. The tube pitch is influenced by the arrangement of the tubes, which can be mounted at angles of 30°, 45°, 60°, or 90°. In order to express the

tube pitch equation as 1.25 [-] multiplied by the outer diameter, the tube arrangement must be triangular, square, or rotated square, corresponding to angles of 30°, 90°, or 45°, respectively. [69] [71]

$$P_t = 1.25 * d_{oST} \quad [m] \quad (30)$$

To calculate the total heat transfer surface area offered by the tubes, equation 31 is employed. Upon examining this equation, it becomes apparent which parameters primarily influence the heat transfer surface area in a HE using the ST. Altering the number of tubes or increasing their length will result in an expanded heating surface area. Naturally, there are distinct limitations within every ST HE, sufficient space for each tube and adequate length, achievable through additional passes or an extended shell.[72]

$$Ah_{oa} = N_t * \pi * d_{oST} * L_t \quad [m^2] \quad (31)$$

In Table 6, the K and n coefficients are utilized to calculate the outside diameter of the baffle within the shell, as demonstrated in equation 33. These coefficients depend on the number of passes and the angle at which the tubes are installed. Both the square and rotated square configurations share the same coefficient values. While the difference between triangular and square arrangements is not substantial, it yields more accurate results. Figure 16 provides an explanation of flow patterns used in Table 6.[71]

Table 6: K1 and n1 values to Shell and Tube HE

Number of passes	Triangular pitch		Square and rotated square pitch	
	K1 [-]	n1 [-]	K1 [-]	n1 [-]
1	0.319	2.142	0.215	2.207
2	0.249	2.207	0.156	2.291
4	0.175	2.285	0.158	2.263

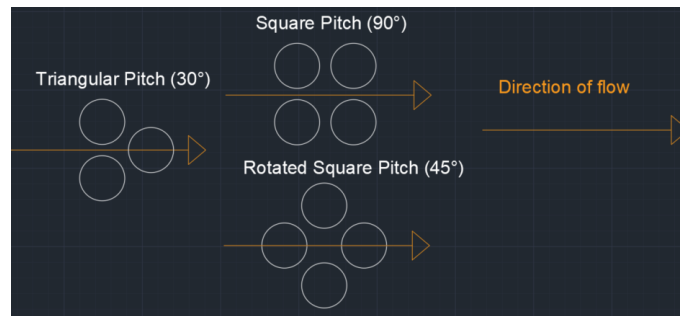


Figure 16: Caption

Then the outside diameter of the baffle is calculated by using the outside diameter of the pipe and relations between K and n coefficients. Equation 33 illustrates how the coefficients are used in the equation. [73] [71]

$$D_{o,b} = d_{o,ST} * \frac{N_t}{K1} \frac{1}{n1_{ST}} \quad [m] \quad (32)$$

The shell diameter can be determined by adding the baffle diameter and the clearance between the shell and baffle diameters, as illustrated in equation 33. Clearance values may vary among different manufacturers, which can affect the required shell diameter size. In situations with limited space, a lower clearance value would be advantageous; however, smaller clearances can lead to increased heat loss between the shell and the fluid.

$$D_{shell} = d_{o,b} * D_{cl} \quad [m^2] \quad (33)$$

The tube side flow area is added to the script to give the possibility of analyzing the available m^2 of flow area to the refrigerant or fluid. Equation 34 describes the parameters needed to perform the calculation. [71] [71]

$$a_t = \left(\frac{N_t}{N_p}\right) * \left(\frac{\pi}{4} * d_{i,ST}^2\right) \quad [m^2] \quad (34)$$

The correction factor can be computed to yield more accurate values for the correction factor. Initially, the correction factor is set to 1, as indicated in Table 5; however, a more precise correction factor is calculated using the updated fluid parameters and h_o and h_i , and then applied to a new U_{ST} . Tables are often enabled to determine the correction factor for various parameters with regard to ST. To calculate the correction factor in Python, using equations is more convenient than tablets. Consequently, these equations are essential 35, 36, 37, and 38.[69][74] [56]

$$R = \frac{T_{f,in,CO} - T_{f,out,CO}}{T_{w,out,CO} - T_{w,in,CO}} \quad [-] \quad (35)$$

$$P = \frac{T_{w,out,CO} - T_{w,in,CO}}{T_{f,in,CO} - T_{w,in,CO}} \quad [-] \quad (36)$$

$$Y = \frac{(1 - P * R)^{\frac{1}{N_p}}}{(1 - P)} \quad [-] \quad (37)$$

$$Z = \frac{(R^2 + 1)^{0.5}}{R - 1} \quad [-] \quad (38)$$

The updated correction factor for the HE can be computed using equation 39. In many books and articles, this is often presented as graphs; however, since extracting values from a graph is not feasible in Python, equation 39 must be employed instead.[74]

$$F_{new} = \frac{S * \log(W)}{\frac{(\log((1+W) - S + S*W))}{(1+W+S-S*W)}} \quad [-] \quad (39)$$

Pressure loss for the shell side of ST is calculated by equation 40. This pressure drop serves as an indicator of the extent of work required by the pump to "push" the water through the HE. Equation 41 is performed when calculating the pressure loss of the refrigerant, subsequent pressure loss must be handled by the pump.[73]

$$\Delta P_s = f_s * \left(\frac{\rho * v_s^2}{2}\right) * \left(\frac{L}{B}\right) * \left(\frac{D_s}{d_e}\right) \quad [Pa] \quad (40)$$

$$\Delta P_t = N_p * \left(\frac{f_t * L_t}{d_{i,st}} + 2.5\right) * \left(\frac{\rho * v_s^2}{2}\right) \quad [Pa] \quad (41)$$

The overall heat transfer coefficient for the ST HE, denoted as U_{st} , is computed using equation 42. While many publications represent this coefficient as U , it may be more appropriate to denote it as K or another symbol, given that in the field of building and energy, U typically signifies heat loss capability. However, in this

context, the focus is on heat transfer, which is the opposite concept [73]. Because it is widely generalized as U still, no change is added to the parameter for this, to not cause confusion. Another approach for calculating U_{st} is outlined in equation 43, wherein k_w is utilized.[70]

$$U_{ST,1} = \frac{1}{\frac{1}{h_s} + R_{f,s} + \frac{d_o}{d_i} * (R_{f,t} + \frac{1}{h_t})} \quad [W/m^2 * K] \quad (42)$$

$$U_{ST,2} = \frac{1}{\frac{1}{h_s} + R_{f,s} + \frac{d_o * \ln(d_o/d_i)}{2 * k_w} * (R_{f,t} * \frac{d_o}{d_i} + \frac{1}{h_t} * \frac{d_o}{d_i})} \quad [W/m^2 * K] \quad (43)$$

The equation for effectiveness is presented with 44. There are found other solutions such as from Sanaye et al. [72] but equation 44 was found to be the most reliable. [56]

$$\epsilon_{st} = N_p * (1 + c + \sqrt{1 + c^2} \frac{1 + \exp[-NTU * \sqrt{1 + c^2}]}{1 - \exp[-NTU * \sqrt{1 + c^2}]})^{-1} \quad [-] \quad (44)$$

Parameter c is found with the same method for all three HEs. First c_x is found by multiplying the mass flow rate by specific heat capacity, shown by equations 45. With these parameters known, the maximum and minimum values of the parameters can be found and used in equations 46.[56]

$$\begin{aligned} c_h &= \dot{m}_h * C_{p,h} \quad [kW/K] \\ c_c &= \dot{m}_c * C_{p,c} \quad [kW/K] \end{aligned} \quad (45)$$

$$\begin{aligned} c_{min} &= \min(c_h, c_c) \quad [kW/K] \\ c_{max} &= \max(c_h, c_c) \quad [kW/K] \\ c &= \frac{c_{min}}{c_{max}} \quad [-] \end{aligned} \quad (46)$$

3.5.2 Double pipe

The essential input values for a DP HE, which are required to execute the script, are shown in Table 7. Compared to ST and plate HE, DP HEs are more simplified, requiring fewer inputs to perform calculations. The provided values for DP represent standardized values from the industry and should closely align with many DP currently in use. The book "Heat and Mass Transfer: Fundamentals Applications"(HM) offers extensive information on DP HEs, and some of the input values have been cross-referenced with the book for accuracy. [56] The parameter that constitutes most from Table 7 is L_{pipe} , an increase in length can increase the total heating area substantially.

The inside area of the pipe can be calculated with the parameters: π , di_{DP} , and L_{pipe} . Equation 47 shows the multiplication of the parameters.[75]

$$A_{i_{surface}} = \pi * di_{DP} * L_{pipe} \quad [m^2] \quad (47)$$

Equation 48 is in reality the outside area of the pipe, but the outside area of the pipe is heating up the fluid running through the shell side. Because of Python and giving output for different cases, this parameter is called $Ah_{overall}$ in the script. But one can still analyze that length of the tube impacts the equation substantially. [75] [76]

$$Ah_{oa} = \pi * do_{DP} * L_{pipe} \quad [m^2] \quad (48)$$

Table 7: Initial input values for double pipe HE

Explanation	Parameter	Value	Unit
Tube outer diameter (Pipe)	$d_{o,DP}$	0.028	[m]
Tube Inner diameter (Pipe)	$d_{i,DP}$	0.030	[m]
Tube outer diameter (Shell)	D_o	0.020	[m]
Tube Inner diameter (Shell)	D_i	0.016	[m]
Length	L_{pipe}	40	[m]
U	U_{DP}	900	[W/m ² * K]
F	F_{DP}	1	[-]

The annulus refers to the flow area for the fluid in the shell side of the DP exchanger. It is important to understand and control this parameter through calculations. A higher $Ah_{annulus}$ influences flow calculations, such as the Re and Nu, for instance. Equation 49 demonstrates these calculations.[75]

$$Ah_{annulus} = \frac{\pi}{4} * D_{i,DP}^2 - d_{o,DP}^2 \quad [m^2] \quad (49)$$

The hydraulic diameter can be calculated using equation 50 and is helpful for computing flow parameters on the shell side, such as Reynolds number and friction factor. Due to the presence of the pipe within the shell, the original inside and outside diameters cannot be utilized. The equivalent diameter can be determined using two different methods, illustrated by equations 51 and 52; however, $De1_{DP}$ is considered the most accurate calculation method in this thesis.[75]

$$D_{h,DP} = D_{i,DP} * d_{i,DP} \quad [m^2] \quad (50)$$

$$De1_{DP} = \frac{D_{i,DP}^2 * d_{o,DP}^2}{d_{o,DP}} \quad [m^2] \quad (51)$$

$$De2_{DP} = D_{i,DP} * d_{o,DP} \quad [m^2] \quad (52)$$

Pressure loss for DP HE is performed with equation 53. When the tube is calculated each parameter with x is substituted by the parameter correlated with the tube. Same for the outer pipe, then the correlated parameter for the annulus is applied. The calculation of pressure loss for the DP HE is conducted using equation 53. In the case of the tube, each parameter denoted with x is replaced by its corresponding tube-related parameter. Similarly, for the outer pipe, the respective parameters corresponding to the annular pipe are employed. [76][75]

$$\Delta P_{DP,x} = f_x * \frac{G_x^2 * L_x}{2 * \rho * D_{e,x}} \quad [m^2] \quad (53)$$

Equation 54 displays a more accurate calculation for the heat transfer coefficient. This will be computed for DP in the Python script.[75]

$$h_{x,DP} = \frac{0.027}{D_e} * k_x * Re_x^{0.8} * \left(\frac{C_{p,x} * \mu_{x1}}{k_x}\right)^{1/3} * \left(\frac{\mu_{x1}}{\mu_{x2}}\right) \quad [m^2] \quad (54)$$

Equation 55 and 56 are two methods presented for DP with regard to calculating U_{DP} . Both equations are computed in Python and the user of the script can easily shift between them.[75]

$$U_{DP,new} = \frac{1}{h_i} + \frac{1}{h_o} \quad [m^2] \quad (55)$$

$$U_{DP,new2} = \frac{1}{h_i * A_i} + \frac{\ln(D_o/D_i)}{2 * \pi * k * L} + \frac{1}{h_o * A_o} \quad [m^2] \quad (56)$$

Effectiveness for DP is calculated with equation 57 for parallel flow. For instance, if counter-flow is chosen equation 58 will run because it's preferred with the flow type. [56]

$$\epsilon_{DP} = 1 - \mathit{math.exp}\left(\frac{-NTU_{DP} * (1 + c)}{(1 + c)}\right) \quad [W/m^2 * K] \quad (57)$$

$$\epsilon_{DP} = 1 - \mathit{math.exp}\left(\frac{-NTU_{DP} * (1 + c)}{(1 + c)}\right) \quad [W/m^2 * K] \quad (58)$$

3.5.3 Plate exchanger

The PE possesses the highest number of input variables among the three HEs, which can make it seem more complex. The inner and outer diameters of the hot and cold pipes are often similar, but they can vary depending on the manufacturer and the specific application. Most manufacturers provide these parameters or offer general values that can be used with a reasonably low margin of error. The PE also boasts a relatively easy installation process, particularly in pre-existing facilities or settings where heat transfer between fluids is required, owing to its compact square structure. The thermal conductivity, as initially set in Table 8, is 50 $[W/m * K]$, and it depends on the material used to construct the PE, whether it be copper, steel, aluminum, etc., as decided by the manufacturer.[62]

Equation 59 is applied to ensure that heat transfer is not over-calculated. This can be handled differently and some articles and calculation tools only used the square plate surface below the pipes as a heating area or transfer of heat regarding a PE. Because this neglects the lower half of the hot pipe, it was decided to use the bottom half of the hot pipe to include calculations for the heating area. [62][77]

$$D_p = \frac{D_o}{2} \quad [m] \quad (59)$$

The height to be used in the heating area are therefore dependent on the calculations from 59, but a safety factor has been added with 0.02 multiplied by 2. This is to ensure that the heating area is not bigger than what occurs in reality. The height for the plate to be used further in heating calculations is illustrated by equation 60. [62]

$$H_v = H_{tot} - D_p - 0.02 * 2 \quad [m] \quad (60)$$

For width the same safety factor from equation 60 is still applied, after reading other research articles the safety factor applied in equation 60 was deemed necessary to subtract the total width by the same factor to yield an accurate result when calculating the width regarding heat transfer. This can be removed if the user of the code has other specifications from the manufacturer.[78] [62]

$$W_p = W_{tot} - (0.02 * 2) \quad [m] \quad (61)$$

Table 8: Initial input values for plate HE

Explanation	Parameter	Value	Unit
Inner diameter, cold water	$d_{i,PE}$	0.070	[m]
Tube outer diameter, cold water	$d_{o,PE}$	0.072	[m]
Tube Inner diameter	D_i	0.070	[m]
Tube outer diameter	D_o	0.072	[m]
Height	H_p	1.066	[m]
Width	W_p	0.460	[-]
Plate spacing	P_s	0.008	[-]
Plate thickness	T_h	0.0003	[m]
Corrugation pitch	b	0.0015	[-]
Angle of plates pattern	B_e	50	degree
Correction factor	F_{pe}	1	[-]
Number of plates	$N_{p,pe}$	20	[m]
Fouling factor, water	R_w	0.0001	[-]
Fouling factor, refrigerant	R_f	0.0003	[-]
Thermal conductivity	K_p	50	[m]
Length first plate	$L_{p,tot}$	2	[m]
Width first plate	$W_{p,tot}$	1.6	[m]
e-P	e_p	0.002	[m]
Overall heat transfer coefficient	U_{ST}	800	[-]
Overall heat transfer coefficient, evap.	$U_{ST,EV}$	1000	[m]

The total plate area is calculated with equation 62 for the first and last plates, which are almost always bigger than the thin heat-transferring plates inside the PE. The total area of the first and last outside plates is not taken into account when calculating the heat transfer area.[62]

$$A_{tot,plate} = h_{tot} * W_{tot} \quad [m] \quad (62)$$

The inner channel aspect ratio is utilized to have a ratio between the corrugation pitch, b , and plate spacing, P_s . To calculate the enlargement factor more precisely a channel aspect ratio is necessary. Equation 63 illustrates the inner channel ratio. [79]

$$\gamma = \frac{2 * b}{P_s} \quad [-] \quad (63)$$

For PE the enlargement factor can either be set between 1.15 - 1.25, but this is a general factor and more an

average between many different PE. In this thesis, there was a desire to have it specifically calculated for the chosen PE. Therefore, equation 64 has been utilized.[79]

$$\phi = \frac{1}{6} * (1 + [1 + (\frac{\pi}{2 * \cos \beta})^2 * \gamma^2]^{0.5} + 4 * [1 + (\frac{\pi}{2 * \sqrt{2} * \cos \beta})^2 * \gamma^2]^{0.5}) \quad [-] \quad (64)$$

The total heating area of one plate can now be calculated by the use of equation 65. This provides a heating area of one plate that is utilized for further calculations regarding PE and size.[62][79]

$$A_p = \phi * W_p * H_p \quad [m^2] \quad (65)$$

The key factors to analyze when applying a PE to a situation that requires heat transfer are the number of plates, height, and width. These are the factors impacting the heating area and can result in higher Q_c , adding more plates are probably the most favorable solution to adding a bigger $Ah_{overall}$, if the space is limited and bigger end plates are not feasible. Equation 66 shows the heating area calculation, where the number of plates is multiplied by the heating area of one plate.[62][78]

$$Ah_{oa} = N_{p_{pe}} * A_p \quad [m^2] \quad (66)$$

There is also an equivalent and hydraulic diameter for the plate exchanger that can be utilized for further calculations on different flow parameters. Equation 67 and 68 show the methods used in this thesis. [62]

$$D_e = 2 * P_s \quad [m] \quad (67)$$

$$D_h = \frac{2 * T_h}{\phi} \quad [m] \quad (68)$$

Pressure loss for a PE can be calculated by the following method. Equation 69 is dependent on the channel friction factor, but the most precise channel friction factor equation also depends on pressure drop. That is why Haaland's Darcy Friction Factor is utilized to find a f_{ha} which then can be used to calculate the pressure drop, more on f_{ha} in section 3.6. With known pressure drop, there is a possibility to then perform equation 70.[77]

$$\Delta P_{pl} = \frac{4 * f_{ha} * L_p * P}{2 * \rho * D_e} * (\frac{W}{N * A})^2 + 1.4 * \frac{P}{2 * \rho} * (\frac{W}{A_p})^2 * \rho * g * L_p \quad [Pa] \quad (69)$$

The channel friction factor for PE can be calculated with equation 70. This method, which yields the most accurate value for a PE could be calculated after the pressure drop is found by using Haaland's formula, as stated above.[77]

$$f_p = \frac{\Delta P_{pl} * D_h}{2 * \rho * V^2 * L_p} \quad [-] \quad (70)$$

Overall heat transfer coefficient, U_{new} for PE is calculated with equation 71. The main difference from calculating U PE to other HE is the thermal conductivity, k , and thickness of the plate, T_h . By performing equation 71 one checks the initial given U . [77][78][62]

$$U_{new} = \frac{1}{\frac{1}{h_f} + \frac{T_h}{k_p} + \frac{1}{h_w} + R_f + R_w} \quad [W/m^2] \quad (71)$$

Effectiveness for PE is calculated with equations 72 and 73. The value c is found by the same method as for ST, equation 45. Then Python will use the equation that fits with the calculated c value. [80] **If: $c < 0.0$**

$$\epsilon_{PE} = 1 - \text{math.exp}\left(\frac{-NTU_{DP} * (1 + c)}{(1 + c)}\right) \quad [-] \quad (72)$$

If: $c > 0.0$

$$\epsilon_{PE,2} = \frac{Q1}{Q2} \quad [-] \quad (73)$$

3.6 General equations

Total Q for the condenser is calculated using a widely recognized equation employed in HP cycles, illustrated in 74. Q_c represents the amount of heat available for transfer between various refrigerants or fluids flowing through pipes in this instance. The overall heat transfer coefficient (U) has been assigned values that fall within the range of limits outlined in the Engineering Toolbox and articles.[81][56]

$$\dot{Q}_c = U_{CO} * A_{h_{overall}} * F_{ST} * LMTD_{CO} \quad [W] \quad (74)$$

The mass flow rate by the water arriving at the HE in the condenser is calculated by using Q_c and its C_p , and temperature differences. The temperature difference will variate because it is dependent on the user input. So this can be differentiated by what ΔT the user provides. The small change in specific heat capacity for water, $C_{p,c}$, is taken into account, and Q_c is divided by 1 000 [-] to get [kW], because $C_{p,c}$ is written in [kJ/kg * K]. As long as water into the H is between 10 and 70 °C the $C_{p,c}$ will be updated.[56]

$$\dot{m}_{water} = \frac{Q_c/1000}{C_{pc} * (T_{w,out} - T_{win})} \quad [kg/s] \quad (75)$$

The mass flow rate in the HP cycle for user-specified refrigerants is determined by employing the heating capacity, Q_c , from equation 74 and considering the enthalpy differences between points two and three, depending on the P-h diagram, more general enthalpy point right before and after the condenser, as shown in equation 76. This stems from the energy balance calculated in 2.3.3. Consequently, a higher Q_c necessitates a greater mass flow rate in the system. The enthalpies are primarily influenced by the choice of refrigerant, heat of vaporization, and pressure.[56]

$$mflow = \frac{Q_c}{h_2 - h_3} \quad [kg/s] \quad (76)$$

The work done by the compressor to elevate the fluid to the desired temperature is computed using the mass flow rate and enthalpies prior to the compressor, commonly noted as points one and two. However, this is subject to the degree of superheating, which in turn impacts the P-h diagram. The enthalpies in equation 77 are affected by factors such as the choice of refrigerant, isentropic efficiency, and compressor losses. If it's desirable to know the isentropic compressor work, equation 78 can be applied.[56]

$$W_{comp} = mflow * h_2 - h_1 \quad [kg/s] \quad (77)$$

$$W_{comp,is} = \frac{mflow * h_2 - h_1}{n_{is}} \quad [kg/s] \quad (78)$$

LMTD depends on two temperature differences, for parallel flow the two ΔT values are collected as equation 79 illustrate. Then these values are used for equation 81. There is possible to calculate the LMTD more

accurately with step-by-step methods, discussed further in section 5.6. [56]

$$\begin{aligned}\Delta T1 &= T_{f,in} - T_{w,in} & [K] \\ \Delta T2 &= T_{f,out} - T_{w,out} & [K]\end{aligned}\tag{79}$$

For counter-flow, the same parameters are utilized, but the configuration is different. As equation 80 demonstrates, $T_{w,out}$ and $T_{w,in}$ has switched place. Then this value is computed by the same equation as parallel flow 81. [56]

$$\begin{aligned}\Delta T1 &= T_{f,in} - T_{w,out} & [K] \\ \Delta T2 &= T_{f,out} - T_{w,in} & [K]\end{aligned}\tag{80}$$

Then general LMTD is computed with equation 81 and either values for parallel flow or counter-flow are utilized, depending on what flow pattern is desirable for the given case.[56]

$$LMTD = \frac{\Delta T1 - \Delta T2}{\ln * \frac{\Delta T1}{\Delta T2}} \quad [K]\tag{81}$$

Two defined equations, referenced as ??, are employed to calculate the evaporator load, Q_{evap} . These equations yield two parameters which are subsequently used to ascertain the absolute difference in evaporator load.

The volumetric flow is used in calculations for the flow can be calculated once the mass flow rate is known. By dividing the mass flow rate by density multiplied by flow area, the volumetric flow is known. This has been calculated for both water and refrigerant and for water this will be correct. With regard to the refrigerant, there is a possibility for a source of error because of the phase change, this is discussed in section 5.4. [52]

$$V_x = \frac{mflow}{Density_{fluid} * A_{surface}} \quad [m/s]\tag{82}$$

Calculation of how much fluid passes through the flow area, also called mass velocity. [72]

$$G_t = \frac{mflow}{a_t} \quad [kg/s * m^2]\tag{83}$$

Calculations of density(ρ), dynamic viscosity(μ), and thermal conductivity(k) are collected by the use of the library CoolProp. Further description of how CoolProp works can be found in section 19. That results in these three parameters being calculated by passing two or more values into the function. Equations are shown with 84.

$$\begin{aligned}\rho_x &= PropsSI('D', 'T', T2, 'Q', 1, myfluid) & [kg/m^3] \\ \mu &= PropsSI('VISCOSITY', 'T', T2, 'Q', 1, myfluid) & [kg/m * s] \\ k_x &= PropsSI('L', 'P', P2, 'Q', 1, myfluid) & [W/m * K]\end{aligned}\tag{84}$$

The calculation of kinematic viscosity(v) is possible to calculate when the dynamic viscosity and density are known.[56]

$$v_x = \frac{\mu}{\rho_x} \quad [m^2/s]\tag{85}$$

Re can be calculated by using different methods and parameters, depending on what parameters are available. For calculations performed in this thesis mass flow rate has been utilized, meaning the second equation written

for Re by 86. The decision was made by testing and analyzing results and the volumetric flow, V_x , was found to be the least accurate. One reason could be it was impacted the most by the phase change of the refrigerant.

$$Re_x = \frac{\rho * V * D}{\mu} = \frac{4 * \dot{m}}{\rho * \mu * d} \quad [-] \quad (86)$$

The Haaland equation for calculating the Darcy friction factor is utilized across all three Reynolds number scenarios and employed in the computation of the Nusselt number. Given its high degree of accuracy, particularly in relation to water as it does not undergo phase transition within the HE, the Haaland equation proves to be a viable choice between the different existing equations. Prior studies have indicated the applicability of Haaland's equation for both single-phase and two-phase flow, acknowledging the negligible error that may occur. [82] There exist methodologies proposed by experts to adapt the Haaland equation to two-phase flow conditions.[83] The implementation of this adaptation within the script is addressed, with section 5.9 discussing this further.

$$f_x = \frac{1}{-1.8 * \ln\left[\left(\frac{e_x/di_x}{3.7}\right)^{1.11} + \left(\frac{6.9}{Re_x}\right)^{0.5}\right]} \quad [-] \quad (87)$$

The value of the Nu is contingent on the nature of the flow, whether it is laminar or turbulent, which is dictated by the Re . Specifically, an Re greater than 10,000 corresponds to turbulent flow, while an Re less than 2,300 signifies laminar flow. When the Re falls between these two values, in this case between 2,300 and 10,000, the flow is considered to be in a transitional state, not fully developed. In such instances, a specific equation is employed to account for this partially developed flow condition. The distinctions among these three conditions, turbulent, transitional, and laminar are illustrated with equations 88, 89, and 90. [56]

For Re that corresponds to turbulent flow: [56]

$$Re_f > \mathbf{10\ 000}$$

$$Nu_x = 0.027 * (Re_x^{0.8}) * (Pr_x^{0.33}) * \left(\frac{\mu_1}{\mu_2}\right) \quad [-] \quad (88)$$

For Re that are not fully developed: [56]

$$\mathbf{10\ 000} < Re_x < \mathbf{3\ 000}$$

$$\mathbf{0.5} < Pr_x < \mathbf{2\ 000}$$

$$Nu_x = \frac{\frac{f_x}{8} * (Re_x - 1000) * Pr_x}{(1 + 12.7 * (\frac{f_x}{8})^{0.5} * (Pr_x^{0.66} - 1))} \quad [-] \quad (89)$$

For Re that corresponds to laminar flow: [56]

$$\mathbf{2\ 300} > Re_x$$

$$\mathbf{5} < Pr_x$$

$$Nu_x = 3.66 + \frac{(0.065 * (\frac{di_x}{L_x}) * Re_x * Pr_x)}{(1 + 0.04 * (((\frac{di_x}{L_x}) * Re_x * Pr_x^{2/3}))} \quad [-] \quad (90)$$

A well-known equation for the Nu is utilized to ascertain the convection heat transfer coefficient, both within and external to the pipe. This approach is applicable when the Nu is determined from the equations above, and the heat transfer coefficient "h" remains to be determined. Equations 91 and 92 shows the connection.

$$Nu_x = \frac{h_x * D}{k} \quad [-] \quad (91)$$

$$h_x = \frac{Nu_x * k}{D} \quad [-] \quad (92)$$

The Prandtl number can be computed utilizing the dynamic viscosity (μ in $[Ns/m^2]$), thermal conductivity (k in $[W/m * K]$), and the specific heat capacity at constant pressure (C_p in $[kJ/kg * K]$), equation 93. Alternatively, the "PropsSI" function can be employed with two known parameters as input to derive the respective Prandtl number, equation 94.

$$Pr = \frac{\mu * C_p}{k} \quad [-] \quad (93)$$

$$Pr_F = PropsSI('PRANDTL', 'T', T2, 'P', P2, myfluid) \quad [-] \quad (94)$$

Volumetric flow and speed of the fluid are to be found by using mass flow rate, density, and flow area. Equation 95 illustrates the volumetric flow and equation 96 shows the speed of the fluid.[]

$$V_x = \frac{mflow}{\rho} \quad [m^3/s] \quad (95)$$

$$Vs_x = \frac{V_x}{A_x} \quad [m/s] \quad (96)$$

The calculation of water pressure loss within the HE if a more specified equation is not to be found, is based on parameters such as the length (L) and diameter (d) and the rest illustrated in equation 97.[56]

$$\Delta P_x = (f_x * (\frac{\rho_x * Vs_x^2}{2}) * (\frac{L_x}{D_x})) \quad [Pa] \quad (97)$$

The overall pump power necessary to circulate the water through the HE is determined by equation 98. The main parameters that pump power are decided by are mass flow rate, pressure loss, density, and efficiency. Here the efficiency, n_{pump} is set to be 0.8 [-], which is 80 [%]. However, this value can be easily adjusted by the user to reflect the desired efficiency. The computation of these parameters is illustrated in equation 98. [56]

$$W_{pump,w} = \frac{\dot{m}_x * \Delta P_x}{Density_x * n_{pump,x}} \quad [W] \quad (98)$$

3.7 Python

Once the relevant equations for each type of HE were identified, as detailed in sections 3.5.1, 3.5.2, and 3.5.3, the Python coding began by developing various scripts to execute the required calculations. The script containing the equations and returning a single output for given input values is now referred to as *HPmain*. The script that utilizes calculations from *HPmain*, iterates until specific conditions are satisfied, and generates plots for all calculations performed is now designated as *HPIteration*. The final script, *App4*, integrates both the *HPmain* and *HPIteration* scripts, forming the app or web page, which is further explained in 3.7.3. Figure 17 describes a path and connection between the scripts.

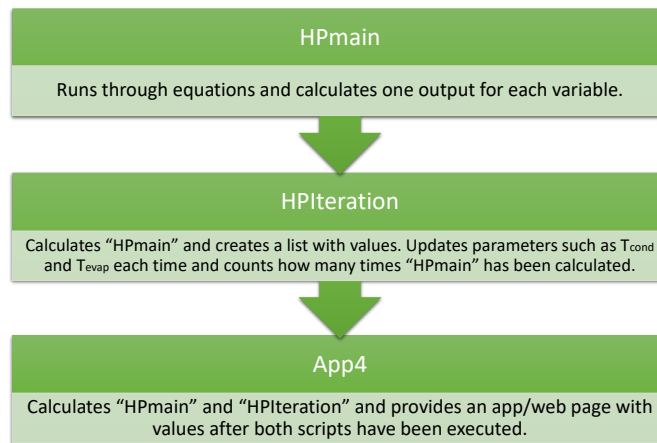


Figure 17: Schematic description of scripts

3.7.1 HPmain

First outlining the structure of the *HPmain* script. The primary libraries employed in this script include numpy, CoolProp, thermopy, math, prettytable, cv2, and matplotlib.pyplot. Numpy and math are libraries that provide a variety of mathematical functions, for instance, 'np.log' is frequently used for LMTD calculations when a natural logarithmic value is required. The pretty-table library was utilized to display output in a tabular format, which was meant to improve visibility compared to structured lists. After the packages are imported, the main function, denoted as *def HPMF(...)* is introduced, and a picture illustrating this from the script can be found in Appendix C.1. All the equations in the script are contained within this function, right up to the point where the results are returned and the function is called. The 'calling' of the function is shown in Python by Appendix C.2, where explanations of all numbers and statements are commented out with an extra line for user clarity.

The package employed for calculating the HP cycle is called CoolProp, which is imported into the script as PropsSI. This explains why parameters are written in the format $P1 = \text{PropsSI}('P', 'T', T_{evap}, 'Q', 1, \text{myfluid})$, using pressure at stage one as an example. Here, pressure is the desired parameter, while the evaporator temperature and saturated vapor state of the fluid ($Q=1$) serve as inputs to calculate pressure ($P1$). Figure

18 shows P1 as an example. CoolProp facilitates the passing of parameters and values, then returns the desired parameter's output, as long as two or more input values and the refrigerant's name are provided as arguments. Pressure, enthalpy, entropy, temperature, and density are the primary calculated parameters for the four stages or components: compressor, condenser, expansion valve, and evaporator. Entropy, enthalpy, and temperatures have been modified and extended from the original script handed over, and provide more extensive calculations with regard to T-s and P-h diagrams. The script concludes the HP cycle by calculating the critical and maximum temperatures and pressures, a feature added to the HP cycle. This information helps users determine whether their calculations are near or far from critical values, which should not be approached too closely.

```
if SH == 0:
    #f(Tev)saturated vapor Q=1
    P1 = PropsSI('P', 'T', Tev, 'Q', 1, myfluid)
```

Figure 18: Illustration of PropsSI used in Python

Next, the input parameters for the ST, DP, and PE HEs are specified. Users are required to input the desired values for each parameter. If, for example, a user wishes to calculate for the PE, the parameters for ST and DP can simply be left as they are, they will not affect the computations. Following this, temperatures with input values from the function being used are listed. An 'if' statement is then deployed: if the water temperature entering the condenser is below 294 [K], a specific heat capacity $C_{p,h}$ is used. This is followed by an 'elif' statement for another temperature range, indicating that if the incoming condenser temperature is between 294 - 304 [K], a different $C_{p,h}$ applicable to this range is used, and this pattern continues. Thus, the 'if' and 'elif' statements deliver an output corresponding to their specified value ranges. Appendix ?? shows a figure of how the input values look in Python.

The subsequent step involves a critical 'if' statement for the three types of HEs. The type selected determines which computational loop the script enters, and the initial calculation is based on whether the flow is parallel or counter, dependent on the user's choice. After several more computations, another significant "if" statement comes into play, calculating the Darcy Friction factor and Nusselt number based on the Reynolds number. Following the fluid and water calculations, additional computations for the U and effectiveness are carried out until the script reaches two 'if' statements. These statements control the printing of the results table based on a True or False condition. This is crucial as when the script is used in *HPIteration*, printing the table for each count would add substantial processing time. The final 'if' statement corresponds to the chosen flow pattern for the HE, specifically if it's parallel- or counter-flow. For the evaporator same equations as the condenser are performed, and the glycol mixture is taken into account for the brine water with regard to density. A flow chart to visually illustrate the methodology of the *HPmain* script is presented in Figure 19

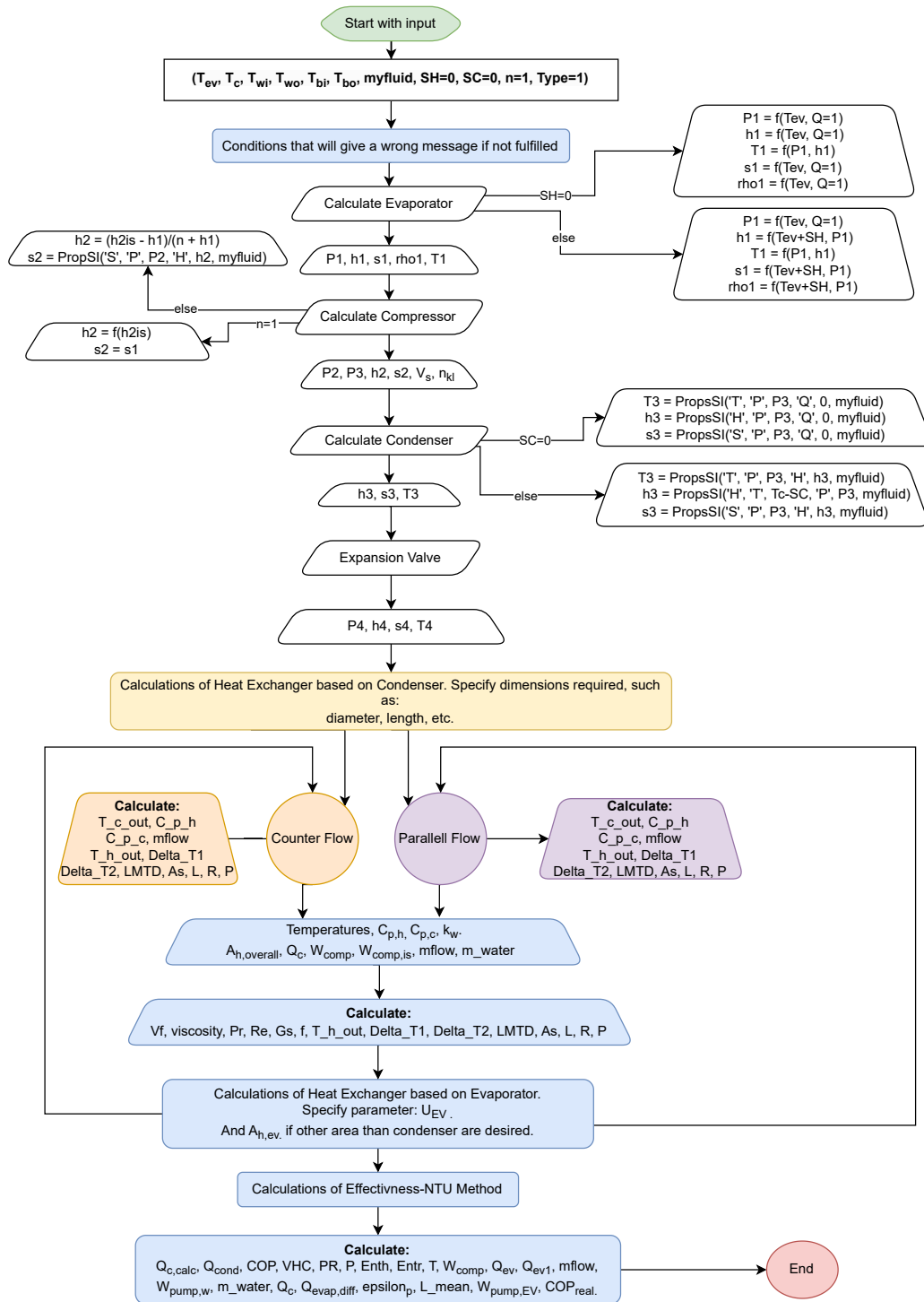


Figure 19: Flow chart of HPmain script.

3.7.2 HPIteration

The only newly introduced library in *HPIteration* is Openpyxl, which enables results to be exported directly to an Excel file, facilitating data storage. The *HPIteration* script imports *HPmain* and executes calculations within a "While loop", allowing the script to run until defined criteria are met. A new function is also embedded within the script to manage the iterative loop. The core objective of *HPIteration* is to satisfy convergence criteria for four variables, as illustrated in Table 9 with $T_{cons,max}$ and $T_{evap,max}$ from case 2 used as an example. $T_{cons,max}$ constantly iterating from initial to max temperature, when max temperature is reached it starts at initial value again, illustrated in section 4.3. Evaporator temperature is increasing step-wise and checks calculation until max temperature is reached. Subsequently, an empty list for all parameters is generated to collect values from each iteration. These lists enable the production of trends and values derived from the iterative 'While loop' to be plotted. If the convergence criteria are successfully met, relevant plots will be displayed. If the convergence criteria are not fulfilled, the 'Not accepted' message from Table 9 is written. The user can choose whatever percentage of desirable tolerance for one and two, depending on the condenser or evaporator. When values are passed into this list, it overwrites the original list from *HPmain*. arydshln

Table 9: Convergence criteria for iterations.

Convergence criteria			
Equation	Criteria	Accepted	Not accepted
$\frac{abs(Q_c - Q_{c,rec})}{Q_{c,rec}} * 100$	Tol 1	If all four criteria are approved: Convergence criteria reached.	If on criteria does not approve: Max temp condenser or evaporator reached.
$\frac{abs(Q_{ev} - Q_{ev1})}{Q_{ev1}} * 100$	Tol 2		
$T_{cond} + 0.05$	$T_{cond,MAX} = 328$		
$T_{evap} + 0.05$	$T_{evap,MAX} = 267.95$		

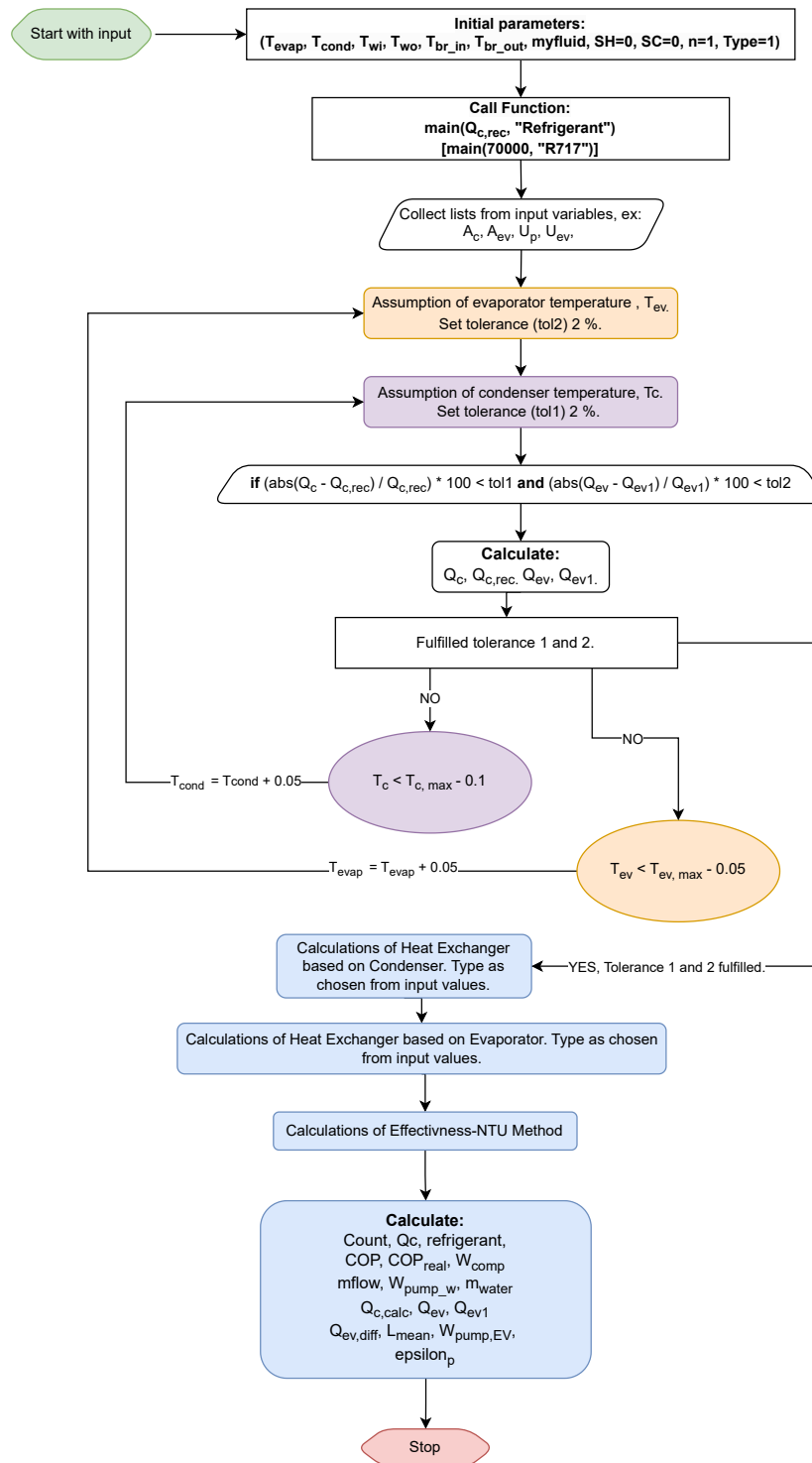


Figure 20: Flow chart of HPIteration script.

3.7.3 App

The packages Streamlit and Pandas have been employed to develop a web application, serving as an interactive way to display the results. The script *app4.py* showcases all the calculations and iterations on a locally hosted web page. It includes a button for users to input their desired Q_{rec} and *Refrigerant* values for script testing. However, achieving a presentable display of all plots and graphs posed a challenge. A flowchart outlining the process and methodology of the script is featured in Figure 21.

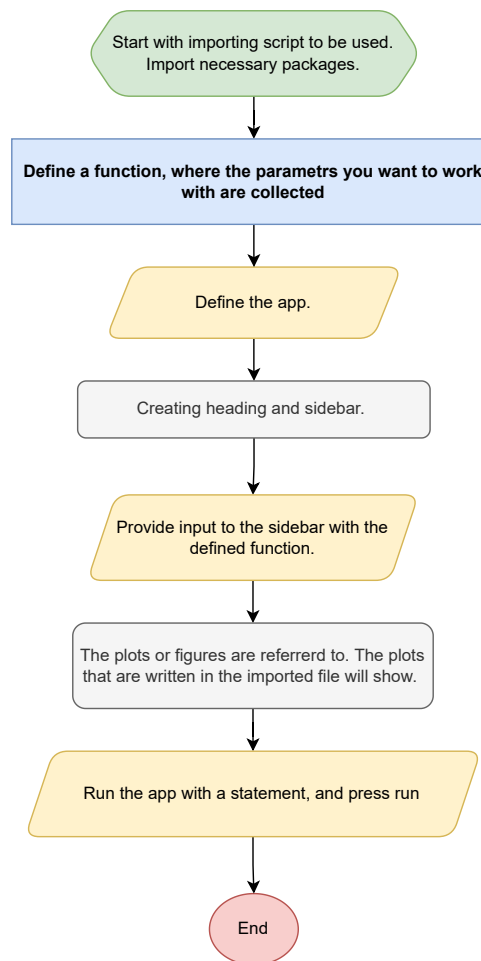


Figure 21: Flow chart of Streamlit app script.

3.8 Interviews with experts

To collect feedback about the most valuable parameters with regard to HPs and HEs, and if a user-friendly Python script could be valuable to the building industry, questions were made. The survey was meant to be performed on a focus group that consisted of five or six experts/experienced people from the building industry. In the end, two individuals answered and signed the necessary document with permission for the answers to be published. Given that the queries were presented to two individuals, the resulting data cannot be deemed representative of a full-scale survey, which would ideally include a minimum of 40-50 respondents. While the sample size is insufficient to constitute a focus group, the extensive industry experience of respondents is enough to give it strength. Jørn Stene has 35 years in the business, and Ole Døsvik has 40 years in the business, which lends weight to their insights on various themes. Table 10 summarizes the most compelling findings and observations. Both said Python is a tool used in their respective companies, but it was utilized by specialists, mostly the younger generation, not them. Can see from the results that indeed PE and counter-flow are the most desired combination. The feedback provided by Ole Døsvik emphasized the complexities encountered in managing the mass flow rate, where high mass flow rates through the HP are often favorable, yet lower rates are preferred for other system components further out on the schematics. Jørn Stene also underscored the importance of selecting an appropriate compressor to optimize the cycle, further illustrated in the Compressors section 1.1 of the literature review. The decision to utilize CoolPack over CoolTools was guided by its broader selection options and advanced capabilities.

Table 10: Interviews with two individuals from the building industry.

Interviews with experts		
Questions	Answers by: Jørn Stene	Answers by: Ole Døsvik
What are your thoughts on Python as a tool for calculations regarding heat pumps?	I will not use Python.	I will not use Python.
What type of program/tool do you prefer for calculations about HPs?	CoolPack and Excel.	IDA-ICE, CoolPack, and Excel.
Designing HEs for a project, the most important parameters are?	\dot{m} , LMTD, A , U , and \dot{Q} .	\dot{m} and LMTD.
What is the most common type of HE you use in projects?	Plate liquid-to-liquid HE.	Plate liquid-to-liquid HE.
What is the most usual type of flow pattern you come across regarding heat exchangers?	Counter-Flow.	Counter-Flow.
What format is the most desirable for reading calculation results in programs/tools?	PDF.	Web page and app.

4 Results

The results section goes through validation, tables from Python, and the web page.

4.1 Validation of the code

The code validation process involved the use of CoolTools, a well-established tool in the field of HP cycle simulations. CoolTools not only perform calculations but also presents the results in a visual VCC. However, as CoolTools does not provide all necessary parameters, data with property values for the refrigerant's density, obtained from the book: 'Heat and Mass Transfer', referred to at the final line in Table 11.[56] Figure 22 offers a detailed representation of the input parameters given to CoolTools, as well as the calculations carried out by the tool. Additionally, it displays various state parameters like pressure, enthalpy, entropy, and mass flow rate. A side-by-side comparison of the results generated by CoolTools and Python can be found in Table 11. R134a was selected as the refrigerant for this validation due to the extent of research available on it, which facilitates the verification of different parameters. Although this refrigerant is in the process of being phased out, it serves as an effective 'benchmark' for validation purposes.

The screenshot shows the CoolTools input interface for R134a. The interface is organized into several sections:

- Temperature Levels:** T_E [°C]: -9.00, ΔT_{SH} [K]: 5.00, T_C [°C]: 40.00, ΔT_{SC} [K]: 0.00
- Pressure Losses:** Δp_{SH} [K]: 1.00, Δp_{OL} [K]: 1.00
- Suction Gas Heat Exchanger:** No SGHX, 0.30
- Refrigerant:** CoolProp, R134a
- Cycle Capacity:** Heating capacity [kW]: 88.00, \dot{Q}_E [kW]: 70.94, \dot{Q}_C [kW]: 88, \dot{m} [kg/s]: 0.5026, \dot{V}_S [m³/h]: 185.6
- Compressor Performance:** Isentropic efficiency [-]: 1.00, η_{lis} [-]: 1, \dot{W} [kW]: 17.83
- Compressor Heat Loss:** Heat loss factor [%]: 5.00, f_{ol} [%]: 5, T_2 [°C]: 51.4, \dot{Q}_{LOSS} [kW]: 0.8917
- Suction Line:** Unuseful superheat [K]: 0.00, \dot{Q}_{SL} [W]: 115.09, T_8 [°C]: -4, $\Delta T_{SH,SL}$ [K]: 0
- Cycle Performance:** COP [-]: 3.978, COP* [-]: 3.9844, COP_{CARNOT} [-]: 5.3908, η_{CARNOT} [-]: 0.73912

Summary: Refrigerant R134a, COP [-]: 3.978, η_{CARNOT} [-]: 0.73912

State Points:

State	T [°C]	p [bar]	h [kJ/kg]	s [kJ/kg/K]	\dot{m} [kg/s]
1	-4.00	2.006	397.78	1.7526	0.5026
2	51.40	10.441	431.48	1.7471	0.5026
3	50.88	10.166	431.48	1.7489	0.5026
4	40.00	10.166	256.41	1.1905	0.5026
5	40.00	10.166	256.41	1.1905	0.5026
6	-9.00	2.086	256.41	1.2145	0.5026
7	-4.00	2.086	397.55	1.7487	0.5026
8	-4.00	2.006	397.78	1.7526	0.5026

Figure 22: CoolTools input screen with R134a as refrigerant.

The Python-generated representation of the HP cycle is shown in Figure 23. These results were obtained by executing a Python script with the same input parameters as those used in CoolTools. Python allows for the modification and variation of a wider range of parameters, however, for this particular case, all adjustable parameters in CoolTools were mirrored identically in the Python script. Appendix B shows a table with input parameters to Python matching input values provided to CoolTools.

Heat Pump			
Parameter	Value	Unit	
Tc	313	K	
Tev	264	K	
myfluid	R134a	-	
Qcond	88617.759	W	
Qevap	71463.593	W	
Qevapl	94417.8	W	
mass flow rate	0.506	kg/s	
W_comp	17154.166	W	
W_comp_IS	19060.184	W	
Temp	[269. 323.838 313. 313. 264. 269.]	K	
P, pressure	[207422.873 1012509.592 1012509.592 207422.873 207422.873]	Pa	
h, enthalpi	[397455.596 431366.199 256185.329 256185.329 397455.596]	J/kg	
s, entropi	[1748.813 1748.813 1711.109 1189.773 1213.85 1748.813]	J/kg * K	
Density fluid	57.221	kg/m ³	
COP	5.166	-	
COP, real	4.144	-	
VHC	1772008.247	J/m ³	
PR	4.881	-	
Calculated Q	205934.85	W	
Compressor stroke volume	200.0	%	
Efficiency(Klammevirkningsgrad)	0.612	-	
Critical temperature, fluid	374.21	K	
Critical pressure, fluid	40592.8	kPa	
Critical temperature, water	647.096	K	
Critical pressure, water	220640.0	kPa	

Figure 23: Heat pump cycle from Python with R134a as refrigerant

The parameters that are available in Python for the HEs results are visually represented in Figure 24. The header information provides clarity on the specific HE model used in the case, in this instance, a DP HE was selected for validation and comparison with CoolTools, as indicated in Figure 24. Can see parameters such as Re , $frictionfactor$, h_{new} , and NTU . The code also functions in Visual Studio Code.

Heat Exchanger CONDENSER, Double Pipe. Counter Flow		
Parameter	Value	Unit
mflow_water	2.647	kg/s
mflow_fluid	0.506	kg/s
Delta_T1_CO	12	K
Delta_T2_CO	20.0	K
LMTD_CO	15.661	K
A_annulus	0.002	m ²
Ah_overall	7.069	m ²
A_total	16.493	m ²
L	75	m
h, fluid	813.791	W/m ² * K
h, water	12437.808	W/m ² * K
k, fluid	0.016	W/m * K
k_water	0.598	W/m * K
Density_water	998.238	kg/m ³
Density_fluid	57.221	kg/m ³
Volumetric flow, water	1.116	m/s
Volumetric flow, fluid	0.001	m/s
Reynolds Number(water)	47328.417	-
Reynolds Number(Fluid)	1790752.487	-
Delta_P_Water	44843.027	N/m ²
Delta_P_Fluid	4073267.296	N/m ²
Friction factor, water	0.362	N/m ²
Friction factor, fluid	0.258	N/m ²
Pump power, water	1016.469	W
U_input(init)	800	W/m ² * K
Qc	88560.425	W
U_new	1860.003	W/m ² * K
Q_calc	205903.29	W
NTU	1187.671	-
epsilon	1.0	-

Figure 24: All heat exchanger parameters possible to read from Python

The three figures referenced (22, 23, 24) are visualized and compared side-by-side to summarize, illustrated in Table 11. Table 11 has a *Percentage deviation* column to illustrate the percentage difference between collected parameters from CoolTools and Python. The results were uplifting with a low percentage of error between most of the parameters. COP was the only parameter where the gap was extensive, COP from Python nearly matched with COP_{carnot} from CoolTools, but COP collected from Python was indeed not COP_{carnot} . This result needs to be investigated further. It's important not to misinterpret the volumetric flow deviation of 836 [%] as an error. This parameter is highly influenced by the pipe diameter. In the script utilized, the diameter is set at 0.028 [m]. However, adjusting this to 0.23 [m] aligns the value with that derived from CoolTools(182.09 [m^3/h]). Notably, CoolTools doesn't permit modifications to this particular parameter. To calculate the COP with regard to CoolTools, equation 24 from section 2.4 has been utilized. This is the same equation used for Python. This is the reason a different COP value from Figure 22 has been listed from CoolTools in Table 11.

Table 11: Initial input values for double pipe HE

Parameter	CoolTools	This work's code	Percentage deviation
Q_c	88.00 [kW]	88.56 [kW]	0.18 [%]
Q_{ev}	70.94 [kW]	71.4 [kW]	0.41 [%]
mass flow rate \dot{m}	0.503 [kg/s]	0.506 [kg/s]	0.20 [%]
Volumetric flow	185.6 [m^3/h]	22.18 [m^3/h]	836.79 [%]
Comp. work \dot{W}_{work}	17.83 [kW]	17.15 [kW]	3.94 [%]
COP_{HP}	4.94 [-]	5.16 [-]	4.45 [%]
P_1	2.006 [Bar]	2.07 [Bar]	3.19 [%]
P_2	10.441 [Bar]	10.125 [Bar]	3.12 [%]
h_1	397.78 [kJ/kg]	397.45 [kJ/kg]	0.08 [%]
h_2	431.48 [kJ/kg]	431.37 [kJ/kg]	0.03 [%]
s_1	1.752 [kJ/kg * K]	1.748 [kJ/kg * K]	0.23 [%]
s_2	1.7471 [kJ/kg * K]	1.748 [kJ/kg * K]	0.05 [%]
Density	46 Book [kg/m ³]	57.22 [kg/m ³]	24.39 [%]

4.2 Cycles that satisfy Q_{cond} values

This selection presents the results for convergence by Q_c , $Q_{c,rec}$, Q_{evap} , and $Q_{ev,1}$ as mentioned in section 3.7.2 for the HPIteration script. The results are presented with three different cases where each case computes results for three different HEs. Results are demonstrated by plots of different HEs modeled in Python. The script does work for both Spyder and Visual Studio Code. Pump efficiency is set at 0.80 [-] for all three cases.

4.2.1 Case 1

Table 12 and Table 13 describe input values used for ST, DP, and PE to calculate *Case 1*.

Table 12: Input values Case 1

Case 1		
Parameter	Value	Unit
T_{wi}	293	K
T_{wo}	303	K
$T_{br,in}$	278	K
$T_{br,out}$	268	K
$T_{cond,init}$	303.05	K
$T_{cond,max}$	318.00	K
$T_{evap,init}$	265.00	K
$T_{evap,max}$	267.95	K

Table 13: Rest of Case 1 input values

Case 1		
Parameter	Value	Unit
SH	0	$^{\circ}C$
SC	0	$^{\circ}C$
n	1	-
U	800	W/m^2K
Ah_{oa}	6.6	m^2
$Ah_{oa,EV}$	10	m^2
U_{EV}	1000	W/m^2K
tol	2.00	%

Case 1

Figure 25 presents $Q_{c,rec}$ represented by the blue line, denoting the required values from the iteration process. The orange points, meanwhile, display Q_c values, which have been produced as output when the convergence criteria are met, with ST as an example, but the same $Q_{c,rec}$ has been utilized for all HE. It is noticeable that Q_c appears to be closer to $Q_{c,rec}$ for lower values, ranging from 40,000 to 50,000 [W]. This observation makes sense, given that the tolerance is set as a percentage, thus, a 2 percent deviation from 40,000 [W] will provide a narrower range than 2 percent of 70,000 [W]. Figure 26 shows COP and COP_{real} for three different refrigerants when the ST HE scenario is applied. Among the refrigerants, R717 delivers the highest COP value for both the highest and lowest $Q_{c,rec}$, but it also displays the largest disparity between COP and COP_{real} . The calculation for COP_{real} incorporates the pump power of water and brine, and thus, the difference between COP values largely depends on the power required for these fluids. The performance of R1270 and R290 are closely matched, with R290, represented by the green and red lines, slightly outperforming R1270. Figure 27 illustrates COP and COP_{real} values for all three refrigerants within the DP scenario. Similar to the previous

figures, R717 continues to yield the highest COP values. Compared to Figure 26 of ST, the difference between COP and COP_{real} is notably larger for DP, likely due to the increased pump power required for water and brine, given the length of the DP, which is significantly longer than that of the ST. Lastly, Figure 28 portrays COP and COP_{real} values for the PE scenario, showing a pattern similar to that observed in Figure 27 for DP. As before, R717 records the highest COP values, with R1270 and R290 remaining closely comparable. Figure 27 illustrates COP and COP_{real} values for all three refrigerants for DP, and COP for R717 still yields the highest values also in this case. In comparison to Figure 26 of ST, the difference between COP and COP_{real} are significantly higher for DP. This is most likely due to the pump power required for water and brine, because of the DP length, which is considerably longer than ST. Figure 28 shows COP and COP_{real} values for PE, and this pattern is most similar to Figure 27 for DP. R717 yields the greatest COP values and R1270 and R290 are still similar.

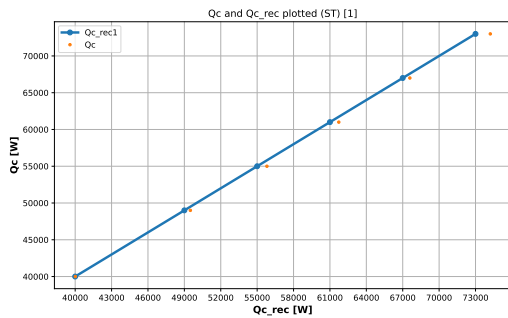


Figure 25: Q_c and $Q_{c,rec}$ for all simulation points, C1,ST.

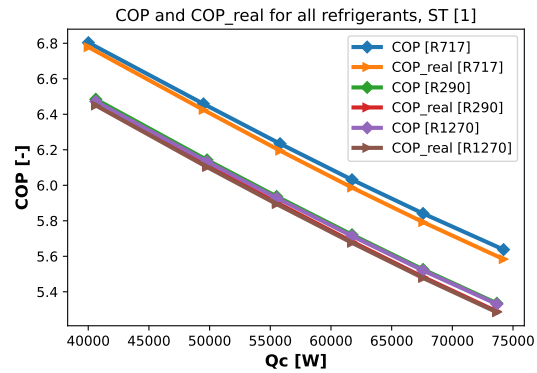


Figure 26: COP and COP_{real} for all refrigerants, C1,ST.

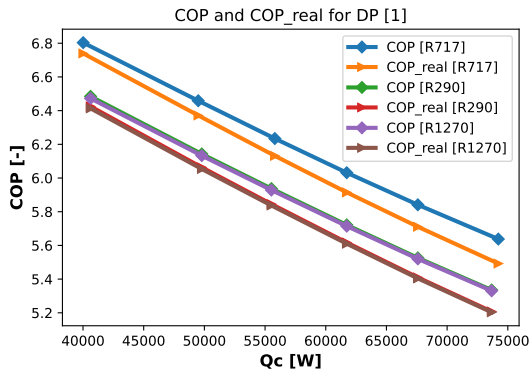


Figure 27: COP and COP_{real} for all refrigerants, C1,DP.

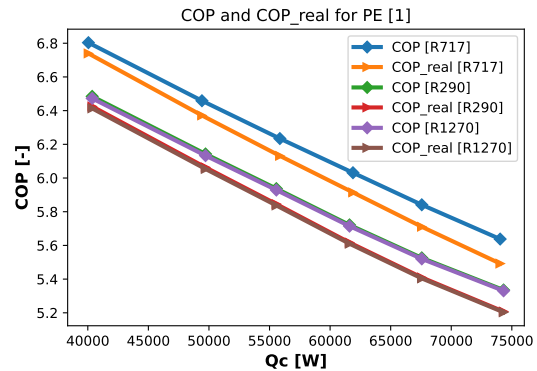


Figure 28: COP and COP_{real} for all refrigerants, C1,PE.

Figure 29 demonstrates the pump power necessary to drive water through the ST HE. It displays a subtle increasing trend with each new simulation involving a different $Q_{c,rec}$. Notably, the power requirements for

all three fluids are identical, which is reasoned to the fact that the fluids don't influence the water that passes through the HE via a separate pipe. Similarly, Figure 30 portrays the pump power needed for the DP HE. It follows a trend similar to that observed in the ST scenario, but the power requirements are markedly higher, peaking above 250 [W]. This is mainly due to the substantially longer length of the DP. Lastly, Figure 31 reveals the pump power needed for the PE scenario. At its highest values, there's a noticeable deviation from the established trend. For R717, there seems to be an outlier which could suggest a slight error; however, the final value returns to the initial trend. PE requires higher power for the pump than ST, but lower than DP.

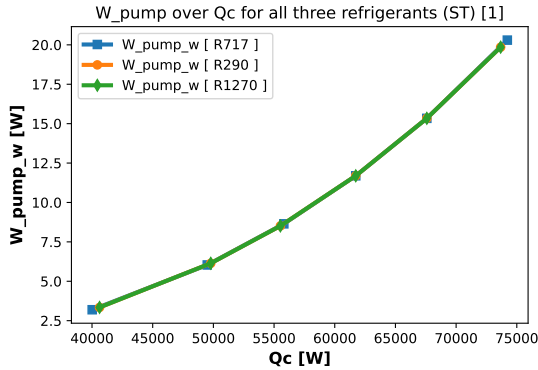


Figure 29: Water pump over Q_c for all refrigerants, C1, ST

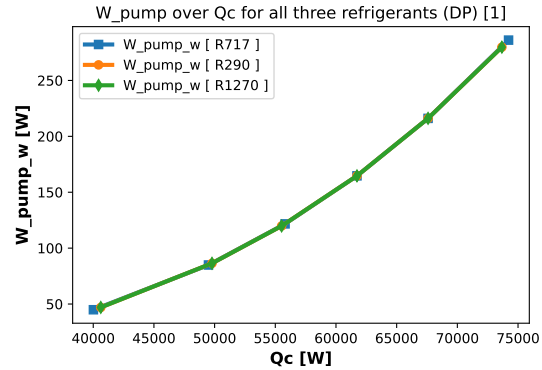


Figure 30: Water pump over Q_c for all refrigerants, C1, DP

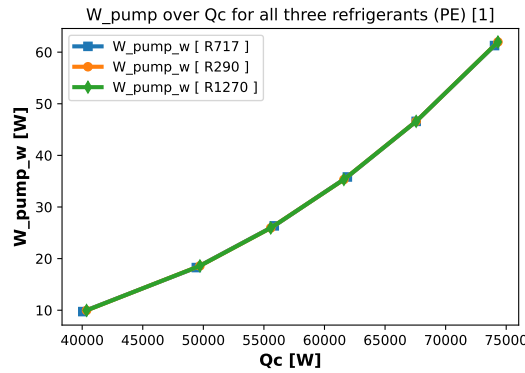


Figure 31: Water pump over Q_c for all refrigerants, C1, PE

Figure 32 showcases the brine pump power needed for the ST HE. Upon comparing this with the water pump power specific to SP, it becomes evident that brine requires more power, even though its \dot{m} and $C_{p,br}$ are lower and the ΔT is identical. This can be explained by the fact that the brine water circulates through the smaller pipes in the ST, while the refrigerant is the fluid that absorbs the heat. Consequently, the smaller diameter and other parameters necessitate a greater power input from the pump. Figure 33 illustrates the pump power

needed for circulating brine water through the DP HE. Due to lower parameters such as \dot{m} and $C_{p,br}$, the pump power needed for DP, in relation to brine water, is less than that required in the condenser. Figure 34 presents the pump power necessary for circulating brine water through the PE. The results bear little difference from the water pump power specific to PE. This is a positive outcome, given that the pipes in both cases are of a similar diameter because all four pipes have the same diameter, which should logically yield comparable results for PE, or the brine pump power requirement should be slightly lower. Same outspring of trend in this case too.

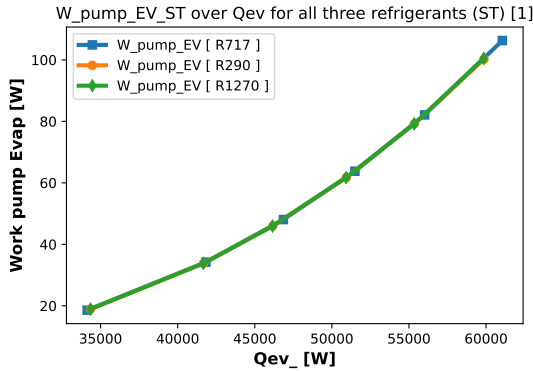


Figure 32: Brine pump power for all three refrigerants, C1,ST

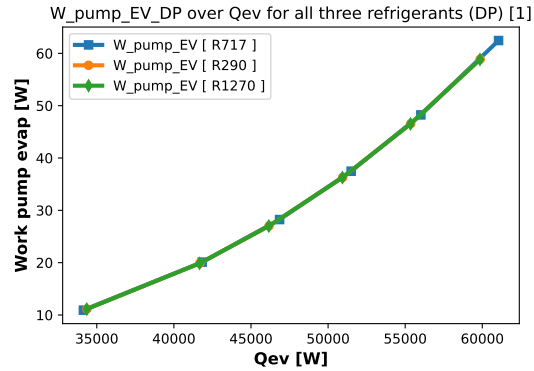


Figure 33: Brine pump power for all three refrigerants, C1,DP

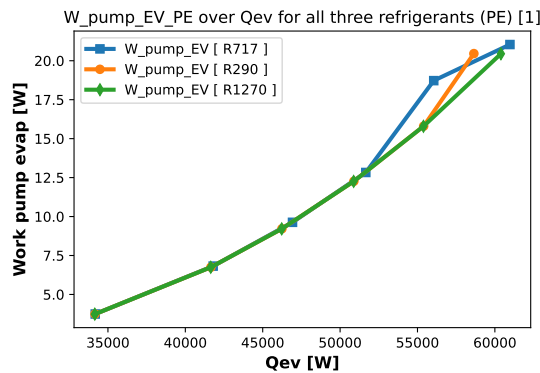


Figure 34: Brine pump power for all three refrigerants, C1,PE

Figure 35 presents the efficiency of the ST HE, for each refrigerant. Here, R717 delivers the highest efficiency, followed by R1270, and finally R290. It is worth noting that the y-axis displays up to three decimal places, mentioning that the difference between R1270 and R290 is about 0.005 [–], relatively marginal. Figure 36 reveals a contrast to the ST results, with R717 now being the refrigerant associated with the lowest efficiency. The disparity between R1270 and R290 has also diminished. As with the previous figure, the y-axis extends to decimals, explaining the difference is not substantial. The efficiency of PE, as portrayed in Figure 37,

unveils interesting findings. There is a marked decrease in efficiency with an increase in $Q_{c,rec}$, amounting to a significant variation of 0.20 [-]. These findings imply that accurate calculations need to be made for specific PE instances, particularly if the desired efficiency is above 0.8 [-]. The divergence in mass flow rates between R717, R290, and R1270 can be attributed to the Δh , as indicated in Figure 38. The mass flow rate for refrigerants is determined by dividing Q_c by Δh as derived from section 3.6. Higher Δh leads to a lower mass flow rate and seemingly higher COP for the refrigerant. Conversely, a low Δh can enhance efficiency but will result in a reduced COP . Given the marginal efficiency differences between ST and DP, it would be more beneficial to prioritize a high Δh and superior COP to optimize energy use and lower costs. Figure 41 illustrates the huge difference in Δh between R717 and R290. The mass flow rate for ST is illustrated in Figure 38, since the rest of the mass flow rate figures are similar, Appendix D.1 and D.2 shows for the two other HEs.

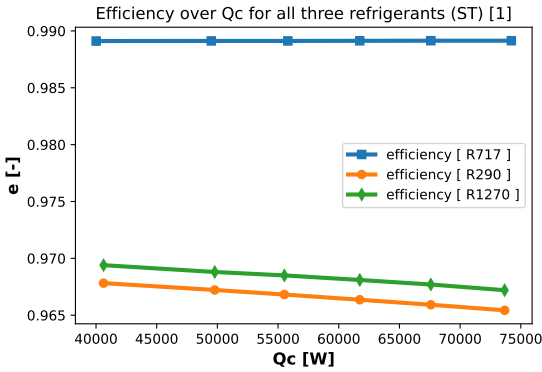


Figure 35: Efficiency for all refrigerants, C1,ST.

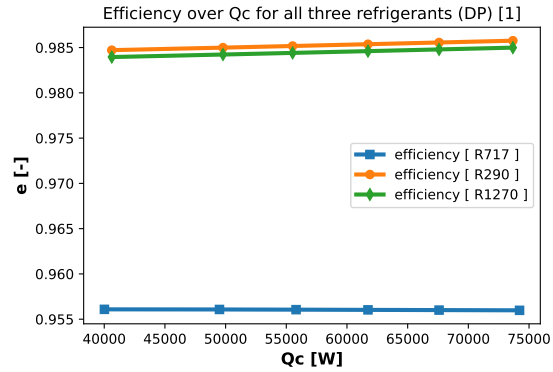


Figure 36: Efficiency for all refrigerants, C1,DP.

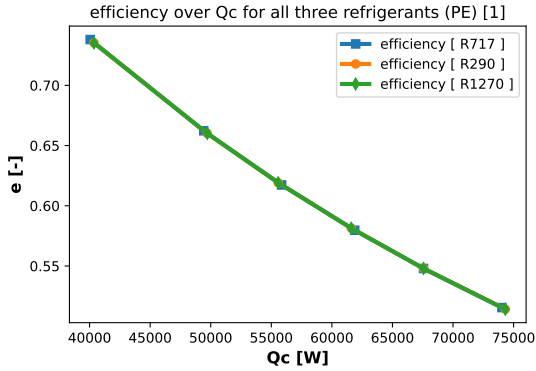


Figure 37: Efficiency for all refrigerants, C1,PE.

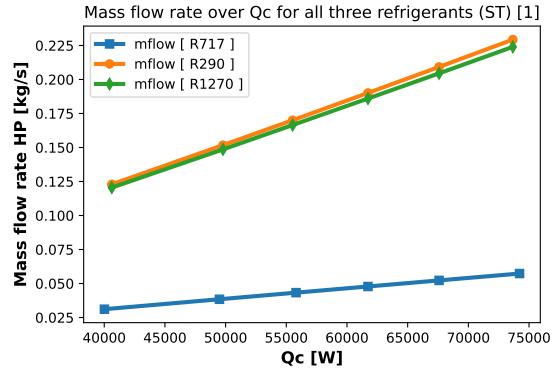


Figure 38: Mass flow rate for all refrigerants, C1,ST.

VCC is illustrated for refrigerants R717 and R290, as calculations showed similarities between R290 and R1270, thus making it sufficient to present only one. Figure 39 illustrate the T-s diagram for R717, calculated for a Q_c of 61 [kW]. The limits of temperatures for the condenser and evaporator are plotted to display that the

VCC falls within the predefined limits. Notably, the peak temperature for R717 substantially exceeds that for R290, as demonstrated in Figure 39. This indicates a higher temperature for R717 post-compression by the compressor in comparison to R290. Furthermore, Figure 40 reveals a significantly lower entropy scale for R290 than for R717. The appendix F further details both P-h and T-s diagrams for R717 and R290 at Q_c values of 61, 67, and 73 [kW], demonstrating the minor variations in VCC with each distinct Q_c . Python script used for plotting P-h and T-s diagram can be found in Appendix H. Appendix 109 displays an example of the extended features of the HP-cycle, by plotting the T-s diagram for 5 [°C] SH and 5 [°C] SC, with R134a as an example.

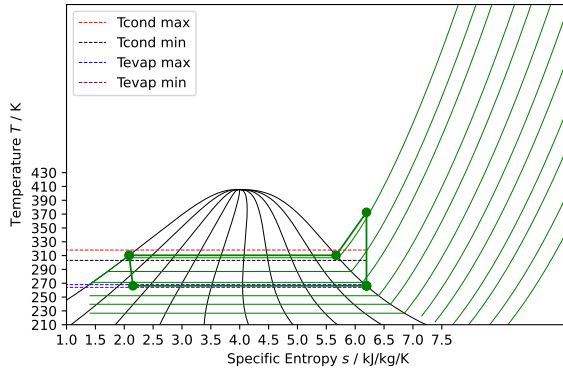


Figure 39: T-s diagram, R717, for Q_c equals 61 [kW], C1.

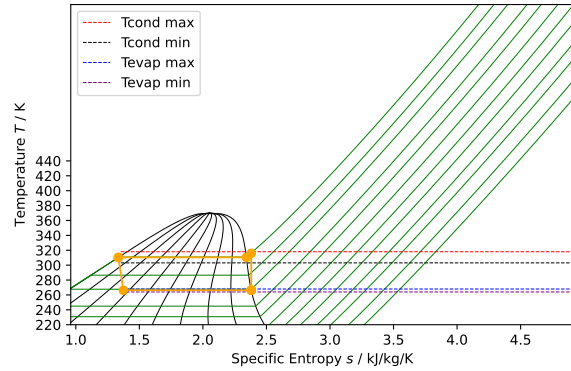


Figure 40: T-s diagram, R290, for Q_c equals 61 [kW], C1.

Figure 41 presents the P-h diagram for R717, showcasing its high temperature in correlation with substantial enthalpy as illustrated in the T-s diagram. The pressure difference between R717 and R290 is insignificant, as Figure 42 displays. Notably, R717 occupies a larger area in the phase domain of saturated vapor and liquid compared to R290. The appendix F further displays P-h diagrams for Q_c values at 61, 67, and 73 [kW] for analysis between different Q_c .

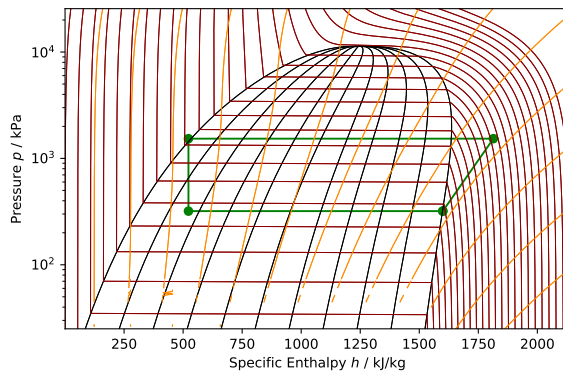


Figure 41: P-h, R717, for Q_c equals 61 [kW], C1.

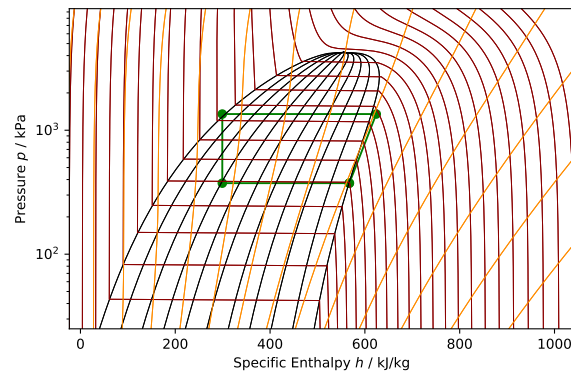


Figure 42: P-h diagram, R290, for Q_c equals 61 [kW], C1.

4.2.2 Case 2

Input values for *Case 2* are presented with Table 14 and Table 17, temperatures for the evaporator and condenser utilized for the calculations are now increased from the first case. Appendix 98 displays how the iterative values from Python were stored in Excel, then plotted.

Table 14: Input values Case 2

Case 2		
Parameter	Value	Unit
T_{wi}	303	K
T_{wo}	318	K
$T_{br,in}$	278	K
$T_{br,out}$	268	K
$T_{cond,init}$	318.05	K
$T_{cond,max}$	328.00	K
$T_{evap,init}$	265.00	K
$T_{evap,max}$	267.95	K

Table 15: Rest of Case 2 input values

Case 2		
Parameter	Value	Unit
SH	0	$^{\circ}C$
SC	0	$^{\circ}C$
n	1	-
U	800	W/m^2K
Ah_{oa}	6.6	m^2
$Ah_{oa,EV}$	10	m^2
U_{EV}	1000	W/m^2K
tol	2.00	%

Case 2

Figure 43 illustrates the Q_c and $Q_{c,rec}$ for results in *Case 2*, and the main difference from *Case 1* is that 12 points are used for measurement instead of 6. Generally the orange points, Q_c are accurate and in this case, it's not necessarily that the higher Q_c the higher deviation. Accuracy on 70 000 [W] as an example to prior values. Figure 44 illustrates COP values for COP and COP_{real} for all three refrigerants. In comparison to *Case 1* one can see that the differences have faded away. There is a small gap with R717, but R290 and R1270 are technically the same. R717 still yields the best COP . Figure 45 indicates small changes in COP and COP_{real} , but the gap has occurred between the COP values. Again length of DP is the main decider in the gap between COP and COP_{real} , because the pump needs to perform more work. R717 highest COP and R1270 next best. Figure 46 indicates a gap between COP and COP_{real} as usual, but there have occurred some strange patterns. But still, a slow decrease of COP and COP_{real} so the results are correct in that regard. Still yields R717 the best COP and R1270 is now the second best.

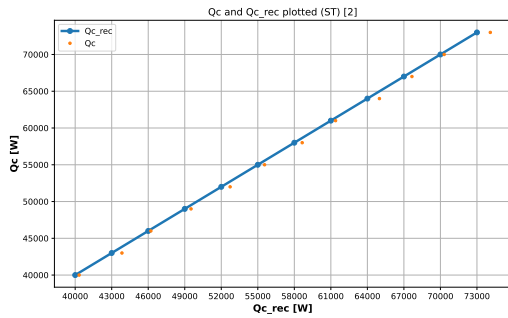
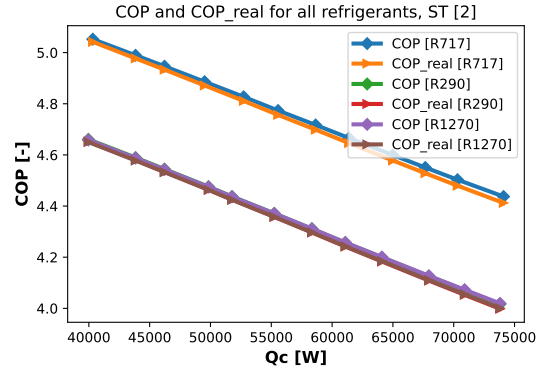
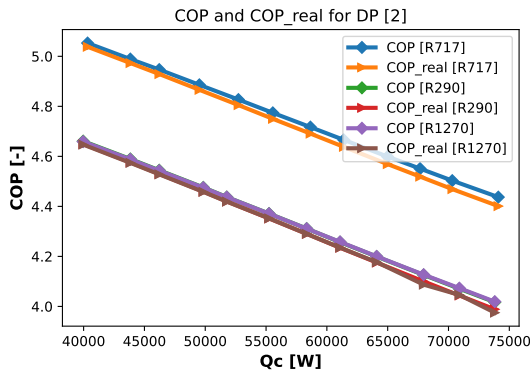
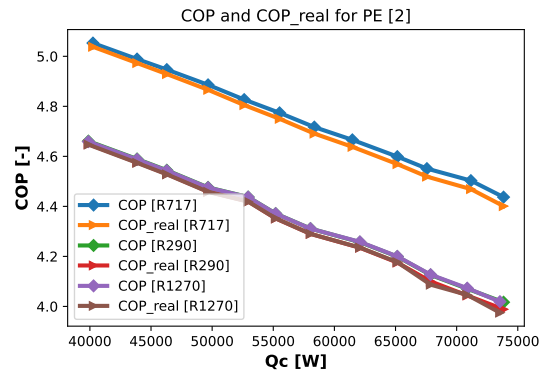
Figure 43: Q_c and $Q_{c,rec}$, C2,ST.Figure 44: COP and COP_{real} for all refrigerants, C2,ST.Figure 45: COP and COP_{real} , C2,DP.Figure 46: COP and COP_{real} all refrigerants, C2,PE.

Figure 47 pictures the water pump power for all three refrigerants in the ST scenario. As anticipated, the difference between the refrigerants is minimal, yet it's clear that ST requires the least pump power compared to the other conditions. In this case, ST demands the lowest, therefore, the most favorable pump power of all three HEs. Each of the three HEs has demonstrated a reduction in pump power from *Case 1*, suggesting that pressure loss and temperature difference are factors at play. The mass flow rate remains consistent between both cases, as demonstrated in Figure 56. Figure 48 illustrates a decrease in pump power from the previous case, with the maximum pump power requirement reduced from over 250 [W] to just above 80 [W]. Consequently, DP follows a similar pattern to ST for *Case 2*. Despite this, DP still demands the highest pump power of all three, attributable to the same previously mentioned factor, length. Figure 49, too, shows a reduction from the previous case, but not significantly, placing it midway between ST and DP in terms of pump power. The PE results also highlight the proximity of each measurement point to one another. While for the other two HEs the symbols fall on the line but at different locations on the x-axis, in the PE case, they are almost precisely at the same point.

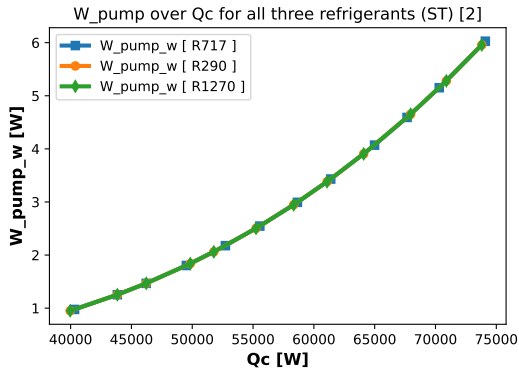


Figure 47: Pump power required, water, C2,ST.

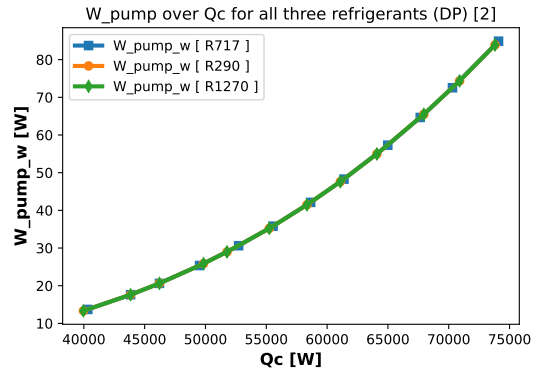


Figure 48: Pump power required, water, C2,DP.

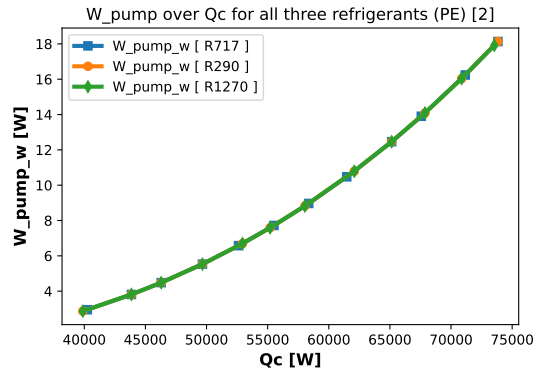


Figure 49: Pump power required, C2,PE.

Figure 50 portrays the brine pump power for ST, characterizing the implications observed in *Case 1*. Here, the brine water is computed to flow through the smaller pipes, while the refrigerant moves through the baffle of the HE. Consequently, a higher pump power is understandable for the evaporator than for the condenser in the ST scenario. In the case of DP, Figure 51 demonstrates a modest reduction in the pump power required for brine compared to water. This decrease is attributable to a reduction in Q since Q_{ev} is less than Q_c , which in turn equals a lower mass flow rate. As a result, with a similar pressure loss for both condensers and the evaporator, the pump requirement will be less. Figure 52 illustrates a pattern consistent with *Case 1*, where the brine pump power requirement closely aligns with the water pump power required for PE.

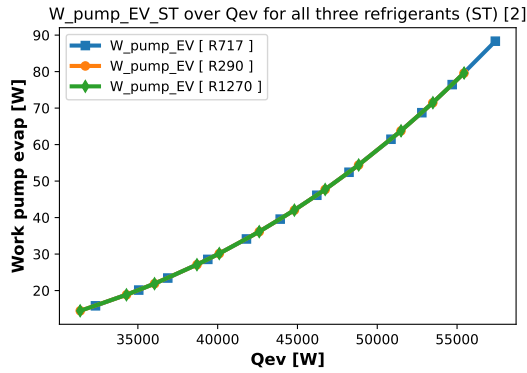


Figure 50: Brine pump power, C2,ST.

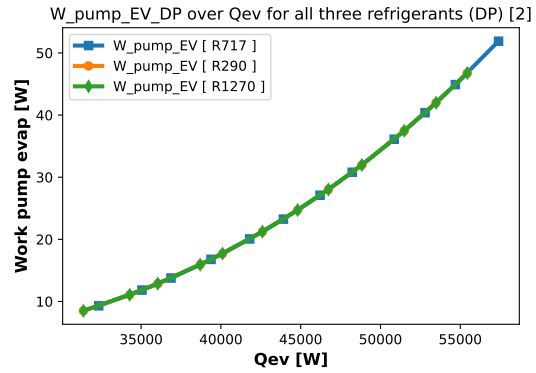


Figure 51: Brine pump power, C2,DP.

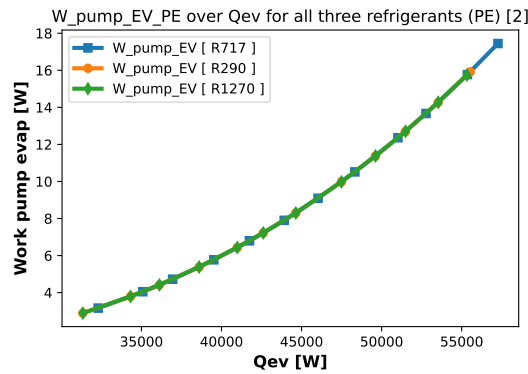


Figure 52: Brine pump power, C2,PE.

Figure 53 demonstrates the efficiency, showcasing a consistent outcome as with ST for *Case 1*, where R717 presents the highest efficiency. There's a slight decrease in efficiency from 0.99 to 0.98 [-] across the two cases. A more considerable gap of 0.04 [-] exists between the efficiencies of the refrigerants in *Case 2* compared to *Case 1*. The gap between R290 and R1270 is also wider, but as the y-axis is expressed in two decimal places, the overall differences remain relatively insignificant. Figure 54 depicts a reversal in efficiency between ST and DP, consistent with the case. The results for DP suggest that R290 and R1270 deliver the highest efficiency, but these differences are again not significant. Figure 55 reflects the significant efficiency drop for PE, similar to previous observations. PE's top efficiency still trails behind the other two HEs in ST and DP. The measurement points remain consistent and closely matched. The principle outlined in section 4.2.1 applies here as well, a greater Δh , and thus a reduced mass flow rate of the refrigerant, yields the best *COP*. Figure 56 presents the mass flow rate for ST HE. Here, R717 stands out as notably smaller, as elaborated in section 4.2.1 via Figure 38. Appendix D.3 and D.4 respectively show the mass flow rate for DP and PE, and illustrate the *COP* for the three refrigerants.

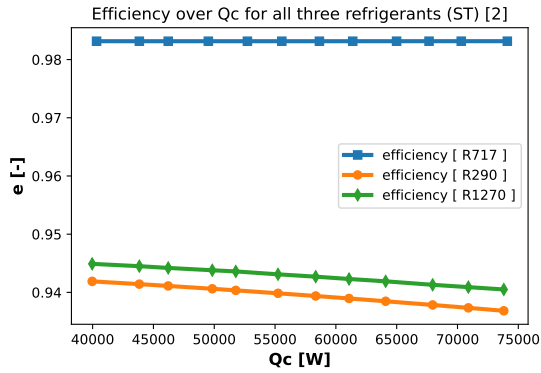


Figure 53: Efficiency for all three refrigerants, C2,ST.

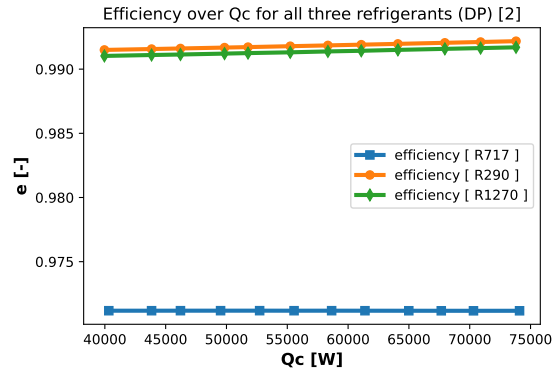


Figure 54: Efficiency for all three refrigerants, C2,DP.

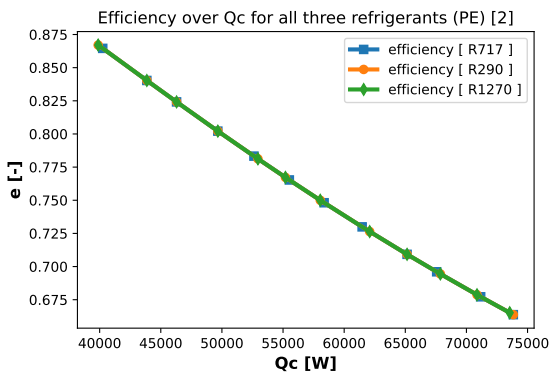


Figure 55: Efficiency for all three refrigerants, C2,PE.

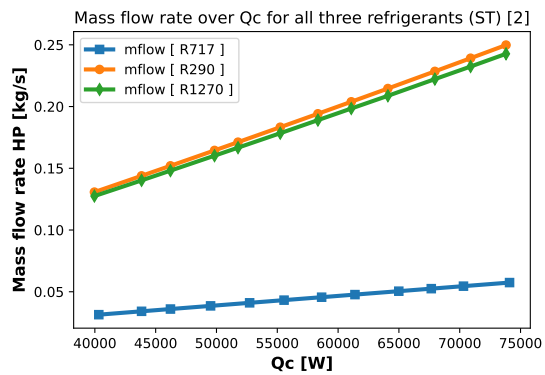


Figure 56: Mass flow rate for all three refrigerants, C2,ST.

Figure 57 illustrates the T-s diagram for R717, and *Case 2* has been calculated with a Q_c value of 61 [kW]. The temperature limits have now increased, as pictured in Figure 57. Observe can be made that the condenser temperature is approximately in the middle of the temperature limits, and the high temperature after the compressor is clearly visible. In Figure 58, R290 is positioned at the upper end of the temperature limits. Once again, a low-temperature lift is necessary for R290. The difference in the saturation curve can be observed in the figures. Appendix G presents the T-s and P-h diagrams for both refrigerants, corresponding to Q_c values of 61, 67, and 73 [kW].

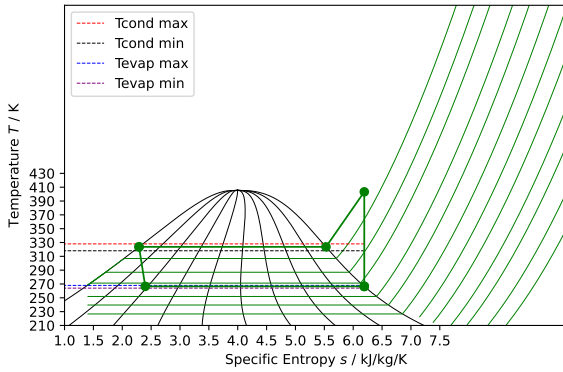


Figure 57: T-s diagram, R717, for Q_c equals 61 [kW], C2.

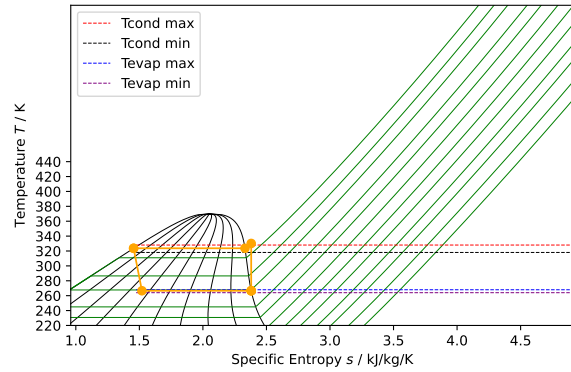


Figure 58: T-s diagram, R290, for Q_c equals 61 [kW], C2.

The P-h diagram for R717, reflecting a Q_c value of 61 [kW], is illustrated in Figure 59. As anticipated, there is an escalation in pressure from *Case 1*. Once again, we observe significantly higher enthalpy values for R717. Correspondingly, Figure 60, with an equivalent Q_c of 61 [kW], demonstrates that the pressure of R290 has also risen, with the values aligning roughly as anticipated. The P-h and T-s diagrams for both refrigerants, featuring Q_c values of 61, 67, and 73 [kW], are presented in Appendix G.

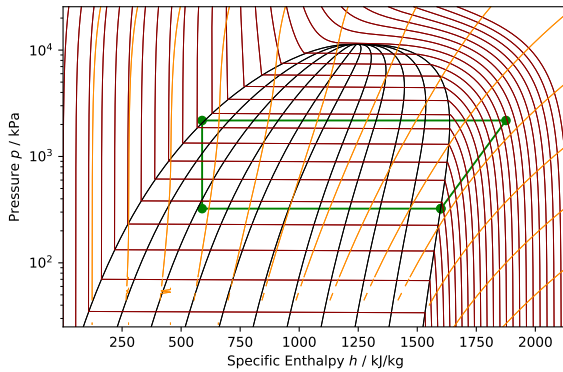


Figure 59: P-h diagram, R717, for Q_c equals 61 [kW], C2.

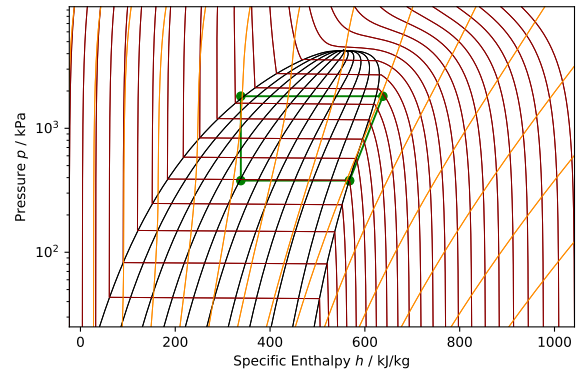


Figure 60: P-h diagram, R290, for Q_c equals 61 [kW], C2.

4.2.3 Case 3

For *Case 3* the input values listed in Table 16 and Table 17 are utilized.

Table 16: Input values Case 3

Case 3		
Parameter	Value	Unit
T_{wi}	313	K
T_{wo}	333	K
$T_{br,in}$	278	K
$T_{br,out}$	268	K
$T_{cond,init}$	333.05	K
$T_{cond,max}$	343.00	K
$T_{evap,init}$	265.00	K
$T_{evap,max}$	267.95	K

Table 17: Rest of Case 3 input values

Case 3		
Parameter	Value	Unit
SH	0	$^{\circ}C$
SC	0	$^{\circ}C$
n	1	-
U	800	W/m^2K
Ah_{oa}	6.6	m^2
$Ah_{oa,EV}$	10	m^2
U_{EV}	1000	W/m^2K
tol	2.00	%

Case 3

For *Case 3* only significant differences in patterns or trends will be thoroughly commented. *Case 3* is mainly computed to analyze if trends do continue, and how much COP and other parameters drops. P-h and T-s diagram is not shown in the results for *Case 3* but follows the trend of previous cases.

Figures 61, 62, and 63 illustrate a subtle disparity between COP and COP_{real} , coupled with a notable overall decrease in COP from the two preceding cases. As temperature differences rise, the disparity between each COP and COP_{real} diminishes.

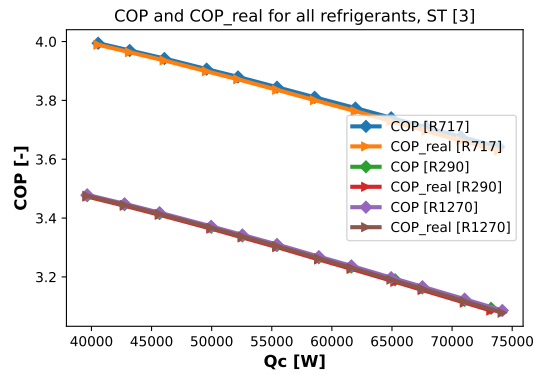


Figure 61: COP and COP_{real} for all refrigerants, C3,ST.

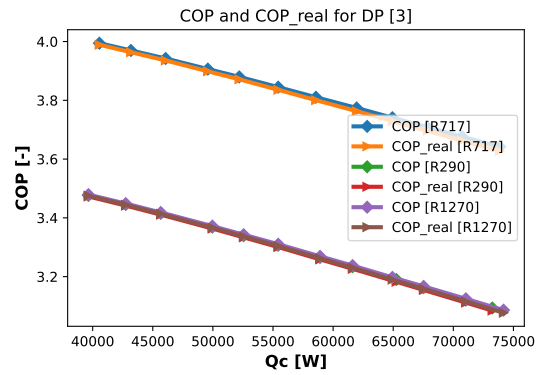


Figure 62: COP and COP_{real} for all refrigerants, C3,DP.

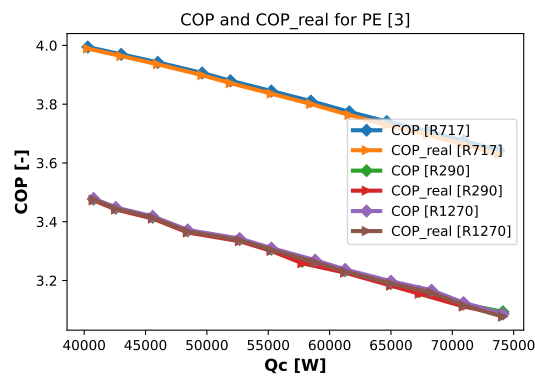


Figure 63: COP and COP_{real} for all refrigerants, C3,PE.

Figures 64, 65, and 66 confirm the continued decline in pump power, in line with the previous trends. The pump power necessary for ST, as pictured in Figure 64, is low. The reduction in mass flow rate is now distinctly noticeable, as elaborated in section 5.1. DP produces the highest pump power by a clear margin.

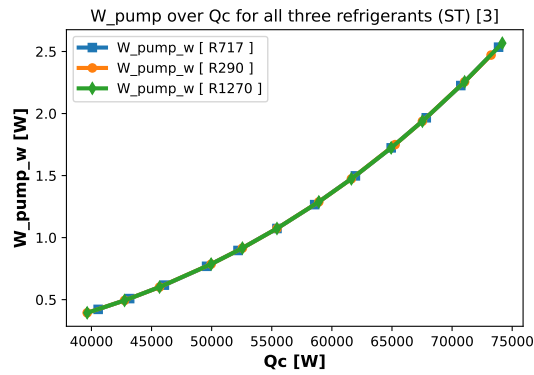


Figure 64: Water pump power for all refrigerants, C3,ST.

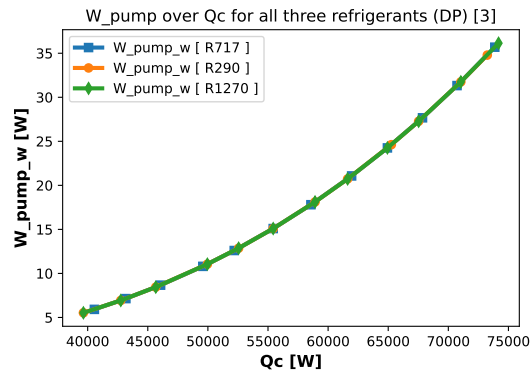


Figure 65: Water pump power for all refrigerants, C3,DP.

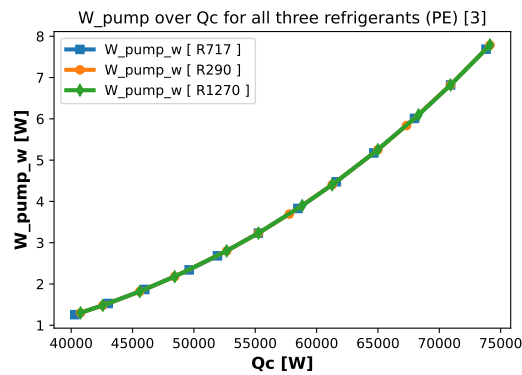


Figure 66: Water pump power for all refrigerants, C3,PE.

Figures 67, 68, and 69 consistently maintain the identified trend. ST has the greatest range of pump power required to brine water through the HE, flowing past in the tubes. Specifically, Figure 69 reveals that the brine power required for PE is comparable to the power demanded by the water pump, whereas, for ST and DP, an increase is observable.

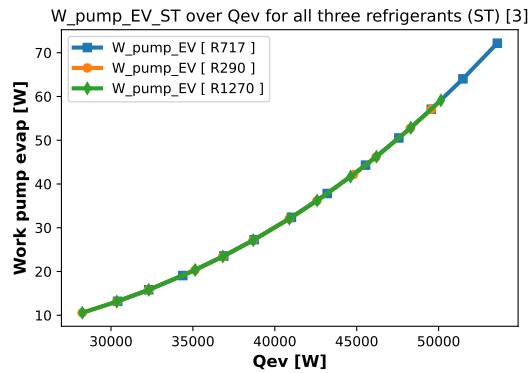


Figure 67: Brine pump power for all refrigerants, C3,ST.

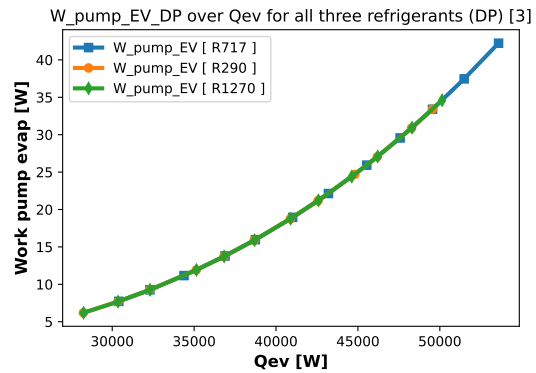


Figure 68: Brine pump power for all refrigerants, C3,DP.

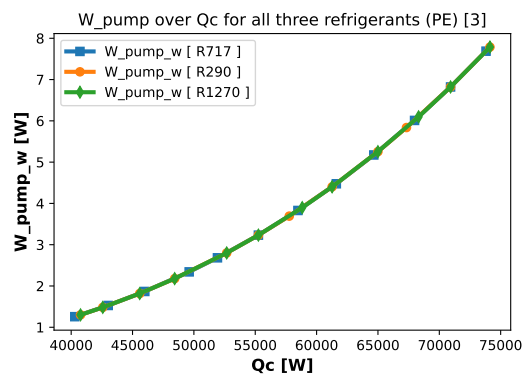


Figure 69: Brine pump power for all refrigerants, C3,PE.

Figure 70 presents a marginal efficiency distinction between R290 and R1270, yet R717 maintains a superior efficiency status. The decline is more pronounced for R290 and R1270 relative to R717. Within Figure 71, the peak efficiency is achieved by R290 and R1270, although R717 is only slightly lagging. The gap between the lowest and highest efficiency is significantly greater for ST compared to DP. Figure 72 continues to exhibit a steep reduction in efficiency, however, the starting efficiency value is higher than those observed in preceding cases. Appendix D.5 and D.6 display the mass flow rate for DP and PE, ST is similar to DP.

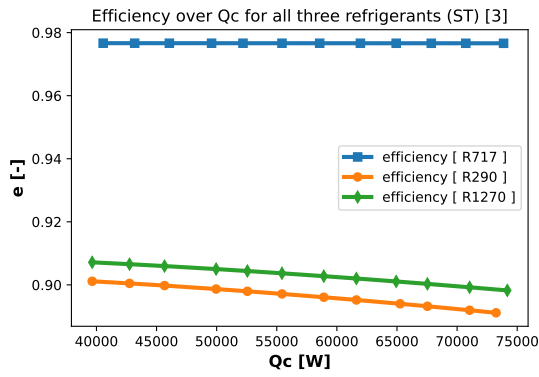


Figure 70: Efficiency for all refrigerants, C3,ST.

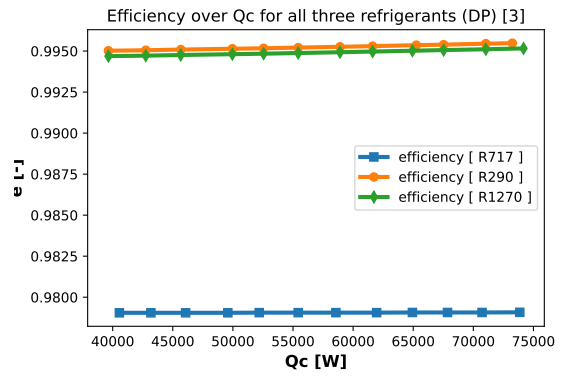


Figure 71: Efficiency for all refrigerants, C3,DP.

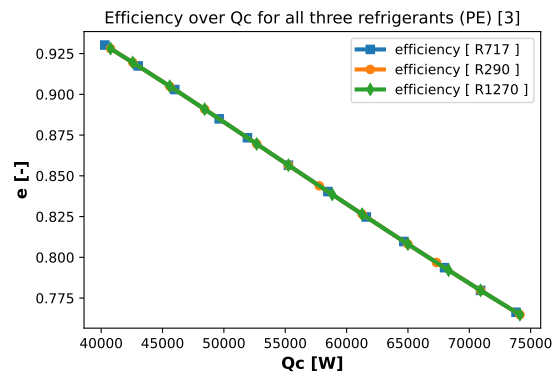


Figure 72: Efficiency for all refrigerants, C3,PE.

4.3 Web page with Streamlit

Streamlit enables the execution of the three cases in Python through its web platform via a local host. Presenting results as a web page serves as a more appealing approach for displaying outcomes by developing an 'Online Modeling Tool' that could potentially be more comprehensible or user-friendly for individuals without Python experience, to fulfill the stated objective of the thesis. Following discussions with Ole Døsvik from the survey, he elaborated on how the web page offers a way to present results to, for instance, a project's leadership using a more simplified approach, rather than revealing complex IDA-ICE graphs or calculations or graphs from CoolPack. A web page can be configured with parameters such as Q_c , refrigerant, and type of HE while excluding other variables, allowing users to adjust these three values as desired while ensuring that the script owner's crucial components remain unchanged, preventing calculation errors. Additionally, an 'Online Modeling Tool' represents an initial step toward a resource that can be utilized for educational purposes, as outlined in the task. Visual aids can assist students in comprehending how the heat pump cycle varies with different input values. Figure 73 and 74 display the aesthetics of the web page before pressing *Generate Plots* and thereby running the script. Figure 75 and 76 illustrate the table showing the value for each favorable parameter and the first pots.

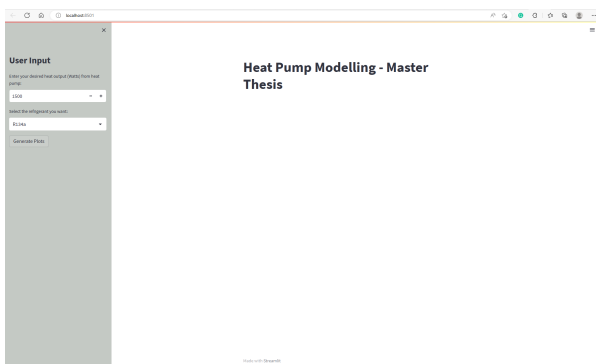


Figure 73: First to see when opening web page.

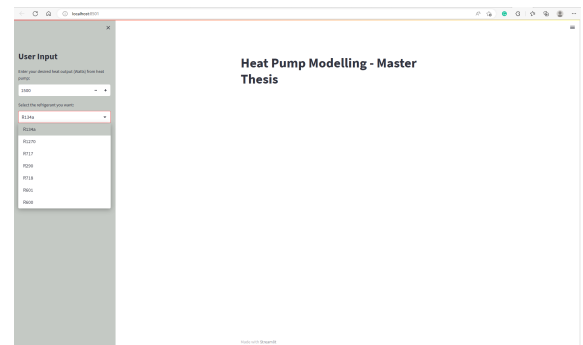


Figure 74: Showing available refrigerants to choose from

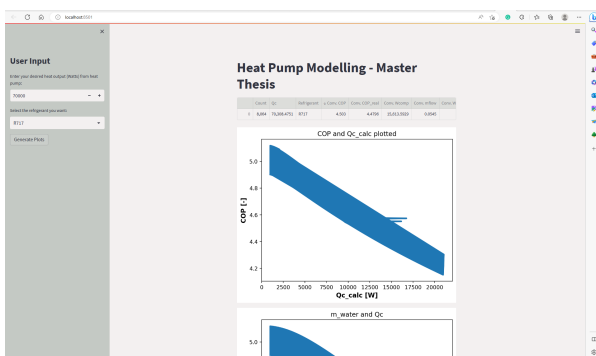


Figure 75: Shows a table of the count, Q_c , etc.

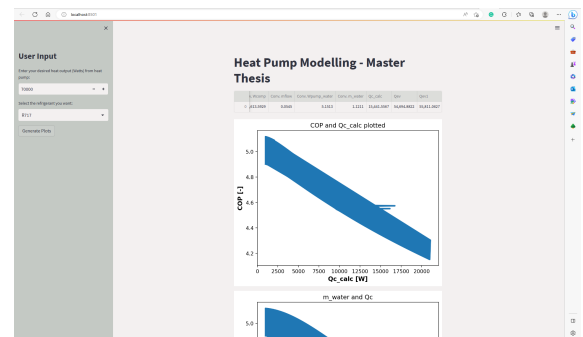


Figure 76: More information of output and start of tables.

The difference between the evaporator heat transfer rates Q_{ev} and Q_{ev1} , equations explained in section 3.6, is plotted to illustrate the decreasing trend of both the difference and the overall evaporator heat transfer rate, in the quest for convergence. Figure 78 showcases the necessary heat transfer for the condenser represented by the orange line, alongside the boundaries for maximum and minimum Q_c , denoted by the blue lines, as well as the variation in the evaporator heat transfer rate.



Figure 77: Q evaporator difference.

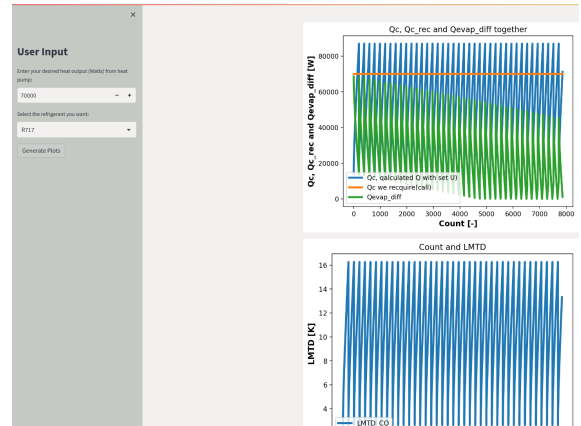


Figure 78: Q condenser and required, with evaporator difference.

The variation of the LMTD within a specific temperature range is demonstrated through calculations presented in Figure 79. The modulation of temperatures in the condenser and evaporator is shown in Figure 80. The temperature of the condenser escalates until it reaches a maximum temperature, then it resets and starts the cycle anew from the initial temperature. Conversely, the evaporator temperature consistently rises to ensure convergence with the lowest temperature lift, thereby maximizing the COP , until it hits maximum temperature, then stops.

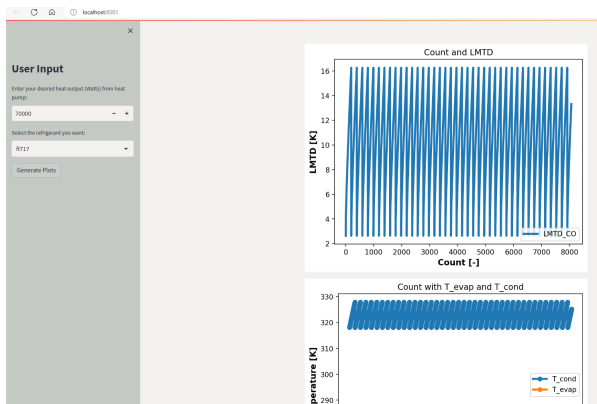


Figure 79: The change in LMTD.

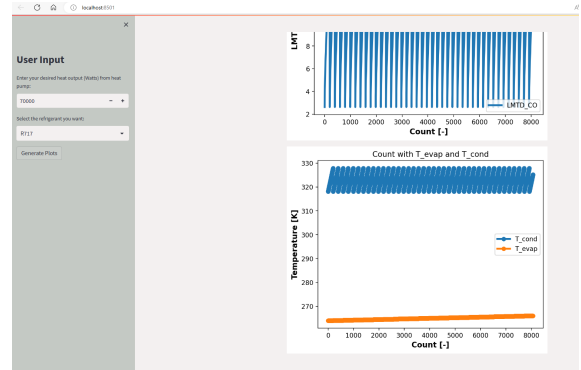


Figure 80: The change of temperature for condenser and evaporator.

5 Discussion

This section discusses some thoughts and reflections regarding the results, components, and general thermodynamics of the thesis.

5.1 Results and cases

Initially, concerns were raised when the required pump power peaked for *Case 1*. However, analyzing the parameters utilized to calculate pump power, the results were encouraging. The Q_c and $Q_{c,rec}$, were consistent across all cases, the primary variable being the inlet and outlet temperatures of the HEs, specifically 20-30 [°C], 30-45 [°C], and 40-60 [°C] with the initial condenser temperature set at 0.05 [K] above the outlet temperature of the HEs. Given the similar Q_c values, this provided a valid comparison between different HEs. In the case of mass flow rate, it would have been intriguing to investigate varying Q_c values with a wider disparity and assess the changes in pump power and mass flow rate.

The pump power for water in the condenser and brine in the evaporator depends on four parameters: mass flow rate, pressure loss, density, and efficiency. The efficiency remained constant at 0.80 [–] across all cases, and water density exhibited minimal variation. The brine water was held constant to the same glycol, 40 [%], mixture across all cases, hence remaining unchanged. It would also be worthwhile to explore how pump power might vary with different glycol mixtures and consequent changes in density to reduce it to the lowest possible level. Thus, pressure loss and mass flow rate become the variable parameters. As explained in section 3.6, these parameters were detailed and expressed through equations. Considering mass flow rate, it's evident that Q_c divided by the product of C_p and temperature indeed decreases if C_p is multiplied by a greater temperature difference in each case. The mass flow rate also affects the water velocity used in the pressure loss calculations, resulting in a slower fluid velocity if a reduction in mass flow rate ensues. From equation 97 in section 3.6, one can detect that a decrease in mass flow rate corresponds to a reduction in pressure loss. This results in a smaller value being divided by two *stable factors*, namely efficiency and density. Consequently, it would be compelling to examine and investigate different cases where density and efficiency are the primary variables and mass flow rate remains relatively constant.

The HE in the evaporator will have a pump power with a small source of error. When the cases were run the evaporator area was computed to be 10 [m^2]. That is totally fine in itself, but calculations are performed with diameters and parameters connected to a HE with an area of 6.7 [m^2]. Then questions can be asked as to how much would the pipe calculations change with diameters and other parameters increased to reach a 3.3 [m^2] greater area. These parameters affect calculations such as $W_{pump,EV}$, but the general patterns and trends would most likely be the same. Probably would the $W_{pump,EV}$ be ten percent higher in each case, but differences are the same. This could have been fixed with separate input values for the evaporator and the condenser and more precise values would be gathered with this integration. For now, this will remain as future work.

The HE in the evaporator carries a minor margin of error regarding pump power. When the cases were executed, the evaporator area was computed to be 10 [m^2]. Although acceptable on its own, computations were conducted using diameters and parameters associated with a HEs of 6.7 [m^2], for the condenser. This leads to questioning how much the pipe calculations would adjust if the diameters and other parameters were increased to account for an additional 3.3 [m^2]. These parameters influence calculations such as $W_{pump,EV}$, however, the general patterns and trends are likely to remain even with this minor error. It's possible that the

$W_{pump, EV}$ could be approximately five to ten percent higher in each case, with differences being consistent. This discrepancy could have been rectified by assigning separate input values for the evaporator and the condenser, thus gathering more precise values with this integration. For now, addressing this remains a future task.

5.2 User-friendliness

The user-friendliness of the Python code is hard to draw strong conclusions from the two individuals questioned. Both individuals have more head of apartment responsibilities in their respective companies, and thus it seems logical that they have more responsibility over many subjects and does not become expert at one simulation tool. Would assume Python also is a tool where each company has two or three individuals that are experts and have high skill sets in a programming language. Then other individuals send cases and ask them to compute the wished scenarios, to save time.

5.3 Web page

The process of developing a web page linked to a code was extensive and thus, had fewer details. Given more time, the subsequent step would involve making the URL accessible even without the Python script owner having Python active on their personal computer. This would require a Streamlit subscription and some script modifications. Furthermore, incorporating more adjustable parameters in the sidebar would allow more direct changes on the web page itself. Initially, the intention was to display the plots and potential capabilities on the web page. Interestingly, one expert under interviews expressed a preference for a web page as a method to present results, thus highlighting the potential value of a web page as a project showcase.

5.4 Phase change on refrigerant

The refrigerant goes through phase changes between the compressor and the expansion valve. This results in the refrigerant either being saturated vapor, vapor-liquid mixture, or liquid. The equations with regard to flow patterns such as Re, Nu, and Prandtl number can differentiate between the different phases. These equations are applicable to saturated vapor and liquid, but for instances where a refrigerant operates as a vapor-liquid mixture, the equations should ideally take into account the 'X', which varies from 0 - 1 dependent on the mixture. This change was difficult to implement with the given time to the thesis because other aspects of the code were deemed more important, such as creating an iterative loop and making the results available on a web page. There would be more accurate calculations if 'X' was integrated into the equations, but again more types of HEs for comparison and other aspects were prioritized.

5.5 Choice of refrigerant

R744 was excluded from the iterative process due to its low critical temperature, which rendered it unsuitable for the tests conducted with refrigerants above its critical point in this thesis. However, R744 operates without error in the *HPmain* script, provided that the condenser temperature is set below its critical temperature from the user. If it were not for its low critical temperature, R744 would likely have been included in the convergence results. However, to do so, one of the three selected refrigerants would need to be replaced. A case could be made to substitute R290, which has a higher GWP than R744 and poses a fire risk, making it less safe. R717 would not be replaced with R744 due to its low GWP, zero ODP, and negligible fire risk. R718 was unsuitable

because its minimum temperature is too high. If the evaporator temperature drops below 274 [K], an error message will appear because it is out of range for R718. Since the convergence was tested with an evaporator temperature of 264 [K], below the critical minimum of R718, it was excluded. R718, however, has a high critical temperature for the condenser, low GWP and ODP, and poses no fire risks. For future projects, R744 and R718 should be given priority for analysis.

5.6 LMTD

The difference in LMTD between parallel and counter flow configurations varies minimally, by only 0.2 - 0.3 [K] This is attributed to the heat transfer being predominantly via phase-changing refrigerant as explained, and thus by conduction. The code can change the LMTD differences if the exit temperature of the condenser, T_3 , is adjusted to a lower value by manually setting T_3 . That should be done if a user wants to perform research on how LMTD could theoretically impact the calculations, but the heat transfer would then probably be more by loss of temperature, comes to mind.

5.7 Components

The script allows for more precise calculations of compressors, by integrating various types like scroll or piston compressors. However, it's worth noting that compressors are complex components, and the time required for detailed research and calculations referring to them was not available. More accurate pressure computations and heat loss analysis from the compressor would be desirable, as well as an investigation into whether the choice of compressor could have any influence on HEs.

The selection of HEs appeared to be appropriate with regard to choosing the most popular HEs. As the thesis progressed and further research was performed, these three HEs emerged consistently, indicating their widespread use and relevance. The inclusion of the most commonly used HEs in Norway was interesting, and to gain insights into components likely to be encountered in professional practice.

5.8 Efficiency

The efficiency of the PE appears lower than anticipated, suggesting a possible source of error with the applied equations. This doesn't imply it is 100 percent an error, just the significant drop was unexpected, prompting reflection on the potential causes. The task of identifying accurate equations connected to PE and efficiency proved challenging. Many formulas utilized in research articles consistently yielded an outcome of 1.0 [-], despite alterations in parameters that should have notably affected efficiency, hence ruling out a constant 1.0 [-] result. Consequently, the steep decline and drop in efficiency for PE might be attributed to some sort of small error, compared to the efficiency equations used for the other two HEs.

5.9 Darcy friction factor

The main reason for using the same equation for Haaland's friction factor was because Re almost every time occurred to be above 10 000, which results in the Nu not taking f into account when computing a value. Other articles also performed calculations by using the same equation for both single-phase and two-phase. Because this is wanted to be illustrated and made known to the user, Haaland's friction factor with adjustment for two-phase is put into the script but just commented out. Since f does impact the pressure loss, it would be interesting to see the difference between using specified equations for single-phase and specified equations for double-phase. Then research the gap between values.[84] [85]

5.10 Overall heat transfer coefficient

In this thesis, the overall heat transfer coefficient is confined to a range of 600 - 1200 $[W/m^2K]$. Although the PE for example can attain a significantly higher U , it was necessary to cap it at this range for comparative purposes. This is because the ST is unable to reach the same high values of 4000 - 5000 $[W/m^2K]$ as the PE. To facilitate an equal comparison of results, it was thus necessary to maintain uniformity in the U -values across different exchanger types. There could maybe be run cases with higher U for PE and then adjusting the area of the two other HEs and analyzing the results. Would be interesting to see the impact, because a thought then is that PE would yield the lowest pump power, since ST is increased with regard to area and diameter. [56]

5.11 Possibilities the script provide

An additional feature of the *HPmain* script worth noting is the option to compute a new U -value. This involves first calculating the Q_c using the initial area A , $U_{initial}$, and $LMTD$. The computed Q_c is then used to determine the mass flow rate, leading to detailed calculations of flow patterns and consequently, the h . This then yields a revised U -value for the Q_c equation. This process is particularly useful for verifying the feasibility of the initial U -value based on the given parameters. For instance, if a high initial U of 4000 $[W/m^2 * K]$ is selected, subsequent calculations might reveal that the chosen pipe diameter is insufficient to achieve this value. This underscores the importance of considering the impact of pipe diameters and HEs on flow patterns in calculations. This calculation yields the most accurate results the less phase change the refrigerant is required to go through, meaning the higher pressure the higher accuracy of the U -value.

6 Conclusion

Numerous results and gathered information are used to conclude the work in this study. The Python script has been significantly improved, incorporating more precise entropy and enthalpy values into a basic HP cycle script. This improvement for instance enables the calculation of seven points from a T-s diagram instead of four, by acknowledging SH and SC. The modified script can also display the critical temperature and critical pressure for the calculated refrigerant. The principal enhancement is the capability to extensively calculate a wide array of parameters for the ST, DP, and PE, including Re , h_{new} , NTU, efficiency, and more. This script operates seamlessly in both Spyder and Visual Studio Code, showing its accessibility to users customized to different programming environments. Discussion with building industry experts Jørn Stene and Ole Døsvik, with no prior knowledge of Python, stated that operating the script would be manageable, making modifications would be just too challenging, signifying its level of user-friendliness to use but not modify, however, this is subjective. In-depth discussions with Jørn Stene and Ole Døsvik provided valuable insights about the industry's preference for counter-flow and PE and the importance of parameters like mass flow rate and temperatures. It was also revealed that Python is indeed utilized in companies, predominantly by the younger generation. Validation of the script using CoolTools found all parameters, except volumetric flow and density, to fall within a 5[%] deviation.

For Q_c and $Q_{c,rec}$ values can occur with higher precision than 1.5 - 2 percent, at significant Q_c values, concluding that precision doesn't necessarily decrease by higher Q_c values. The VCC revealed variations of enthalpy and entropy values for R717 and R290, with R717 yielding significantly higher values than those for R290. Pressure values in the VCC were relatively similar between R290 and R717. Refrigerant R717 yielded the highest COP through all results and consistently provided a COP of 0.2 - 0.6 [-] better than R290 and R1270. A conclusion is R717 yields higher Δh and therefore lower mass flow rate.

The difference between cases displayed that *Case 3* yielded a reduction of 2.4 - 2.8 [-] compared to *Case 1* regarding COP . Refrigerant R1270 had in most cases the second-best COP and R290 the lowest, but these two refrigerants behaved similarly regarding results. The highest gap between COP and COP_{real} was for DP, because of the length. Therefore water pump power required results to be greatest for DP for the same reason, length. Consistently lowest pump power required is ST, because of its minimal length and minimal pressure loss. Brine pump power and water pump power are greatest for *case 1* and decrease for each case, because of similar Q_c and increased temperature difference, which was an interesting finding. For ST R717 yield the highest efficiency, but regarding DP the greatest efficiency was with R290, and R717 smallest but by fine margins. PE consistently yielded the lowest and steepest decline in efficiency across all cases, but efficiency for PE did yield higher efficiency for *Case 3* compared to *Case 1*. C_p was a parameter with interesting findings, where smaller C_p impacts the pump power for water in the condenser and brine water-glycol mixture in the evaporator.

Streamlit was utilized to make the code available online, although the web page lacks a dedicated URL, requiring the script to be open in Python for displaying the web page. Nevertheless, the web page serves as a valuable tool for demonstrating various parameters, such as changes in condenser temperatures and illustrating results in a better format, as Ole Døsvik answered in the interview.

7 Acknowledgements

Want to state that a new tool has been used in some aspects of this thesis.

- ChatGPT has been used to replace Grammarly. Only correcting grammar errors, not writing any text.
- ChatGPT has also been used to help create figures in overleaf latex, replacing searching for answers in youtube videos.

References

- [1] C. Davis, “Ground source heat pump for flats,” 29.07.2016. [Online]. Available: <https://phpdonline.co.uk/features/ground-source-heat-pump-flats/>
- [2] C. P. Morice, J. J. Kennedy, N. A. Rayner, J. Winn, E. Hogan, R. Killick, R. Dunn, T. Osborn, P. Jones, and I. Simpson, “An updated assessment of near-surface temperature change from 1850: The hadcrut5 data set,” *Journal of Geophysical Research: Atmospheres*, vol. 126, no. 3, pp. 15–17, 2021. [Online]. Available: <https://doi.org/10.1029/2019JD032361>
- [3] FN-Samandet. (2022) Klimaendringer. [Accessed 24-Feb-2023]. [Online]. Available: <https://www.fn.no/tema/klima-og-miljoe/klimaendringer>
- [4] L. C. M. Eberhardt, H. Birgisdottir, and M. Birkved, “Potential of circular economy in sustainable buildings,” vol. 471, no. 9. IOP Publishing, 2019, pp. 7–9. [Online]. Available: <https://doi.org/10.1088/1757-899X/471/9/092051>
- [5] S. Erdogan, “Dynamic nexus between technological innovation and building sector carbon emissions in the brics countries,” *Journal of Environmental Management*, vol. 293, pp. 1–4, 2021. [Online]. Available: <https://doi.org/10.1016/j.jenvman.2021.112780>
- [6] R. H. Crawford, “Greenhouse gas emissions of global construction industries,” vol. 1218, no. 1, pp. 1–3, 2022.
- [7] E. Comission. (2021) Nearly zero-energy buildings. [Accessed 21-Feb-2023]. [Online]. Available: https://energy.ec.europa.eu/topics/energy-efficiency/energy-efficient-buildings/nearly-zero-energy-buildings_en
- [8] RICS, “Maintenance and update of the eu building stock observatory,” 2022.
- [9] Eurostat. (2022) Electricity and gas prices in the first half of 2022. [Accessed 22-Feb-2023]. [Online]. Available: <https://ec.europa.eu/eurostat/web/products-eurostat-news/-/ddn-20221031-1>
- [10] EMBER. (2021) Average monthly electricity wholesale prices in selected countries in the european union (eu) from january 2020 to january 2023. [Accessed 22-Feb-2023]. [Online]. Available: <https://www.statista.com/statistics/1267500/eu-monthly-wholesale-electricity-price-country/>
- [11] FN-Samandet. (2020) Parisavtalen. [Accessed 24-Feb-2023]. [Online]. Available: <https://www.fn.no/om-fn/avtaler/miljoe-og-klima/parisavtalen>
- [12] IEA. (2022) Increase in heat pumps sales in selected regions, 2021 relative to 2020. [Accessed 20-Feb-2023]. [Online]. Available: <https://www.iea.org/data-and-statistics/charts/increase-in-heat-pumps-sales-in-selected-regions-2021-relative-to-2020>
- [13] D. Zijdemans, *Vannbaserte oppvarmings- og kjøleystemer*, 2nd ed. Nemitek AS, 2014.
- [14] H. Sadeghi, A. Ijaz, and R. M. Singh, “Current status of heat pumps in norway and analysis of their performance and payback time,” *Sustainable Energy Technologies and Assessments*, vol. 54, pp. 0–3, 2022.

- [15] NOVAP. (2022) Om varmepumper. [Accessed 24-Feb-2023]. [Online]. Available: <https://www.novap.no/om-varmepumper>
- [16] J. Rosenow, D. Gibb, T. Nowak, and R. Lowes, "Heating up the global heat pump market," *Nature Energy*, vol. 7, no. 10, pp. 901–904, 2022.
- [17] ENOVA. (2023) varmepumper. [Accessed 20-May-2023]. [Online]. Available: <https://www.enova.no/privat/alle-energitiltak/varmepumper/>
- [18] L. Yanda, Z. Yuwei, and N. Razmjooy, "Optimal arrangement of a micro-chp system in the presence of fuel cell-heat pump based on metaheuristics," *International Journal of Ambient Energy*, pp. 1–12, 2020.
- [19] X. Cao, X. Liang, L. Shao, and C. Zhang, "Performance analysis of an ejector-assisted two-stage evaporation single-stage vapor-compression cycle," *Applied Thermal Engineering*, pp. 11–805, 2022.
- [20] S. Ioan and C. Sebarchievici, "General review of ground-source heat pump systems for heating and cooling of buildings," *Energy and buildings*, vol. 70, pp. 441–454, 2014.
- [21] S. Malavika, C. Chiranjeevi, Y. R. Sekhar, T. Srinivas, M. Natarajan, W. P. P. Myo, and A. Singh, "Performance optimization of a heat pump for high temperature application," *Materials Today: Proceedings*, vol. 46, pp. 5278–5285, 2021.
- [22] D. Junqi, W. Yibiao, J. Shiwei, Z. Xianhui, and H. Linjie, "Experimental study of r744 heat pump system for electric vehicle application," *Applied Thermal Engineering*, vol. 183, p. 116191, 2021.
- [23] W. Cai, F. Wang, J. Liu, Z. Wang, and Z. Ma, "Experimental and numerical investigation of heat transfer performance and sustainability of deep borehole heat exchangers coupled with ground source heat pump systems," *Applied Thermal Engineering*, vol. 149, pp. 975–986, 2019.
- [24] F. Alsouda, N. S. Bennett, S. C. Saha, F. Salehi, and M. S. Islam, "Vapor compression cycle: A state-of-the-art review on cycle improvements, water and other natural refrigerants," *Clean Technologies*, vol. 5, no. 2, pp. 584–608, 2023.
- [25] H. Li and K. Tang, "A comprehensive study of drop-in alternative mixtures for r134a in a mobile air-conditioning system," *Applied Thermal Engineering*, vol. 203, p. 117914, 2022.
- [26] Z. Zhang, X. Feng, D. Tian, J. Yang, and L. Chang, "Progress in ejector-expansion vapor compression refrigeration and heat pump systems," *Energy Conversion and Management*, vol. 207, p. 112529, 2020.
- [27] A. Ustaoglu, B. Kursuncu, M. Alptekin, and M. S. Gok, "Performance optimization and parametric evaluation of the cascade vapor compression refrigeration cycle using taguchi and anova methods," *Applied Thermal Engineering*, vol. 180, p. 115816, 2020.
- [28] C. Vering, M. Engelpracht, S. Göbel, S. Hoseinpoori, F. Wüllhorst, C. Schwenzer, M. Rademacher, S. Hinrichs, F. Chandra, P. Mehrfeld *et al.*, "Open-source vapor compression library (vclib): Heat pump modeling for education and research," *Computer Applications in Engineering Education*, vol. 30, no. 5, pp. 1498–1509, 2022.

- [29] J. Persson and M. Westermarkb, "Simultaneous production of domestic hot water and space cooling with a heat pump in a swedish passive house," in *25th International Conference on Efficiency, Cost, Optimization and Simulation of Energy Conversion Systems and Processes, ECOS 2012, Perugia, Italy, 26 June 2012 through 29 June 2012*, vol. 7, 2012, pp. 251–260.
- [30] J. Clauß, S. Stinner, I. Sartori, and L. Georges, "Predictive rule-based control to activate the energy flexibility of norwegian residential buildings: Case of an air-source heat pump and direct electric heating," *Applied Energy*, vol. 237, pp. 500–518, 2019.
- [31] J. Ling, H. Qiao, A. Alabdulkarem, V. Aute, and R. Radermacher, "Modelica-based heat pump model for transient and steady-state simulation using low-gwp refrigerants," 2014.
- [32] M. Verdnik, R. Rieberer, and H. Moisi, "Trans-critical vapor compression cycle using butane (r600) as refrigerant for industrial waste heat recovery," in *Proceedings of the 25th IIR International Congress of Refrigeration*, 2019.
- [33] D. Qian and Z. O'Neill, "Modelica-based dynamic modeling of a solar-powered ground source heat pump system: A preliminary case study," in *Proceedings of The American Modelica Conference 2018, October 9-10, Somberg Conference Center, Cambridge MA, USA*, no. 154. Linköping University Electronic Press, 2019, pp. 85–92.
- [34] U. Camdali, M. Bulut, and N. Sozbir, "Numerical modeling of a ground source heat pump: The bolu case," *Renewable Energy*, vol. 83, pp. 352–361, 2015.
- [35] B. Luo and P. Zou, "Performance analysis of different single stage advanced vapor compression cycles and refrigerants for high temperature heat pumps," *International Journal of Refrigeration*, vol. 104, pp. 246–258, 2019.
- [36] M. M. Ozturk, B. Doğan, and L. B. Erbay, "Performance assessment of an air source heat pump water heater from exergy aspect," *Sustainable Energy Technologies and Assessments*, vol. 42, p. 100809, 2020.
- [37] T. K. Ritschel, J. Gaspar, and J. B. Jørgensen, "A thermodynamic library for simulation and optimization of dynamic processes," *IFAC-PapersOnLine*, vol. 50, no. 1, pp. 3542–3547, 2017.
- [38] S. S. Vali, T. P. Setty, and A. Babu, "Analytical computation of thermodynamic performance parameters of actual vapour compression refrigeration system with r22, r32, r134a, r152a, r290 and r1270," in *MATEC Web of Conferences*, vol. 144. EDP Sciences, 2018, p. 04009.
- [39] P. Acharya, B. K. Choudhury, and S. K. Rout, "Effect of speed of condenser fan motor on vapor compression refrigeration system," in *Advances in Air Conditioning and Refrigeration: Select Proceedings of RAAR 2019*. Springer, 2020, pp. 395–403.
- [40] Z. Kolev, P. Mushakov, and S. Kadirova, "Experimental investigation of the refrigeration cycle of water-to-water heat pump," in *IOP Conference Series: Materials Science and Engineering*, vol. 1032, no. 1. IOP Publishing, 2021, p. 012031.
- [41] D. J. M. Rosado, S. B. R. Chávez, J. A. de Carvalho Jr, and R. C. C. Huallpachoque, "Comparison between the steam compression refrigeration system with intercooler and with compressor scale system: A case study," *Energy Conversion and Management*, vol. 183, pp. 406–417, 2019.

- [42] M. N. Šarevski and V. N. Šarevski, “Thermal characteristics of high-temperature r718 heat pumps with turbo compressor thermal vapor recompression,” *Applied Thermal Engineering*, vol. 117, pp. 355–365, 2017.
- [43] C. Mateu-Royo, J. Navarro-Esbrí, A. Mota-Babiloni, F. Molés, and M. Amat-Albuixech, “Experimental exergy and energy analysis of a novel high-temperature heat pump with scroll compressor for waste heat recovery,” *Applied Energy*, vol. 253, p. 113504, 2019.
- [44] C. Ermel, M. V. Bianchi, and P. S. Schneider, “Energy model of an air source heat pump to explore performance improvements under cold conditions: A python framework,” National Renewable Energy Lab.(NREL), Golden, CO (United States), Tech. Rep., 2023. [Online]. Available: <https://www.osti.gov/biblio/1923484>
- [45] D. Roskosch, V. Venzik, and B. Atakan, “Fluid retrofit for existing vapor compression refrigeration systems and heat pumps: Evaluation of different models,” *Energies*, vol. 12, no. 12, p. 2417, 2019.
- [46] M. Kamesh and V. Koshti, “Modelling and simulation of combined vapor compression system and organic rankine cycle using python,” EasyChair, Tech. Rep., 2022.
- [47] L. P. Brendel, S. L. Caskey, J. E. Braun, and E. A. Groll, “Effect of orientation on the steady-state performance of vapor compression cycles,” *Applied Thermal Engineering*, vol. 207, p. 118174, 2022.
- [48] C. Vering, F. Wüllhorst, P. Mehrfeld, and D. Müller, “Towards an integrated design of heat pump systems: Application of process intensification using two-stage optimization,” *Energy Conversion and Management*, vol. 250, p. 114888, 2021.
- [49] A. Aulicino and S. Bakrania, “A python-based lab module to conduct thermodynamic cycle analysis,” in *2022 IEEE Frontiers in Education Conference (FIE)*. IEEE, 2022, pp. 1–6.
- [50] S. Li, J. Lu, W. Li, Y. Zhang, S. Huang, L. Tian, Y. Lv, Y. Hu, and Y. Zeng, “Thermodynamic analyses of a novel ejector enhanced dual-temperature air source heat pump cycle with self-defrosting,” *Applied Thermal Engineering*, vol. 215, p. 118944, 2022.
- [51] S. Li, J. Lu, W. Li, S. Huang, and L. Tian, “Comparative performance of ternary azeotropic mixtures as substitutes for r134a in dual-temperature air source heat pump combined ejector,” *Thermal Science and Engineering Progress*, vol. 37, p. 101577, 2023.
- [52] M. Lysbo, “Termodynamikk for ingeniørstudenter,” 2020, [Accessed 02-Apr-2023]. [Online]. Available: [EMTS1400_termo_kompendium.pdf](#)
- [53] N. Parmar. (2023) Enthalpy formula. [Accessed 5-Apr-2023]. [Online]. Available: <https://www.collegesearch.in/articles/enthalpy-formula>
- [54] G. W. Drake. (2023) Entropy. [Accessed 5-Apr-2023]. [Online]. Available: <https://www.britannica.com/science/entropy-physics>
- [55] C. Sejkora, L. Kühberger, F. Radner, A. Trattner, and T. Kienberger, “Exergy as criteria for efficient energy systems—a spatially resolved comparison of the current exergy consumption, the current useful exergy demand and renewable exergy potential,” *Energies*, vol. 13, no. 4, p. 843, 2020.

- [56] . G. A. Cengel, Y.A., *Heat and Mass Transfer, Fundamentals Applications*. Mc Graw Hill Education, 2020, pp. 492–730.
- [57] J. C. K. Jørn Stene, “Varmepumper i bygninger. funksjonsbeskrivelse,” 2009. [Online]. Available: https://www.byggforsk.no/dokument/541/varmepumper_i_bygninger_funksjonsbeskrivelse
- [58] N. G. Undersøkelse, “Grunnvarme,” 2023. [Online]. Available: <https://www.ngu.no/geologiske-ressurser/grunnvarme>
- [59] R. Brogan. (2011) Shell and tube heat exchangers. [Accessed 29-Apr-2023].
- [60] S. . MAQUINARIAS. (2023) Varmevexslere. [Accessed 10-May-2023]. [Online]. Available: <http://sumimaqecuador.com/intercambiadores/>
- [61] L. Team. (2022) What are double pipe heat exchangers and their working principles? [Accessed 10-May-2023]. [Online]. Available: <https://www.linquip.com/blog/double-pipe-heat-exchangers/>
- [62] E. C. Fábio A.S. Mota and M. A. Ravagnani, *Heat Transfer Studies and Applications*. InTech, 2015, pp. 0–406.
- [63] M. Waugh. (2011) Generic plate heat exchanger model. [Accessed 5-May-2023]. [Online]. Available: https://grabcad.com/library/plate-heat-exchanger/details?folder_id=49135
- [64] M. W. Faruque, Y. Khan, M. H. Nabil, M. M. Ehsan, and A. Karim, “Thermal performance evaluation of a novel ejector-injection cascade refrigeration system,” *Thermal Science and Engineering Progress*, vol. 39, pp. 101–745, 2023.
- [65] B. Tashtoush and M. Bani Younes, “Comparative thermodynamic study of refrigerants to select the best environment-friendly refrigerant for use in a solar ejector cooling system,” *Arabian Journal for Science and Engineering*, vol. 44, no. 2, pp. 1165–1184, 2019.
- [66] E. Comission. (2023) Climate-friendly alternatives to hfcs. [Accessed 20-Apr-2023]. [Online]. Available: https://climate.ec.europa.eu/eu-action/fluorinated-greenhouse-gases/climate-friendly-alternatives-hfcs_en
- [67] H. H. Simon Yuill, “Python,” *Python Releases Wind*, vol. 24, 2006.
- [68] S. E. B. H. Allen, R., “A python-based code for modeling the thermodynamics of the vapor compression cycle applied to residential heat pumps,” *Conference Proceedings for the 64th International Conference of Scandinavian Simulation Society, SIMS*, 2023.
- [69] V. Patel and R. Rao, “Design optimization of shell-and-tube heat exchanger using particle swarm optimization technique,” *Applied Thermal Engineering*, vol. 30, no. 11-12, pp. 1417–1425, 2010.
- [70] F. Vera-García, J. García-Cascales, J. González-Maciá, R. Cabello, R. Llopis, D. Sanchez, and E. Torrella, “A simplified model for shell-and-tubes heat exchangers: Practical application,” *Applied Thermal Engineering*, vol. 30, no. 10, pp. 1231–1241, 2010.
- [71] S. Fettaka, J. Thibault, and Y. Gupta, “Design of shell-and-tube heat exchangers using multiobjective optimization,” *International Journal of Heat and Mass Transfer*, vol. 60, pp. 343–354, 2013.

- [72] S. Sanaye and H. Hajabdollahi, "Multi-objective optimization of shell and tube heat exchangers," *Applied Thermal Engineering*, vol. 30, no. 14-15, pp. 1937–1945, 2010.
- [73] V. Patel and R. Rao, "Design optimization of shell-and-tube heat exchanger using particle swarm optimization technique," *Applied Thermal Engineering*, vol. 30, no. 11-12, pp. 1417–1425, 2010.
- [74] Wolfram. (2023) Correctionfactorforshellandtubeheatexchanger. [Accessed 25-Apr-2023]. [Online]. Available: <https://www.wolframcloud.com/objects/demonstrations/CorrectionFactorForShellAndTubeHeatExchanger-source.nb>
- [75] P. K. Swamee, N. Aggarwal, and V. Aggarwal, "Optimum design of double pipe heat exchanger," *International Journal of Heat and Mass Transfer*, vol. 51, no. 9-10, pp. 2260–2266, 2008.
- [76] I. Bashtani and J. A. Esfahani, " ε -ntu analysis of turbulent flow in a corrugated double pipe heat exchanger: A numerical investigation," *Applied Thermal Engineering*, vol. 159, p. 113886, 2019.
- [77] J. A. Gut and J. M. Pinto, "Optimal configuration design for plate heat exchangers," *International Journal of Heat and Mass Transfer*, vol. 47, no. 22, pp. 4833–4848, 2004.
- [78] A. Jokar, M. H. Hosni, and S. J. Eckels, "Dimensional analysis on the evaporation and condensation of refrigerant r-134a in minichannel plate heat exchangers," *Applied thermal engineering*, vol. 26, no. 17-18, pp. 2287–2300, 2006.
- [79] B. Kumar, A. Soni, and S. Singh, "Effect of geometrical parameters on the performance of chevron type plate heat exchanger," *Experimental Thermal and Fluid Science*, vol. 91, pp. 126–133, 2018.
- [80] J. Ibarra-Bahena, R. Romero, L. Velazquez-Avelar, C. Valdez-Morales, and Y. Galindo-Luna, "Evaluation of the thermodynamic effectiveness of a plate heat exchanger integrated into an experimental single stage heat transformer operating with water/carrol mixture," *Experimental thermal and fluid science*, vol. 51, pp. 257–263, 2013.
- [81] E. ToolBox, "Heat exchangers - heat transfer coefficients," 2003. [Online]. Available: https://www.engineeringtoolbox.com/heat-transfer-coefficients-exchangers-d_450.html
- [82] J. Ko, K. Thu, and T. Miyazaki, "Investigation of a cascaded co2 refrigeration system using phase change materials for energy-saving potentials," *Applied Thermal Engineering*, vol. 182, pp. 1–15, 2021.
- [83] EngineerExcel. (2023) Haaland equation for friction factor. [Accessed 1-Apr-2023]. [Online]. Available: <https://engineerexcel.com/haaland-equation-for-friction-factor/>
- [84] B. Higgins, J. Scherer, A. Amaya, H. Chandrasekar, and A. Van, "Closed-loop geothermal in steam dominated reservoirs," in *GreenFire Energy. Geothermal Rising Conference Transactions*, vol. 45, 2021.
- [85] A. Dalkilic, S. Laohalertdecha, and S. Wongwises, "Two-phase friction factor in vertical downward flow in high mass flux region of refrigerant hfc-134a during condensation," *International Communications in Heat and Mass Transfer*, vol. 35, no. 9, pp. 1147–1152, 2008.

Appendix

A Initial Code

A.1 Main script

```
7 # Call the function with default values using for example: HPMF(280, 310, 'R134a', option = 'Qcond', 5000)
8 # Call the function with specified values using for example: HPMF(280, 310, 'R134a', option = 'mf', 2.5, SH
9 # Temperatures need to be in kelvin
10 # input value for QH should be in watts
11 # mass flow rate should be in [kg/s]
12
13 import numpy as np
14 from CoolProp.CoolProp import PropsSI
15
16 def HPMF(Tev, Tc, myfluid, option_value, option_name, SH=0, SC=0, n=1):
17
18     # Make sure the user input is correct
19     if option_name != 'Qcond' and option_name != 'mflow':
20         print('Problem: option_name should be specified as either Qcond or mflow')
21         return
22
23     if isinstance(option_value, str):
24         print('option_value must be a float or an int')
25         return
26
27     if n <= 0 or n > 1:
28         print('Problem: n should be specified 0 < n <=1. Check calculations.')
29         return
30
31     # subcooling can not be less than 0.
32     if SC < 0:
33         print('Problem: can not specify negative value. Check calculations.')
34         return
35
36     #evaporator
37     if SH == 0:
38         #f(Tev)saturated vapor Q=1
39         P1 = PropsSI('P', 'T', Tev, 'Q', 1, myfluid)
40         h1 = PropsSI('H', 'T', Tev, 'Q', 1, myfluid) #f(Tev) [J/kg]
41         s1 = PropsSI('S', 'T', Tev, 'Q', 1, myfluid) #f(Tev) [J/K]
42         rho1 = PropsSI('D', 'T', Tev, 'Q', 1, myfluid) #f(Tev) [kg/m^3]
43
44     else:
45         P1 = PropsSI('P', 'T', Tev, 'Q', 1, myfluid)
46         h1 = PropsSI('H', 'T', Tev+SH, 'P', P1, myfluid) #f(T1,P1) [J/kg]
47         s1 = PropsSI('S', 'P', P1, 'T', Tev+SH, myfluid) #f(T1,P1) [J/K]
48         rho1 = PropsSI('D', 'T', Tev+SH, 'P', P1, myfluid) #f(T1,P1) [kg/m^3]
49
50     #compressor
51     P3 = PropsSI('P', 'T', Tc, 'Q', 0, myfluid) #f(Tc)
52     s2=s1
53     P2 = P3
54     h2is = PropsSI('H', 'P', P2, 'S', s2, myfluid) #f(P3,s1)
55
56     if n == 1:
57         h2=h2is
58         s2=s1
59
60     else:
61         h2 = (h2is-h1)/n + h1
62         s2 = PropsSI('S', 'P', P2, 'H', h2, myfluid) #f(P2,h2)
63
64
65     # h2 should be larger than h1
66     if h2is < h1:
67         print('Problem: h2 is less than h1. Check calculations.')
68         return
69
70     # state between point 2. and 3.
71     T23 = Tc
72     s23 = PropsSI('S', 'T', Tc, 'Q', 1, myfluid)
73
74     #condenser
75     if SC == 0:
76         h3 = PropsSI('H', 'T', Tc, 'Q', 0, myfluid) #f(Tc), Q=0 saturated liquid
77         s3 = PropsSI('S', 'P', P3, 'Q', 0, myfluid)
78     else:
79         T2 = Tc+SH;
80         h3 = PropsSI('H', 'T', Tc-SC, 'P', P3, myfluid) #f(T3,P3)
81         s3 = PropsSI('S', 'P', P3, 'H', h3, myfluid)
82
83     # h2 should be greater than h3
84     if h2is < h3:
85         print('Problem: h2 is less than h3. Check calculations.')
86         return
87
88
89     #exp valve
90     P4 = P1
91     h4 = h3
92     s4 = PropsSI('S', 'P', P4, 'H', h4, myfluid)
93
94
95
96
97
98
99
100
```



```

110
111     COP = (h2-h3)/(h2-h1)
112     VHC = (h2-h3)*rho1 #[J/ (m^3)]
113     PR = P2/P1
114     Pres = np.round([P1, P2, P3, P4], Dec)
115     Enth = np.round([h1, h2, h3, h4], Dec)
116     Entr = np.round([s1, s2, s23, s3, s4], Dec)
117
118     # Include variables you want to return from the function
119     result = [Tev, Tc, option_value, myfluid, SH, SC, n, COP, Pres, Enth, Entr, W_comp]
120
121     #pass values out
122     print("Tc: ", Tc)
123     print("myfluid: ", myfluid)
124     print("COP: ", round(COP, Dec))
125     print("P: ", ', '.join(map(str, Pres)))
126     print("h: ", ', '.join(map(str, Enth)))
127     print("S: ", ', '.join(map(str, Entr)))
128     print("rho1: ", round(rho1, Dec))
129     print("Qev: ", round(Qev, Dec))
130     print("W_comp: ", round(W_comp, Dec))
131     print("VHC: ", round(VHC, Dec))
132     print("PR: ", round(PR, Dec))
133
134     return result

```

Figure 81: Initial script handed over by bachelor groupe

A.2 P-h Plot

```

"""
Created on Thu Aug 18 09:36:31 2022

@author: 47456
"""

import matplotlib.pyplot as plt
from CoolProp.Plots import PropertyPlot
from CoolProp.Plots import SimpleCompressionCycle
import CoolProp
from HPModelfunction import HPMF

# Call the function "HPMF" with input arguments to get a PH-plot
output = HPMF(280, 310, 'R134a', 5000, "Qcond")

# Get ready to plot in Ph-diagram
# Use the correct argument position returned from the function starting from [0]
Fluid = 'HEOS:.' + output[3]
plot = PropertyPlot(Fluid, 'PH', unit_system='KSI', tp_limits = 'ACHP')

# Lines of constant values
plot.calc_isolines(CoolProp.iQ, num=11)
plot.calc_isolines(CoolProp.iT, num=25)
plot.calc_isolines(CoolProp.iSmass, num=15)

# Vapor compression cycle from coolprop (Doesn't like SH = SC = 0)
'''
cycle = SimpleCompressionCycle(Fluid, 'PH', unit_system='KSI')
cycle.simple_solve_dt(output['some1'][0], output['some1'][1], output['some1'][3], output['some1'][4], output['some1'][2])
cycle.steps = 50
sc = cycle.get_state_changes()
plot.draw_process(sc, line_opts={'color': 'red', 'lw': 0.5})
plt.close(cycle.figure)
plot.draw_process(sc)
'''

# Own plot
plt.plot((output[9]/1000), (output[8]/1000), color='green', marker = 'o')
plt.show()

```

Figure 82: P-h plot made by bachelor group

A.3 T-s Plot

```
"""
Created on Thu Aug 18 19:32:20 2022

@author: 47456
"""

import matplotlib.pyplot as plt
from CoolProp.Plots import PropertyPlot
import CoolProp
from HPmodelfunction import HPMF

output = HPMF(280, 320, 'R134a')

# Isolines
Fluid = 'HEOS::' + output['Gr1'][1]
plot = PropertyPlot(Fluid, 'TS', unit_system='EUR', tp_limits='ORC')
plot.calc_isolines(CoolProp.iQ, num=11)
plot.calc_isolines(CoolProp.iP, iso_range=[1,50], num=10, rounding=True)
plot.draw()
plot.isolines.clear()
plot.props[CoolProp.iP]['color'] = 'green'
plot.props[CoolProp.iP]['lw'] = '0.5'

# Lines from points
plt.plot(output['Gr4'][2]/1000, output['Gr4'][3]-273.15, color='r')
plt.show()
```

Figure 83: T-s plot made by bachelor group

B Python values for validation

Table 18: Initial input values for validation

Explanation	Parameter	Value	Unit
Evaporator temperature	T_{ev}	264	[K]
Condensator temperature	T_c	313	[K]
Water In temperature	T_{wi}	293	[K]
Water out temperature	T_{wo}	302	[K]
Brine water In temperature	T_{bi}	278	[K]
Brine water out temperature	T_{bo}	268	[K]
Chosen fluid for VCC	$myfluid$	R134a	[-]
Super-heating	SH	5	[K]
Sub-cooling	SC	0	[K]
Isentropic efficiency	n	1	[-]
Type of HE	$Type$	4	[-]
Printed tables	$printtable$	True/False	[-]

C Python scripts

C.1 Start of function

```

import numpy as np
from CoolProp.CoolProp import PropsSI
import thermopy
import math
from math import pi
from tabulate import tabulate
from prettytable import PrettyTable
import os
import sys
import matplotlib.pyplot as plt

def HPWF(Tev, Tc, Twi, Tbo, Tbi, Tbo, myfluid, SH=0, SC=0, n=1, Type=1, printtable=True):
    # This function calculates thermodynamic parameters of a heat pump (VCC) and heat exchangers.

```

Figure 84: Start of function

C.2 Calling function

```

HPWF(275, 338, 312, 325, 278, 276, 'R134a', 0, 0, 1, 3, printtable=True)

```

Figure 85: End of script "calling" the function

D Mass flow rate and COP figures

D.1 Mass flow rate and COP, C1, DP

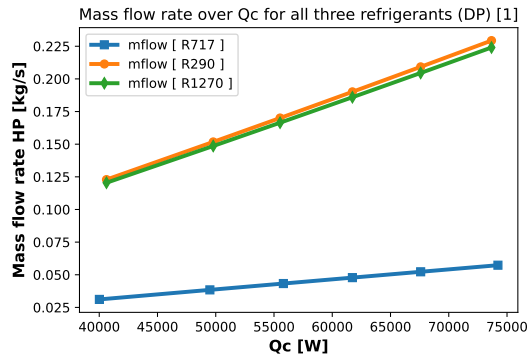


Figure 86: Mass flow rate for all refrigerants, C1,DP

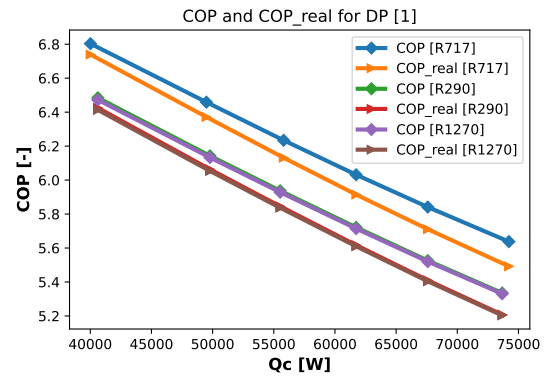


Figure 87: COP for all refrigerants, C1,DP

D.2 Mass flow rate and COP, C1, PE

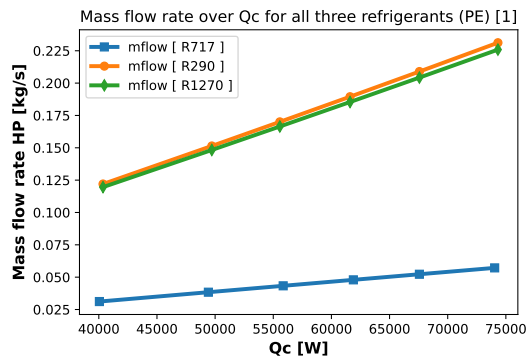


Figure 88: Mass flow rate for all refrigerants, C1,PE

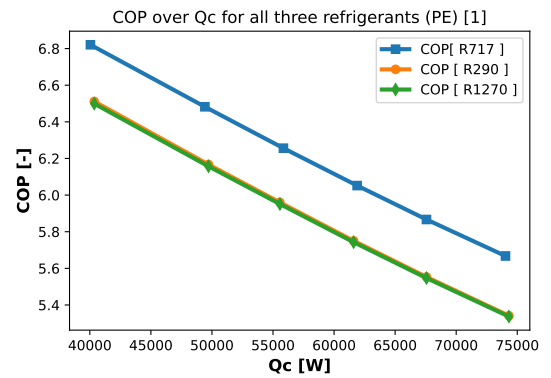


Figure 89: COP for all refrigerants, C1,PE

D.3 Mass flow rate and COP, C2, DP

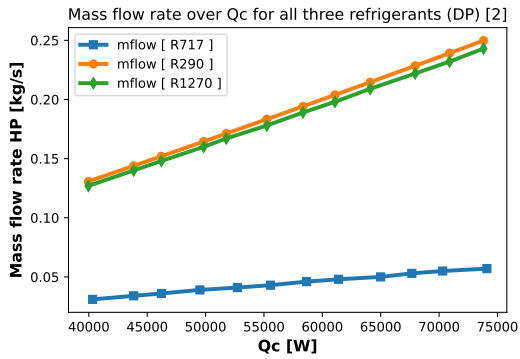


Figure 90: Mass flow rate for all refrigerants, C2,DP

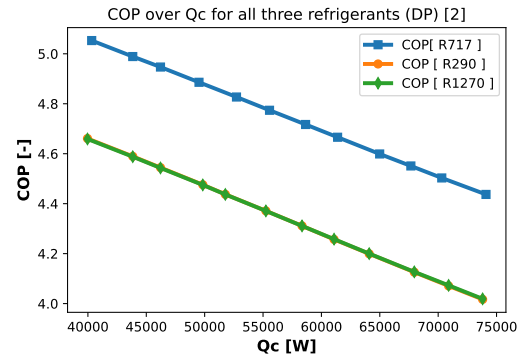


Figure 91: COP for all refrigerants, C2,DP

D.4 Mass flow rate and COP, C2, PE

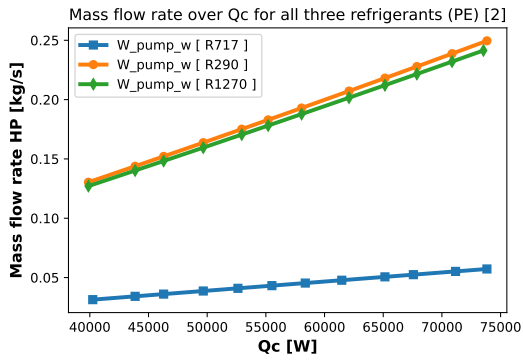


Figure 92: Mass flow rate for all refrigerants, C2,PE

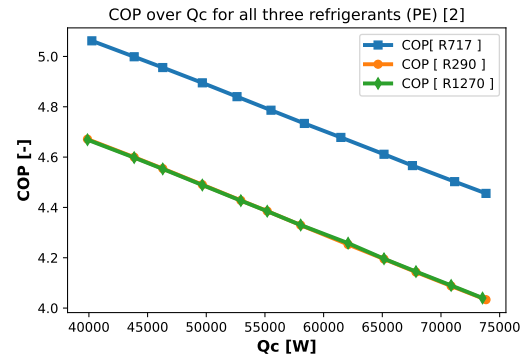


Figure 93: COP for all refrigerants, C2,PE

D.5 Mass flow rate and COP, C3, DP

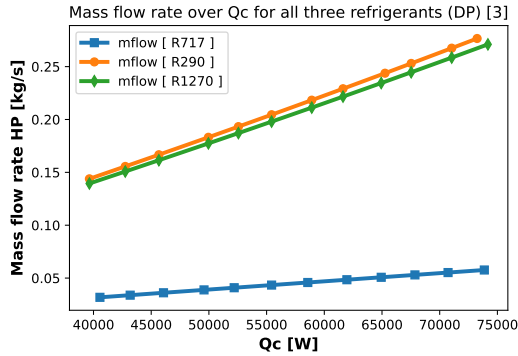


Figure 94: Mass flow rate for all refrigerants, C3,DP

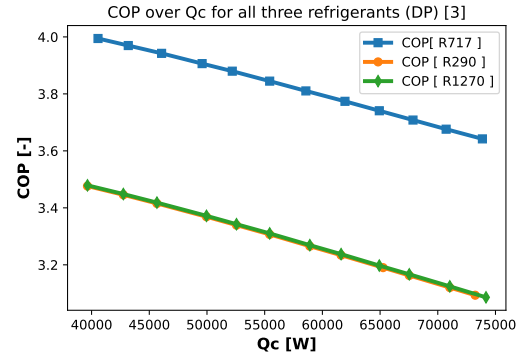


Figure 95: COP for all refrigerants, C3,DP

D.6 Mass flow rate and COP, C3, PE

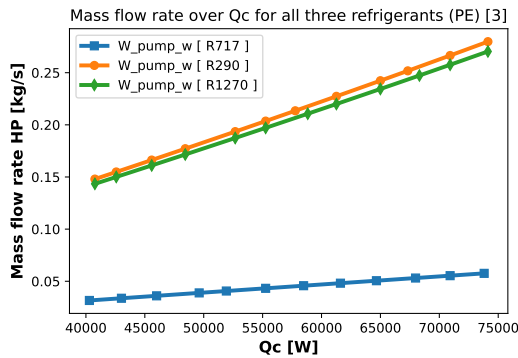


Figure 96: Mass flow rate for all refrigerants, C3,PE

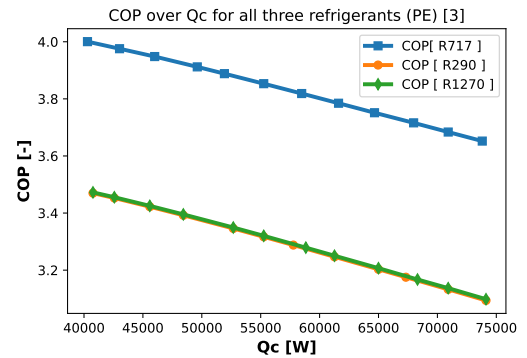


Figure 97: COP for all refrigerants, C3,PE

E Excel

ST_R717_Parallel_Flow															
Count	Qc [W]	Refrigerant [-]	Conv. COP [-]	Conv. COP_real [-]	Conv. Wcomp [W]	Conv. mflow [kg/s]	Conv. Wpump _{water} [W]	Conv. m _{water} [kg/s]	Q _{c,calc} [W]	Q _{ev} [W]	Q _{con} [W]	Conv. Qevap _{water} [W]	LMTD [K]	W_pump _{ev} [W]	epsilon _{ev} [-]
13909	40325.01	R717	5.05254123	5.041931223	7981.133618	0.031443873	0.976210508	0.643018987	6186.309	32344	32845.9	502.0008058	7.64039	15.81892222	0.98315546
13325	43841.4	R717	4.98946383	4.977347612	8786.795257	0.034168556	1.253474162	0.699091037	7125.183	35055	35761	706.3927119	8.30664	20.13597714	0.98315528
12936	46216.65	R717	4.94674037	4.933590534	9342.849669	0.036007753	1.467729138	0.736966636	7784.911	36874	37557.4	683.6445533	8.75668	23.43441454	0.98315441
12352	49515.49	R717	4.88620268	4.871612684	10133.73721	0.038558354	1.803900651	0.789569683	8733.418	39382	40094.2	712.4919149	9.38171	28.54564634	0.98315405
11768	52726.38	R717	4.82709495	4.811099419	10923.00435	0.041037853	2.176955361	0.840770174	9691.045	41803	42487.4	684.0016992	9.99008	34.1389131	0.9831536
11183	55556.24	R717	4.77361221	4.75639455	11638.19713	0.043217799	2.545587969	0.885894883	10561.85	43918	44770.9	852.8867557	10.5263	39.58348849	0.98315516
10599	58646.25	R717	4.71711843	4.698558494	12432.64237	0.045598263	2.993208336	0.935167853	11540.97	46214	46967.9	754.3083708	11.1117	46.11738398	0.98315451
10014	61386.47	R717	4.66597345	4.646249168	13156.19754	0.047703769	3.431585764	0.978863191	12433.5	48230	49094.6	864.3764735	11.6309	52.41918393	0.98315591
9234	64990.07	R717	4.5994378	4.578203642	14130.0026	0.050468694	4.070541119	1.036325871	13611.31	50860	51841.4	981.3254514	12.3137	61.46578788	0.98315765
8649	67660.95	R717	4.55073671	4.528401932	14868.13155	0.052515048	4.592126306	1.078915551	14538.6	52793	53846.2	1053.351611	12.8197	68.73978997	0.98315886
8064	70308.48	R717	4.50302986	4.479621609	15613.59292	0.054541032	5.151338523	1.12113272	15441.56	54695	55811.1	1116.180443	13.3214	76.43745086	0.98315999
7285	74097.11	R717	4.43723292	4.412299523	16698.94483	0.057440146	6.027909507	1.18154592	16759.38	57398	58377.8	979.6828732	14.0392	88.33589946	0.98315919

Figure 98: Values from Excel.

F T-s and P-h diagrams, Case 1

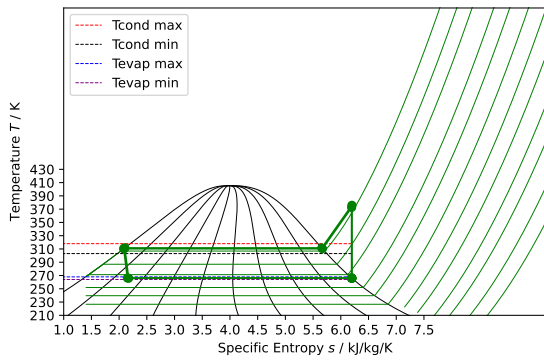


Figure 99: T-s diagram, R717, for Q_c equals to 61, 67, and 73 [kW], C1

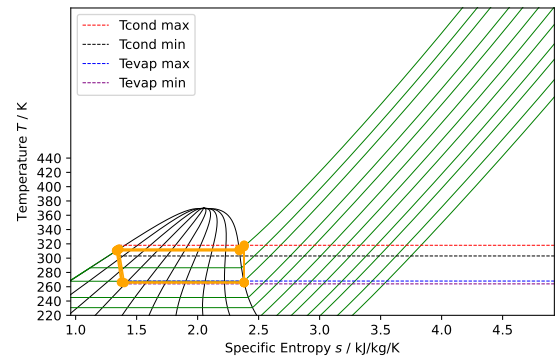


Figure 100: T-s diagram, R290, for Q_c equals to 61, 67, and 73 [kW], C1

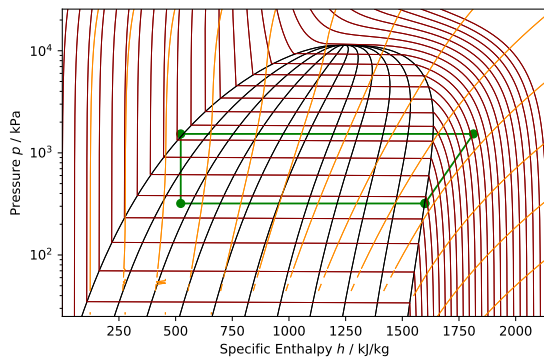


Figure 101: P-h diagram, R717, for Q_c equals to 61, 67, and 73 [kW], C1

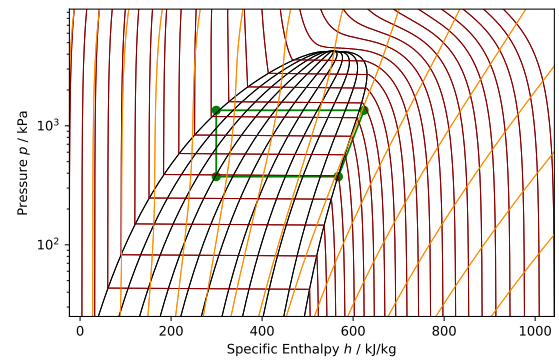


Figure 102: P-h diagram, R290 for Q_c equals to 61, 67, and 73 [kW], C1

G T-s and P-h diagrams, Case 2

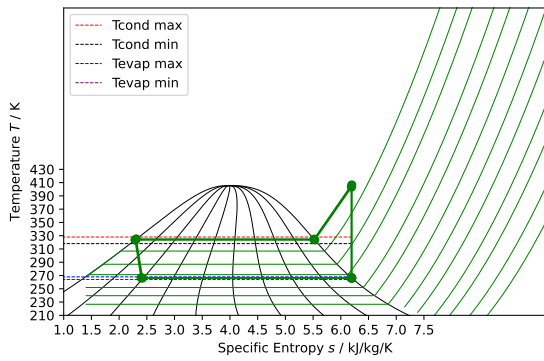


Figure 103: T-s diagram, R717, for Q_c equals to 61, 67, and 73 [kW], C2

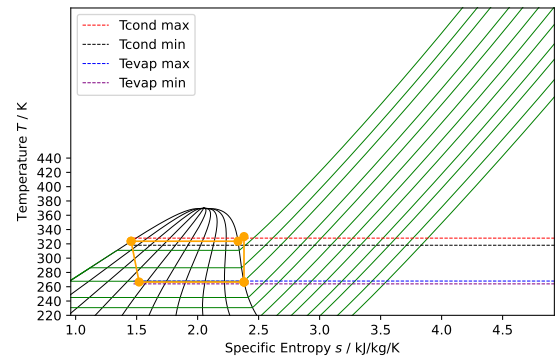


Figure 104: T-s diagram, R290, for Q_c equals to 61, 67, and 73 [kW], C2

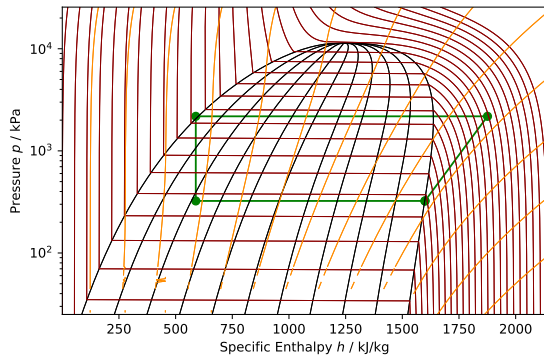


Figure 105: P-h diagram, R717, for Q_c equals to 61, 67, and 73 [kW], C2

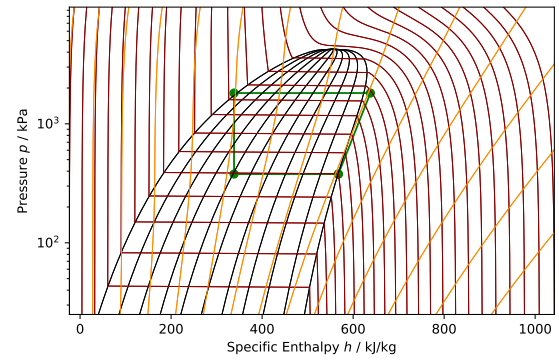


Figure 106: P-h diagram, R290, for Q_c equals to 61, 67, and 73 [kW], C2

H T-h og T-s Python

```
import matplotlib.pyplot as plt
from CoolProp.Plots import PropertyPlot
from CoolProp.Plots import SimpleCompressionCycle
import CoolProp
import numpy as np
#from HPmodelfunction_Uten_Q import HPMF

# Call the function "HPMF" with input arguments to get a PH-plot
#output = HPMF(264, 305, 293, 303, 278, 268, 'R134a', 1, 0, 0.7, 2, printable=False)
# Get ready to plot in Ph-diagram
# Use the correct argument position returned from the function starting from [0]
Fluid = 'HEOS::' + 'R290'
plot = PropertyPlot(Fluid, 'PH', unit_system='KSI', tp_limits = 'ACHP')

# Lines of constant values
plot.calc_isolines(CoolProp.iQ, num=11)
plot.calc_isolines(CoolProp.iT, num=25)
plot.calc_isolines(CoolProp.iSmass, num=15)

x_coords = [567222.742, 623979.339, 299239.011, 299239.011, 567222.742]
x_coords = [x/1000 for x in x_coords]
y_coords = [382693.958, 1284468.013, 1284468.013, 382693.958, 382693.958]
y_coords = [y/1000 for y in y_coords]

x1_coords1 = [566827.713, 625285.303, 302247.28, 302247.28, 566827.713]
x_coords1 = [x/1000 for x in x1_coords1]
y_coords1 = [378393.344, 1316435.228, 1316435.228, 378393.344, 378393.344]
y_coords1 = [y/1000 for y in y_coords1]

x2_coords2 = [566432.277, 626639.983, 305414.013, 305414.013, 566432.277]
x_coords2 = [x/1000 for x in x2_coords2]
y_coords2 = [374129.055, 1350544.924, 1350544.924, 374129.055, 374129.055]
y_coords2 = [y/1000 for y in y_coords2]

# Own plot
plt.plot((x_coords), (y_coords), color='green', marker = 'o', linewidth=1.4)
#plt.plot((x_coords1), (y_coords1), color='green', marker = 'o', linewidth=1.4)
#plt.plot((x_coords2), (y_coords2), color='green', marker = 'o', linewidth=1.4)
plot.show()
#plot.savefig('P-h_C1_R290_61.pdf')
```

Figure 107: P-h plot.

```

import CoolProp
from CoolProp.Plots import PropertyPlot
import matplotlib.pyplot as plt
import numpy as np
#from HPmodelfunction_Uten_Q_CASE_3 import HPMF

# Call the function "HPMF" with input arguments to get a Ps-plot
#output = HPMF(275, 330, 312, 325, 279, 276, 'R134a', 5, 5, 0.7, 1, printtable=True)
output_entro = [6195.421, 6195.421, 5668.212, 2084.575, 2084.575, 2150.009, 6195.421, 6195.421]

# Get ready to plot in Ps-diagram
# Use the correct argument position returned from the function starting from [0]
Fluid = 'HEOS::' + "R290"
plot = PropertyPlot(Fluid, 'TS', unit_system='KSI', tp_limits='ORC')

plot.calc_isolines(CoolProp.iQ, num=10)
plot.calc_isolines(CoolProp.iP, iso_range=[1,1300], num=12, rounding=True)
plot.draw()
plot.isolines.clear()
plot.props[CoolProp.iP]['color'] = 'green'
plot.props[CoolProp.iP]['Lw'] = '0.5'
plt.yticks(np.arange(220, 450, 20))
#plt.xticks(np.arange(1, 8, 0.5))

x90_coords90 = [2380.048, 2380.048, 2331.242, 1454.777, 1454.777, 1520.196, 2380.048, 2380.048]
x_coords90 = [x/1000 for x in x90_coords90]
y_coords90 = [266.6, 330.16, 323.65, 323.65, 323.65, 266.6, 266.6, 266.6]

x91_coords91 = [2380.491, 2380.491, 2330.156, 1465.331, 1465.331, 1534.209, 2380.491, 2380.491]
x_coords91 = [x/1000 for x in x91_coords91]
y_coords91 = [266.25, 331.466, 324.8, 324.8, 324.8, 266.25, 266.25, 266.25]

x92_coords92 = [2380.873, 2380.873, 2329.183, 1474.529, 1474.529, 1546.487, 2380.873, 2380.873]
x_coords92 = [x/1000 for x in x92_coords92]
y_coords92 = [265.95, 332.601, 325.8, 325.8, 325.8, 265.95, 265.95, 265.95]

y_point = 328
y_point3 = 318.05
y_point1 = 267.95
y_point2 = 264
x_range = np.linspace(min(min(x90_coords90), min(x91_coords91), min(x_coords92))), max(max(x90_coords90), max(x91_coords91), max(x_coords92)), 100)
plt.plot(x_range, [y_point]*len(x_range), 'r--', linewidth=0.7, label='Tcond max', color='red')
plt.plot(x_range, [y_point3]*len(x_range), 'k--', linewidth=0.7, label='Tcond min', color='black')
plt.plot(x_range, [y_point1]*len(x_range), 'k--', linewidth=0.7, label='Tevap max', color='blue')
plt.plot(x_range, [y_point2]*len(x_range), 'k--', linewidth=0.7, label='Tevap min', color='purple')

plt.plot(x_coords90, y_coords90, color='orange', marker = 'o', linewidth=1.3)
plt.plot(x91_coords91, y_coords91, color='orange', marker = 'o', linewidth=1.3)
plt.plot(x92_coords92, y_coords92, color='orange', marker = 'o', linewidth=1.3)
plt.legend()

plot.show()

plot.savefig('T-s_C2_R290_61_67_73.pdf')

```

Figure 108: T-s plot

I T-s diagram modification

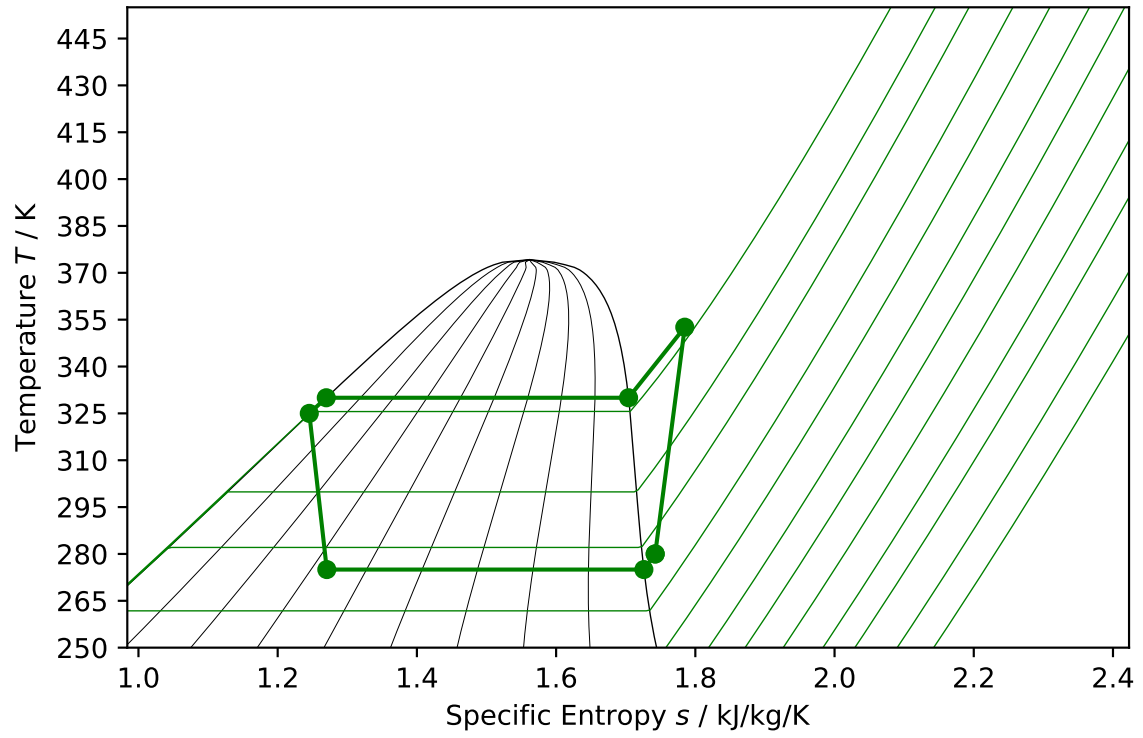


Figure 109: T-s plot of 5 °C SH and 5 °C SC.